YU ISSN 0042-8450

ВОЈНОСАНИТЕТСКИ ПРЕГЛЕД

Часопис лекара и фармацеута Војске Србије

Military Medical and Pharmaceutical Journal of Serbia

Vojnosanitetski pregled

Vojnosanit Pregl 2023; September Vol. 80 (No. 9): pp. 725–806.

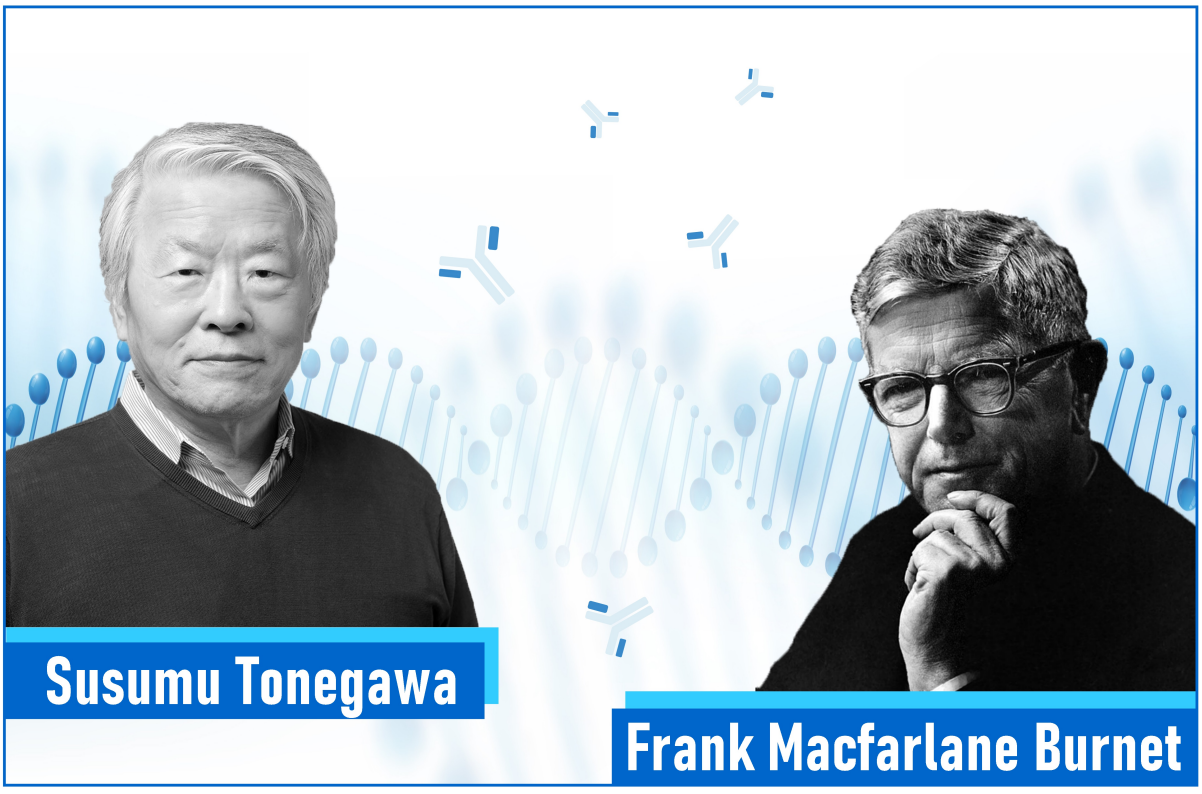

Vojnosanitetski Pregled 2023 September Vol. 80 (No. 9): pp. 725–806.

Vol. 80, No. 9, 2023

VOJNOSANITETSKI PREGLED

The first issue of *Vojnosanitetski pregled* was published in September 1944
The Journal continues the tradition of Vojno-sanitetski glasnik which was published between 1930 and 1941

PUBLISHER
Ministry of Defence of the Republic of Serbia, University of Defence, Belgrade, Serbia

ISSN 0042-8450
eISSN 2406-0720

Editorial Office: University of Defence, Faculty of Medicine of the Military Medical Academy, Center for Medical Scientific Information, Crnotravska 17, 11 040 Belgrade, Serbia. E-mail: **vsp@vma.mod.gov.rs**

Papers published in the Vojnosanitetski pregled are indexed in: Science Citation Index Expanded (SCIE), Journal Citation Reports/Science Edition, SCOPUS, Excerpta Medica (EMBASE), Google Scholar, EBSCO, Biomedicina Serbica, Serbian Citation Index (SCIndex), DOAJ. Contents are published in Giornale di Medicine Militare and Revista de Medicina Militara. Reviews of original papers and abstracts of contents are published in International Review of the Armed Forces Medical Services.

The Journal is published monthly. Subscription: Giro Account No. 840-19540845-28, refer to number 122742313338117. To subscribe from abroad phone to +381 11 3608 997. Subscription prices per year: individuals 5,000.00 RSD, institutions 10,000.00 RSD, and foreign subscribers 150 €.

Printed by: Vojna štamparija, Beograd, Resavska 40b

Vol.80, br. 9, 2023

VOJNOSANITETSKI PREGLED

Prvi broj *Vojnosanitetskog pregleda* izašao je septembra meseca 1944. godine
Časopis nastavlja tradiciju *Vojno-sanitetskog glasnika*, koji je izlazio od 1930. do 1941. godine

IZDAVAČ
Ministarstvo odbrane Republike Srbije, Univerzitet odbrane, Beograd, Srbija

ISSN 0042-8450
eISSN 2406-0720
Open Access
(CC BY-SA)

Adresa redakcije: Univerzitet odbrane, Medicinski fakultet Vojnomedicinske akademije, Centar za medicinske naučne informacije, Crnotravska 17, 11 040 Beograd, Srbija. Informacije o pretplati (tel.): +381 11 3608 997. E-mail (redakcija): **vsp@vma.mod.gov.rs**

Radove objavljene u „Vojnosanitetskom pregledu“ indeksiraju: Science Citation Index Expanded (SCIE), Journal Citation Reports/Science Edition, SCOPUS, Excerpta Medica (EMBASE), Google Scholar, EBSCO, Biomedicina Serbica, Srpski citatni indeks (SCIndeks), DOAJ. Sadržaje objavljuju Giornale di Medicine Militare i Revista de Medicina Militara. Prikaze originalnih radova i izvoda iz sadržaja objavljuje International Review of the Armed Forces Medical Services.

Časopis izlazi dvanaest puta godišnje. Pretplate: Žiro račun br. 840-19540845-28, poziv na broj 122742313338117. Za pretplatu iz inostranstva obratiti se službi pretplate na tel. +381 11 3608 997. Godišnja pretplata: 5 000 dinara za građane Srbije, 10 000 dinara za ustanove iz Srbije i 150 € za pretplatnike iz inostranstva. Kopiju uplatnice dostaviti na gornju adresu.

Štampa: Vojna štamparija, Beograd, Resavska 40b

CONTENTS / SADRŽAJ

CURRENT TOPIC / AKTUELNA TEMA

Vesna Rudić Grujić, Nina Rodić Vukmir, Mirjana Djermanović
Nutrition in COVID-19 recovery
Ishrana u oporavku od COVID-19 729

ORIGINAL ARTICLES / ORIGINALNI RADOVI

Dejan Kostić, Miroslav Mišović, Filip Vučković, Djuro Crevar, Igor Sekulić, Biljana Georgievski-Brkić, Smiljana Kostić, Evica Dinčić
Gadolinium deposition in the brain of patients with relapsing-remitting multiple sclerosis after 10 years of follow-up
Taloženje gadolinijuma u mozgu bolesnika sa relapsno-remitentnom multiplom sklerozom nakon 10 godina praćenja..... 736

Ljubiša Ristić, Vojkan Lazić, Srdjan Postić, Nenad Jelić, Igor Djordjević, Raša Mladenović
The connection between discolored gingiva of abutment teeth and the presence of cast post
Povezanost prebojene gingive pored zuba nosača sa prisustvom livene nadogradnje 743

Boris Gluščević, Aleksandar Stanojković, Dragica Bukumirić, Danilo Jeremić
Clinical results of scarf osteotomy
Klinički rezultati *scarf* osteotomije 748

Aleksandar Djordjević, Jelena Todić, Sanja Simić, Dragoslav Lazić, Zoran Vlahović, Ljiljana Šubarić
The effect of different cementation techniques on the amount of remaining excess cement depending on the crown-abutment margin level
Uticaj različitih tehnika cementiranja na količinu rezidualnog cementa u zavisnosti od lokalizacije margine krunica-nosač 754

Lora Novaković Lacković, Ljilja Latinović Tadić, Mirko Stanetić, Marko Lacković
Prognostic value of tumor-infiltrating T-lymphocytes density in the therapeutic response to initial platinum-based chemotherapy in patients with non-small cell lung cancer
Prognostička vrednost „gustine“ tumor-infiltrišućih T-limfocita u terapijskom odgovoru na inicijalnu hemioterapiju zasnovanu na platini kod bolesnika sa nesitnoćelijskim karcinomom pluća..... 761

Tina Pajević, Dina Vasović, Jovana Juloski, Ljiljana Vučić, Branislav Glišić
Evaluation of the impacted maxillary canines position, determination of the possible indicators of the impaction difficulty, and the risk factors for adjacent teeth root resorption
Procena položaja impaktiranih gornjih očnjaka, određivanje mogućih pokazatelja težine impakcije i faktora rizika od resorpcije korenova susednih zuba 768

Maja Stanković, Nemanja Turković, Silva Dobrić, Nemanja Rančić
Prescription patterns of diclofenac in patients with cardiovascular diseases or at high risk for cardiovascular diseases at primary health care level in Montenegro: retrospective, national, drug utilization study
Propisivanje diklofenaka bolesnicima sa kardiovaskularnim bolestima ili visokim rizikom od razvoja kardiovaskularnih bolesti na nivou primarne zdravstvene zaštite u Crnoj Gori: retrospektivna, nacionalna, studija upotrebe leka 778

CASE REPORTS / KAZUISTIKA

Aleksandar Vlahović, Milana Živković, Velibor Majić, Zorka Badnjar-Ilić, Ninoslav Begović, Ivan Dizdarević
Solid ectopic cervical thymus in an infant
Ektopični cervikalni timus čvrste strukture kod odojčeta 789

Dijana Damnjanović, Milena Zamurović, Aleksandar Vranjanac
Longitudinally extensive transverse myelitis after epidural anaesthesia in childbirth
Longitudinalni ekstenzivni transverzalni mijelitis posle epiduralne anestezije primenjene tokom porođaja..... 794

Srdjan Stošić, Mirela Juković, Jagoš Golubović, Milana Panjković, Sanja Stojanović
Squamous cell carcinoma of the scalp with intracranial extension – the importance of various imaging modalities
Planocelularni karcinom poglavine sa intrakranijalnim širenjem – značaj različitih modaliteta snimanja 797

Vesna Martić, Aleksandar Stojanov
Neurophysiological confirmation of phrenic nerve affection in a patient with dyspnea and herpes zoster
Neurofiziološka potvrda zahvaćenosti frenićnog nerva kod bolesnika sa dispnejom i herpesom zosterom 802

INSTRUCTIONS TO THE AUTHORS / UPUTSTVO AUTORIMA..... 805

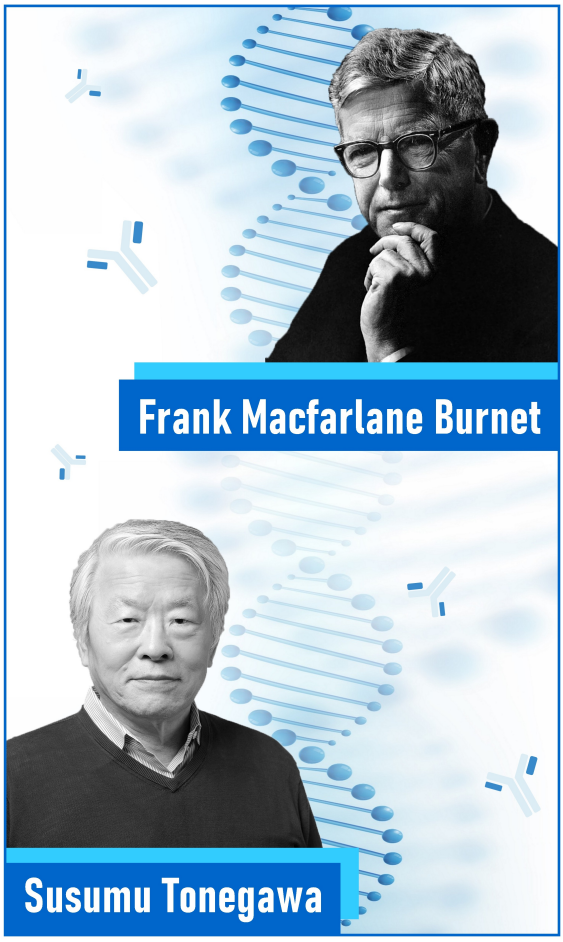

Two scientists born in September left an indelible impression on medicine, especially on immunology.

Susumu Tonegawa (born September 5, 1939) was the first Japanese winner of the Nobel Prize for Physiology or Medicine in 1987. He discovered a fundamental mechanism in the immune system, which explained that millions of antibodies of different specificities in the human body arise as a result of the rearrangement of a limited number of genes.

Frank Macfarlane Burnet (September 3, 1899–August 31, 1985), an Australian virologist, is the creator of the clonal selection theory of immunity, according to which antigen-specific lymphocyte clones develop before and independently of exposure to antigens. Together with Peter Medawar, he received the Nobel Prize in Physiology or Medicine in 1960 “for the discovery of acquired immunological tolerance” which was key to understanding self vs. foreign recognition and laying the foundation for successful solid organ transplantation.

Dva naučnika rođena u septembru ostavila su neizbrisiv trag u medicini, posebno u imunologiji.

Susumu Tonegava (rođen 05.09.1939.) bio je prvi japanski dobitnik Nobelove nagrade za fiziologiju ili medicinu 1987. godine. On je otkrio fundamentalni mehanizam u imunskom sistemu kojim je objašnjeno da milioni antitela različitih specifičnosti u organizmu čoveka nastaju kao posledica preuređenja ograničenog broja gena.

Frenk Makfarlejn Bernet (03.09.1899–31.08.1985), australijski virusolog, tvorac je teorije klonske selekcije imuniteta prema kojoj se antigen-specifični klonovi limfocita razvijaju pre i nezavisno od izlaganja antigenima. Zajedno sa Piterom Medavarom dobio je Nobelovu nagradu za fiziologiju ili medicinu 1960. godine „za otkriće stečene imunološke tolerancije“ što je bilo ključno za razumevanje prepoznavanja sopstvenog naspram stranog i postavljanje temelja uspešne transplantacije solidnih organa.

GENERAL REVIEW

UDC: 613.2::616.98-036.82
DOI: https://doi.org/10.2298/VSP230512041R

Nutrition in COVID-19 recovery

Ishrana u oporavku od COVID-19

Vesna Rudić Grujić, Nina Rodić Vukmir, Mirjana Djermanović

University of Banja Luka, Faculty of Medicine, Banja Luka, Republic of Srpska, Bosnia and Herzegovina; Public Health Institute of Republic of Srpska, Banja Luka, Republic of Srpska, Bosnia and Herzegovina

Key words:
covid-19; nutrition assessment; nutrition disorders; nutritional status; post-acute covid-19 syndrome.

Ključne reči:
covid-19; ishrana, procena; ishrana, poremećaji; nutritivni status; covid-19, post-akutni sindrom.

Introduction

Severe acute respiratory syndrome coronavirus 2 (SARS-CoV-2) appeared at the end of 2019, causing a worldwide pandemic. Most people experienced asymptomatic or mild-to-moderate acute coronavirus disease 2019 (COVID-19) symptoms; however, it was estimated that around 15% of people progressed to a more severe form of the disease requiring hospitalization, and approximately 5% became critically ill [1]. Although the acute phase of the disease has been well described so far, less data is available on the long-term outcomes [2]. Variable terms and definitions are still used to describe prolonged recovery or condition after acute SARS-CoV-2 infection with infection sequelae, such as "post-COVID-19 condition" or "long COVID condition". Long COVID represents a complex condition with different prolonged symptoms. According to the definition given by the World Health Organization (WHO), post-COVID-19 condition, also known as long COVID, occurs in individuals with a history of probable or confirmed SARS-CoV-2 infection, usually three months from the onset of COVID-19. Symptoms last at least two months and cannot be explained by an "alternative diagnosis" [3]. Michelen et al. [4] conducted the most comprehensive review of evidence on long COVID to date. Their findings suggest that this multiorgan syndrome is characterized by fatigue, weakness, malaise, breathlessness, and concentration impairment, among other less frequent symptoms. Symptoms of long-lasting COVID-19 sequelae and complications have been reported worldwide. A study from Italy showed that 87% of inpatients, who recovered from COVID-19, had at least one of the symptoms, even after 60 days [5]. A study in the United States found the prevalence of residual symptoms in 35% of patients treated for COVID-19 on an outpatient basis within 14–21 days after a positive test [6]. Lopez et al. [7] reported that 80% of patients with COVID-19 had long-term symptoms, including an estimate for at least one symptom.

While the focus during the COVID-19 pandemic was on the prevention and treatment of SARS-CoV-2 infection, today, significant attention must be paid to the health status of those who have recovered from COVID-19 or are still recovering from it. Many symptoms and conditions of long COVID, such as fatigue syndrome, sarcopenia, malnutrition, and gut microbiota alteration, are closely related to nutrition. On the other hand, the role of nutrition in the immune system's functioning is well documented today [8, 9]. In this context, it is essential to investigate and better understand the role of nutrition in the prevention of the severe form of the disease and improvement of the SARS-CoV-2 infection recovery. In this article, we present symptoms and conditions in patients with post-COVID-19 conditions closely related to nutrition, and we consider possible nutritional interventions for better outcomes.

Malnutrition

Data from different studies confirm the high prevalence of malnutrition in patients with COVID-19 [10, 11]. A Chinese study reported a prevalence of 52.7% of malnutrition in elderly patients (mean age 68.5 years) with COVID-19 [12]. The Nutricov study describes 37.5% of malnourished COVID-19 patients with pneumonia, with a mean age of 59.5 years, based on Global Leadership Initiative on Malnutrition (GLIM) criteria (weight loss, low body mass index-BMI, and reduced muscle mass) for malnutrition [10]. Malnutrition is a factor that can slow or prevent recovery [2, 13]. Insufficient

Correspondence to: Vesna Rudić Grujić, University of Banja Luka, Faculty of Medicine, Save Mrkalja 14, 78 000 Banja Luka, Republic of Srpska, Bosnia and Herzegovina. E-mail: vesna.rudic.grujic@med.unibl.org

consumption of energy, protein, and certain micronutrients can lead to reduced immune response and increased sensitivity to infections. Sufficient intake of vitamins D, C, A, E, B_6, and B_{12} and minerals zinc, iron, copper, and selenium are necessary to maintain immune function [2, 14–16]. Keeping in mind that some nutrients are crucial in the activation and functional expression of immune cells, it is important to prevent the lack of these nutrients in order to maintain a functional immune system. Screening for malnutrition is important for all COVID-19 patients, but special attention is needed for patients with multiple long-term conditions and people over 65 years of age [17].

Obesity

A different study on SARS-CoV-2 infected patients showed that obesity was strongly associated with negative outcomes [18-21]. Higher in-hospital mortality and the need for mechanical ventilation were documented even in younger patients (18–45 years) with obesity [18]. Simonnet et al. [19] reported that 90% of obese patients (BMI $\geq$ 35 kg/m^2) in the intensive care unit needed mechanical ventilation and that obesity was a strong risk factor for a bad outcome in patients with COVID-19. Earlier studies also support the fact that obesity is a risk factor for more severe clinical outcomes in viral diseases. Such was the case with the study conducted during the 2009 H1N1 pandemic [20]. Furthermore, an Italian study [21] discovered that obese patients required more time to recover from SARS-CoV-2 shedding. Obese people with COVID-19 have higher C-reactive protein (CRP) and tumor necrosis factor alpha (TNF-α) levels.

Sarcopenia

Sarcopenia occurs during COVID-19, also more often in elderly patients, affecting hospital prognosis and post-COVID-19 recovery. The degree of muscle mass loss and muscle function impairment is influenced by the health status before the infection, the degree of inflammation, anorexia, diminished food intake, lack of physical activity, cardiovascular status, intestinal microbiota [22], and medications such as steroids [23]. A study in the Netherlands found a prevalence of malnutrition in 35% of patients with COVID-19 after hospital admission [24]. About 20% of those hospitalized patients showed an acute weight loss of more than 5 kg. About 73% of all patients were at high risk of sarcopenia. Malnutrition is a proven predictor of sarcopenia [24–26].

Fatigue syndrome

Fatigue is a common symptom in post-COVID-19 patients. An Italian study [5], in which 143 patients (mean age 56.5) were monitored about 60 days after the appearance of the first COVID-19 symptom, showed the frequency of fatigue in 53.1% of respondents. Many other studies have shown a high prevalence of chronic fatigue after acute COVID-19 [27–29]. Fatigue occurs as a "physical" symptom, such as loss of energy and feeling powerless, and a "mental" symptom known as "brain fog". On the other hand, low physical or mental activity prolongs and worsens fatigue and other symptoms [29, 30]. The fatigue significantly affects the ability to perform daily activities and further complicates recovery after the acute phase of COVID-19 [30]. Fatigue that lasts for six months or more is called chronic fatigue [31].

Gut microbiota impairment

The gut microbiota has a number of functions that affect human health. Intestinal bacteria play a role in the digestion and metabolism of fatty acids, producing short-chain fatty acids, vitamins, and amino acids [32, 33]. In addition to the above, their role in the immune response is well recognized. Intestinal bacteria prevent colonization by pathogenic bacteria by maintaining the integrity of the intestinal barrier and producing antimicrobial proteins and lactic acid, which negatively affect the growth of pathogens [32–34]. Intestinal microbiota affects the function of immune cells, development of dendritic cells and T cells, synthesis of the cytokine interleukin (IL)-10, and has an impact on the inflammatory response [14, 35, 36]. Studies in mice have shown that disturbances in the intestinal microbiota lead to impaired immune response and exacerbation of respiratory infections, whether bacterial or viral [37, 38]. SARS-CoV-2 binds to the angiotensin-converting enzyme 2 (ACE2) receptor located in the alveolar epithelial cells and thus enters the cell and causes lung inflammation [14]. ACE2s are also expressed on enterocytes, which indicates a link between gut microbiota and the immune response to SARS-CoV-2 infection [14, 39].

Due to the proven role of intestinal microbiota in immune function, many studies have investigated the effect of different probiotics on immune response and infection in humans [34, 40].

The role of micronutrients and the consequences of their deficiency

Vitamins and trace elements and their role as immunomodulators were the subject of great interest during the COVID-19 pandemic. Vitamin D has multiple roles in the immune response, modulating the production of proinflammatory and anti-inflammatory cytokines and inducing antimicrobial peptides at mucosal surfaces [41–43]. A deficiency in vitamin D is linked to a higher risk for infection of the respiratory tract [43]. Vitamin D prevents excessive inflammatory responses in the lungs and strengthens innate defense mechanisms against respiratory pathogens [44]. A pilot study [45] in hospitalized patients with COVID-19 found micronutrient deficits, primarily vitamin D deficiency, in 76% of patients and selenium deficiency in 42% of those examined. Vitamin A plays a role in the proliferation and differentiation of regulatory T cells and participates in the regulation of some inflammatory mediators [36].

Vitamin C has antioxidant, anti-inflammatory, and immunomodulatory effects; this makes it desirable in the treatment of post-COVID-19 [46]. It is considered that vitamin C strengthens the immune system in various ways, for instance,

by increasing the activity of immune cells as well as other immune agents [47]. It was found that the elderly, diabetics, hypertensives, and patients with chronic obstructive pulmonary disease, who have a higher risk of severe COVID-19 infection, also have lower levels of vitamin C in their blood [46].

It has been shown that vitamin B_9 and other vitamins of the B group normalize homocysteine concentrations in the blood and thus play a protective role in patients suffering from COVID-19 [48, 49]. Zinc plays an important role in the innate and adaptive immune system and the production of inflammatory mediators. Zinc also has an antioxidant effect, and studies have shown that it can prevent the multiplication of viruses [50, 51]; on the other hand, zinc deficiency is associated with a higher risk of complications from COVID-19, hospitalization, and a severe clinical outcome of the disease [52]. Zinc inhibits coronavirus and arterivirus RNA polymerase activity *in vitro*, and zinc ionophores block the replication of these viruses in cell culture [53]. Because of their greater susceptibility to infections due to micronutrient deficiency, these patients can be expected to suffer from more severe and long-lasting forms of the disease.

The role of omega-3 fatty acids is well known, and it includes reducing the risk of cardiovascular diseases and blood clots, maintaining the normal function of the blood vessel wall, lowering the level of triglycerides, and slowing down the production of inflammatory mediators. In recovery from COVID-19, omega-3 fatty acids help reduce excessive inflammation [54].

Nutrition intervention for post-COVID-19

The goal of nutritional therapy in post-COVID-19 patients should be to provide an adequate intake of energy, macro and micronutrients, focusing on correcting nutritional deficiencies, as well as enabling full physical and mental health recovery. Many COVID-19 symptoms and conditions, including post-COVID-19, can result in eating disorders and changes in nutritional status. These symptoms and conditions include the following: smell and taste impairment, loss of appetite, difficulty swallowing, nausea, diarrhea, vomiting, fatigue, and isolation during the infection that limits movement and physical activity, which often leads to anxiety and depression [4, 8, 9, 19, 54]. Research in Poland showed that, during the lockdown, about three-fourths of respondents consumed meat and vegetables once a day, and almost half avoided going shopping [55]. Some studies reported more frequent consumption of unhealthy foods [56]. There was a trend toward increased intake of canned food, flour-made food, and rice [22].

The Chinese authors suggest that the nutritional status of each infected patient should be assessed before starting general treatment [48]. The first step in nutritional management for COVID-19 patients is to identify those at risk of malnutrition, particularly those with comorbidity and older adults, who are thought to be at high risk of poor outcomes [57, 58]. According to the Academy of Nutrition and Dietetics, nutritional screening in long COVID patients includes nutritional history, anthropometric measurements, biochemical parameters, physical examination, and personal and family history. In addition to the basic anthropometric parameters of height, weight, and body mass index, it is necessary to obtain information about body composition (fat mass and fat-free mass) [1, 58]. Anamnestic data should include information on dysphagia, changes in taste and smell, fatigue, and muscle weakness [1]. In patients diagnosed with malnutrition, it is necessary to improve their nutritional status [58].

The European Society for Clinical Nutrition and Metabolism (ESPEN) guidelines provide recommendations for an energy intake of 27 kcal/kg/day for patients with polymorbidity over 65 years of age and 30 kcal/kg/day for severely malnourished patients with polymorbidity as well as for elderly patients, individually adapted, depending on their nutritional status, physical activity, and disease state [58–60]. Patients who are malnourished may be advised to eat several smaller meals during the day, not to drink liquids during meals, and, if necessary, to take low-volume nutritional supplements to increase energy intake [1, 58]. In obese patients with post-COVID-19, weight reduction is recommended to reduce the risk of obesity-related complications [1].

Recommendations for protein intake are 1 g/kg/day in the elderly, also adapted to nutritional status, physical activity, and disease status, and > 1 g/kg/day in polymorbid inpatients to improve recovery and prevent weight loss [58–60]. In post-COVID-19 patients, protein intake should be higher to prevent loss of muscle mass or improve symptoms of sarcopenia. High-quality protein from animal and plant sources is recommended to provide all the essential amino acids important for the anti-inflammatory response and immunomodulation [1, 61]. Nutritional therapy for restoring muscle mass and improving muscle strength is an important aspect of treatment for patients with post-COVID-19 syndrome. Data from a systematic review and meta-analysis indicate the possibility of using protein supplementation with resistance training in order to restore muscle mass and strength in post-COVID-19 elderly people who have sarcopenia. The use of the amino acid leucine in a balanced diet or as a supplement for muscle restoration in post-COVID-19 patients has shown effectiveness [61, 62].

Fat and carbohydrate intake are recommended according to energy intake in the ratio of 30 : 70 to 50 : 50 in ventilated patients [60]. Adequate intake of omega-3 fatty acids, eicosapentaenoic acid, and docosahexaenoic acid can interfere with viral replication and help reduce prostaglandin production as well. On the other hand, lipids (phospholipids, glycolipids, and sphingolipids) can block the activation of platelets, which can prevent thrombotic complications in patients with COVID-19 [61, 63].

The consumption of carbohydrates with a high glycemic index can lead to the synthesis of free radicals and an increase in the level of inflammatory cytokines, which is a characteristic of respiratory infections. Because of all of the above, giving priority to the intake of carbohydrates with a lower glycemic index is recommended [61, 64]. Fiber consumption has been shown to have numerous health benefits. A recommended fiber intake of 25–35 g/day helps reduce systemic and intestinal inflammation. Consuming fiber-rich foods lowers the levels of inflammatory mediators (CRP,

Table 1

Summary table of symptoms and conditions in post-COVID-19 related to nutrition and recommended nutritional intervention

Post-COVID-19 conditions closely related to nutrition	Nutritional interventions
Malnutrition	Adequate intake of energy and macro and micronutrients. Energy intake of 27 kcal/kg/day for patients with polymorbidity over 65 years of age; 30 kcal/kg/day for severely malnourished patients with polymorbidity and elderly patients, individually adapted, depending on their nutritional status, physical activity, and disease state. Protein intake of 1 g/kg/day in the elderly, adapted to nutritional status, physical activity, and disease status, and > 1 g/kg/day in polymorbid inpatients to improve recovery and prevent weight loss. Protein intake should be higher to prevent loss of muscle mass or improve symptoms of sarcopenia. Fat and carbohydrate intake are recommended according to energy intake in the ratio of 30 : 70. Intake of carbohydrates with a lower glycemic index. Fiber intake of 25–35 g/day.
Undernutrition	Advice to eat several smaller meals during the day, not to drink liquids during meals, and, if necessary, to take low-volume nutritional supplements to increase energy intake.
Obesity	Weight reduction is recommended.
Sarcopenia	Protein supplementation with resistance training in order to restore muscle mass and strength in post-COVID-19 elderly people who have sarcopenia. The use of the amino acid leucine in a balanced diet or as a supplement for muscle restoration in post-COVID-19 patients has shown effectiveness.
Fatigue syndrome	Taking antioxidants and essential fatty acids as supplements or in a balanced diet.
Inflammation, impaired immune response	Mediterranean diet: rich in fiber, bioactive compounds such as omega-3 fatty acids, antioxidants, whole grains, fruits, vegetables, virgin olive oil, high-quality proteins from eggs, dairy products, and fish; low in meat, saturated fatty acids, and refined carbohydrates. Plant-based dietary patterns.
Gut microbiota impairment/imbalance of gut microbiota	Intake of probiotics. Probiotics, especially some species of *Lactobacillus* and *Bifidobacteria*, have the potential to modify the microbiota and the immune response, contributing to the protection and improved outcomes of airway viral infection.
Micronutrient deficiency	Supplements of vitamins and minerals are recommended for those with micronutrient deficiency who cannot get enough micronutrients from food. Adequate intake of vitamins D, A, B6, B12, and C, and minerals zinc, selenium, and iron must be provided for better clinical outcomes of infection.

TNF-α, and IL-6) while increasing the levels of short-chain fatty acids [54, 61].

Special attention should be paid to adequate intake of vitamins D, A, B_6, B_{12}, and C and minerals zinc, selenium, and iron, as well as omega-3 fatty acids [48, 58] for better clinical outcomes in viral infection, including COVID-19. Antioxidants and essential fatty acids as supplements or in a balanced diet can help mitigate chronic fatigue syndrome in post-COVID-19 cases. Supplements are recommended for malnourished patients or those with nutritional deficits who cannot get enough macro and micronutrients from food [1].

Positive changes in the intestinal microflora can be supported by the intake of polyphenols and probiotics [1, 65]. Although probiotics are mostly mentioned because of their

beneficial effect on immunity during viral intestinal infections, they also play an important role in the immune response when it comes to upper and lower respiratory tract infections and sepsis. In patients suffering from COVID-19, probiotics help restore the altered intestinal flora. By having a favorable effect on the body's immune response, they also help protect against severe complications of COVID-19, such as acute respiratory distress syndrome and multiorgan dysfunction syndrome. Studies have shown the clinical benefits of using *Lactobacillus* and *Bifidobacterium* in patients on mechanical ventilation in intensive care, showing a lower incidence of upper respiratory tract infections and respiratory-related pneumonia [66].

Adequate hydration should be met in patients with COVID-19 as well as those with post-COVID-19 syndrome. The Dietary Reference Intake for water of 2.7 L/day in adult women and 3.7 L/day in men, respectively [67], may be increased, depending on the patient's condition. It is necessary to keep track of the patient's hydration level.

There is increasing evidence suggesting that diet can affect inflammation and the immune system. Studies conducted in different populations [68–70] have shown a link between the Mediterranean diet and a lower risk of COVID-19 as well as better outcomes in patients with COVID-19. Mediterranean diet (rich in fiber, bioactive compounds such as omega-3 fatty acids, antioxidants, whole grains, fruits, vegetables, virgin olive oil, high-quality proteins from eggs, dairy products, and fish, and low in meat, saturated fatty acids, and refined carbohydrates) can be recommended for patients with COVID-19, including those with post-COVID-19 syndrome [1, 71].

Considering that psychological well-being is often impaired in post-COVID-19, including the appearance of anxiety, depression, and impaired cognitive functions, a diet rich in fruits and vegetables has its advantages. Specifically, studies have shown that an increased intake of fruits and vegetables in the diet reduces the risk of depression [72, 73]. A case-control population-based study that investigated the relationship between COVID-19 and diet determined a 73% lower risk for a moderate to severe form of the disease in subjects with a plant-based diet compared to those with other diet patterns [74]. It should be kept in mind that the study was conducted on a small sample, and the dietary survey was based on self-reporting. Studies conducted before the COVID-19 pandemic have shown that a plant-based diet can be beneficial for some conditions that can occur in COVID-19 patients, including fatigue, muscle pain, depression, and headaches [75–76]. Plant-based dietary patterns reduce inflammatory biomarkers and positively affect immune status [77]. Table 1 shows the summary of symptoms and conditions in post-COVID-19 related to nutrition and recommended nutritional intervention.

Conclusion

Nutritional recommendations for patients during recovery from COVID-19 will depend on the patient's condition, disease-related symptoms, and comorbidities and require an individual approach. In this sense, it is necessary to increase awareness of the importance of nutrition and make access to healthy food one of the priorities, especially for members of sensitive groups, such as the elderly, people with comorbidities, etc., in order to reduce the prolonged effects of COVID-19. Information on dietary recommendations for post-COVID-19 patients available in the literature is often obtained from studies related to the treatment of conditions similar to the post-COVID-19 syndrome.

REFERENCES

1. *Barrea L, Grant WB, Frias-Toral E, Vetrani C, Verde L, de Alteriis G*, et al. Dietary Recommendations for Post-COVID-19 Syndrome. Nutrients 2022; 14(6): 1305.
2. *Mentella MC, Scaldaferri F, Gasbarrini A, Miggiano GAD*. The Role of Nutrition in the COVID-19 Pandemic. Nutrients 2021; 13(4): 1093.
3. *Soriano JB, Murthy S, Marshall JC, Relan P, Diaz JV; WHO Clinical Case Definition Working Group on Post-COVID-19 Condition*. A clinical case definition of post-COVID-19 condition by a Delphi consensus. Lancet Infect Dis 2022; 22(4): e102–7.
4. *Michelen M, Manoharan L, Elkheir N, Cheng V, Dagens A, Hastie C,* et al. Characterising long COVID: a living systematic review. BMJ Glob Health 2021; 6(9): e005427.
5. *Carfì A, Bernabei R, Landi F; Gemelli Against COVID-19 Post-Acute Care Study Group*. Persistent Symptoms in Patients After Acute COVID-19. JAMA 2020; 324(6): 603–5.
6. *Tenforde MW, Kim SS, Lindsell CJ, Billig Rose E, Shapiro NI, Files DC,* et al. Symptom Duration and Risk Factors for Delayed Return to Usual Health Among Outpatients with COVID-19 in a Multistate Health Care Systems Network — United States, March – June 2020. MMWR Morb Mortal Wkly Rep 2020; 69(30): 993–8.
7. *Lopez-Leon S, Wegman-Ostrosky T, Perelman C, Sepulveda R, Rebolledo PA, Cuapio A*, et al. More than 50 long-term effects of COVID-19 : a systematic review and meta-analysis. Sci Rep 2021; 11(1): Article No. 16144.
8. *Messina G, Polito R, Monda V, Cipolloni L, Di Nunno N, Di Mizio G*, et al. Functional Role of Dietary Intervention to Improve the Outcome of COVID-19: A Hypothesis of Work. Int J Mol Sci 2020; 21(9): 3104.
9. *Childs CE, Calder PC, Miles EA*. Diet and Immune Function. Nutrients 2019; 11(8): 1933.
10. *Rouget A, Vardon-Bounes F, Lorber P, Vavasseur A, Marion O, Marcheix B,* et al. Prevalence of malnutrition in coronavirus disease 19: the NUTRICOV study. Br J Nutr 2021; 126(9): 1296–303.
11. *Pironi L, Sasdelli AS, Ravaioli F, Baracco B, Battaiola C, Bocedi G*, et al. Malnutrition and nutritional therapy in patients with SARS-CoV-2 disease. Clin Nutr 2021; 40(3): 1330–7.
12. *Li T, Zhang Y, Gong C, Wang J, Liu B, Shi L,* et al. Prevalence of malnutrition and analysis of related factors in elderly patients with COVID-19 in Wuhan, China. Eur J Clin Nutr 2020; 74(6): 871–5.
13. *Vellas B, Guigoz Y, Garry PJ, Nourhashemi F, Bennahum D, Lauque S,* et al. The Mini Nutritional Assessment (MNA) and its use in grading the nutritional state of elderly patients. Nutrition 1999; 15(2): 116–22.

14. *Bold J, Harris M, Fellows L, Chouchane M.* Nutrition, the digestive system and immunity in COVID-19 infection. Gastroenterol Hepatol Bed Bench 2020; 13(4): 331–40.
15. *Naja F, Hamadeh R.* Nutrition amid the COVID-19 pandemic: a multi-level framework for action. Eur J Clin Nutr 2020; 74(8): 1117–21.
16. *Galmés S, Serra F, Palou A.* Current State of Evidence: Influence of Nutritional and Nutrigenetic Factors on Immunity in the COVID-19 Pandemic framework. Nutrients 2020; 12(9): 2738.
17. *Tsagari A, Risvas G, Papathanasiou JV, Dionyssiotis Y.* Nutritional management of individuals with SARS-CoV-2 infection during rehabilitation. J Frailty Sarcopenia Falls 2022; 7(2): 88–94.
18. *Steinberg E, Wright E, Kushner B.* In Young Adults with COVID-19, Obesity Is Associated with Adverse Outcomes. West J Emerg Med 2020; 21(4): 752–5.
19. *Simonnet A, Chetboun M, Poissy J, Raverdy V, Noulette J, Duhamel A,* et al. High Prevalence of Obesity in Severe Acute Respiratory Syndrome Coronavirus-2 (SARS-CoV-2) Requiring Invasive Mechanical Ventilation. Obesity (Silver Spring) 2020; 28(7): 1195–9. Erratum in: Obesity (Silver Spring) 2020; 28(10): 1994.
20. *Louie JK, Acosta M, Samuel MC, Schechter R, Vugia DJ, Harriman K,* et al. A novel risk factor for a novel virus: obesity and 2009 pandemic influenza A (H1N1). Clin Infect Dis 2011; 52(3): 301–12.
21. *Moriconi D, Masi S, Rebelos E, Virdis A, Manca ML, De Marco S,* et al. Obesity prolongs the hospital stay in patients affected by COVID-19, and may impact on SARS-COV-2 shedding. Obes Res Clin Pract 2020; 14(3): 205–9.
22. *Piotrowicz K, Gąsowski J, Michel JP, Veronese N.* Post-COVID-19 acute sarcopenia: physiopathology and management. Aging Clin Exp Res 2021; 33(10): 2887–98.
23. *Schakman O, Kalista S, Barbé C, Loumaye A, Thissen JP.* Glucocorticoid-induced skeletal muscle atrophy. Int J Biochem Cell Biol 2013; 45(10): 2163–72.
24. *Wierdsma NJ, Kruizenga HM, Konings LA, Krebbers D, Jorissen JR, Joosten MI,* et al. Poor nutritional status, risk of sarcopenia and nutrition related complaints are prevalent in COVID-19 patients during and after hospital admission. Clin Nutr ESPEN 2021; 43: 369–76.
25. *Soares MN, Eggelbusch M, Naddaf E, Gerrits KHL, van der Schaaf M, van den Borst B,* et al. Skeletal muscle alterations in patients with acute Covid-19 and post-acute sequelae of Covid-19. J Cachexia Sarcopenia Muscle 2022; 13(1): 11–22.
26. *Beaudart C, Sanchez-Rodriguez D, Locquet M, Reginster JY, Lengelé L, Bruyére O.* Malnutrition as a Strong Predictor of the Onset of Sarcopenia. Nutrients 2019; 11(12): 2883.
27. *Halpin SJ, McIvor C, Whyatt G, Adams A, Harvey O, McLean L,* et al. Postdischarge symptoms and rehabilitation needs in survivors of COVID-19 infection: A cross-sectional evaluation. J Med Virol 2021; 93(2): 1013–22.
28. *Townsend L, Dyer AH, Jones K, Dunne J, Mooney A, Gaffney F,* et al. Persistent fatigue following SARS-CoV-2 infection is common and independent of severity of initial infection. PLoS One 2020; 15(11): e0240784.
29. *Bennett BK, Goldstein D, Chen M, Davenport TA, Vollmer-Conna U, Scott EM,* et al. Characterization of fatigue states in medicine and psychiatry by structured interview. Psychosom Med 2014; 76(5): 379–88.
30. *Sandler CX, Wyller VBB, Moss-Morris R, Buchwald D, Crawley E, Hautvast J,* et al. Long COVID and Post-infective Fatigue Syndrome: A Review. Open Forum Infect Dis 2021; 8(10): ofab440.
31. *Fukuda K, Straus SE, Hickie I, Sharpe MC, Dobbins JG, Komaroff A.* The chronic fatigue syndrome: a comprehensive approach to its definition and study. International Chronic Fatigue Syndrome Study Group. Ann Intern Med 1994; 121(12): 953–9.
32. *Bäckhed F, Ley RE, Sonnenburg JL, Peterson DA, Gordon JI.* Host-bacterial mutualism in the human intestine. Science 2005; 307(5717): 1915–20.
33. *Hawryłkowicz V, Lietz-Kijak D, Kaźmierczak-Siedlecka K, Sołek-Pastuszka J, Stachowska L, Folwarski M,* et al. Patient Nutrition and Probiotic Therapy in COVID-19: What Do We Know in 2021? Nutrients 2021; 13(10): 3385.
34. *Calder PC.* Nutrition and immunity: lessons for COVID-19. Eur J Clin Nutr 2021; 75(9): 1309–18.
35. *Bermudez-Brito M, Plaza-Díaz J, Muñoz-Quezada S, Gómez-Llorente C, Gil A.* Probiotic mechanisms of action. Ann Nutr Metab 2012; 61(2): 160–74.
36. *Vinolo MA, Rodrigues HG, Nachbar RT, Curi R.* Regulation of inflammation by short chain fatty acids. Nutrients 2011; 3(10): 858–76.
37. *Clarke TB.* Early innate immunity to bacterial infection in the lung is regulated systemically by the commensal microbiota via NOD-like receptor ligands. Infect Immun 2014; 82(11): 4596–606.
38. *Zhang N, He QS.* Commensal microbiome promotes resistance to local and systemic infections. Chin Med J (Engl) 2015; 128(16): 2250–5.
39. *Dhar D, Mohanty A.* Gut microbiota and Covid-19- possible link and implications. Virus Res 2020; 285: 198018.
40. *Lei WT, Shih PC, Liu SJ, Lin CY, Yeh TL.* Effect of Probiotics and Prebiotics on Immune Response to Influenza Vaccination in Adults: A Systematic Review and Meta-Analysis of Randomized Controlled Trials. Nutrients 2017; 9(11): 1175.
41. *Voelkle M, Gregoriano C, Neyer P, Koch D, Kutz A, Bernasconi L,* et al. Prevalence of Micronutrient Deficiencies in Patients Hospitalized with COVID-19: An Observational Cohort Study. Nutrients 2022; 14(9): 1862.
42. *Gombart AF.* The vitamin D-antimicrobial peptide pathway and its role in protection against infection. Futur Microbiol 2009; 4(9): 1151–65.
43. *Lin Z, Li W.* The Roles of Vitamin D and Its Analogs in Inflammatory Diseases. Curr Top Med Chem 2016; 16(11): 1242–61.
44. *Gönen MS, Alaylıoğlu M, Durcan E, Özdemir Y, Şahin S, Konukoğlu D,* et al. Rapid and Effective Vitamin D Supplementation May Present Better Clinical Outcomes in COVID-19 (SARS-CoV-2) Patients by Altering Serum INOS1, IL1B, IFNg, Cathelici-din-LL37, and ICAM1. Nutrients 2021; 13(11): 4047.
45. *Cawood AL, Walters ER, Smith TR, Sipaul RH, Stratton RJ.* A Review of Nutrition Support Guidelines for Individuals with or Recovering from COVID-19 in the Community. Nutrients 2020; 12(11): 3230.
46. *Holford P, Carr AC, Jovic TH, Ali SR, Whitaker IS, Marik PE,* et al. Vitamin C-An Adjunctive Therapy for Respiratory Infection, Sepsis and COVID-19. Nutrients 2020; 12(12): 3760.
47. *Schönrich G, Raftery MJ, Samstag Y.* Devilishly radical NETwork in COVID-19: Oxidative stress, neutrophil extracellular traps (NETs), and T cell suppression. Adv Biol Regul 2020; 77: 100741.
48. *Zhang L, Liu Y.* Potential interventions for novel coronavirus in China: A systematic review. J Med Virol 2020; 92(5): 479–90.
49. *Shakoor H, Feehan J, Mikkelsen K, Al Dhaheri AS, Ali HI, Platat C,* et al. Be well: A potential role for vitamin B in COVID-19. Maturitas 2021; 144: 108–11.
50. *Chasapis CT, Loutsidou AC, Spiliopoulou CA, Stefanidou ME.* Zinc and human health: an update. Arch Toxicol 2012; 86(4): 521–34.
51. *Read SA, Obeid S, Ahlenstiel C, Ahlenstiel G.* The Role of Zinc in Antiviral Immunity. Adv Nutr 2019; 10(4): 696–710.

52. *Jothimani D, Kailasam E, Danielraj S, Nallathambi B, Ramachandran H, Sekar P,* et al. COVID-19: Poor outcomes in patients with zinc deficiency. Int J Infect Dis 2020; 100: 343–9.
53. *te Velthuis AJ, van den Worm SH, Sims AC, Baric RS, Snijder EJ, van Hemert MJ*. Zn (2+) inhibits coronavirus and arterivirus RNA polymerase activity in vitro and zinc ionophores block the replication of these viruses in cell culture. PLoS Pathog 2010; 6(11): e1001176.
54. *Iddir M, Brito A, Dingeo G, Fernandez Del Campo SS, Samouda H, La Frano MR,* et al. Strengthening the Immune System and Reducing Inflammation and Oxidative Stress through Diet and Nutrition: Considerations during the COVID-19 Crisis. Nutrients 2020; 12(6): 1562.
55. *Sidor A, Rzymski P*. Dietary Choices and Habits during COVID-19 Lockdown: Experience from Poland. Nutrients 2020; 12(6): 1657.
56. *Ammar A, Brach M, Trabelsi K, Chtourou H, Boukhris O, Masmoudi L,* et al. Effects of COVID-19 Home Confinement on Eating Behaviour and Physical Activity: Results of the ECLB-COVID19 International Online Survey. Nutrients 2020; 12(6): 1583.
57. *Handu D, Moloney L, Rozga M, Cheng FW*. Malnutrition Care During the COVID-19 Pandemic: Considerations for Registered Dietitian Nutritionists. J Acad Nutr Diet 2021; 121(5): 979–87.
58. *Barazzoni R, Bischoff SC, Breda J, Wickramasinghe K, Krznaric Z, Nitzan D,* et al. ESPEN expert statements and practical guidance for nutritional management of individuals with SARS-CoV-2 infection. Clin Nutr 2020; 39(6): 1631–8.
59. *Gomes F, Schuetz P, Bounoure L, Austin P, Ballesteros-Pomar M, Cederholm T,* et al. ESPEN guidelines on nutritional support for polymorbid internal medicine patients. Clin Nutr 2018; 37(1): 336–53.
60. *Volkert D, Beck AM, Cederholm T, Cruz-Jentoft A, Goisser S, Hooper L*, et al. ESPEN guideline on clinical nutrition and hydration in geriatrics. Clin Nutr 2019; 38(1): 10–47.
61. *Fernández-Quintela A, Milton-Laskibar I, Trepiana J, Gómez-Zorita S, Kajarabille N, Léniz A,* et al. Key Aspects in Nutritional Management of COVID-19 Patients. J Clin Med 2020; 9(8): 2589.
62. *Gielen E, Beckwée D, Delaere A, De Breucker S, Vandewoude M, Bautmans I,* et al. Nutritional interventions to improve muscle mass, muscle strength, and physical performance in older people: an umbrella review of systematic reviews and meta-analyses. Nutr Rev 2020; 79(2): 121–47.
63. *Zabetakis I, Lordan R, Norton C, Tsoupras A*. COVID-19 : The Inflammation Link and the Role of Nutrition in Potential Mitigation. Nutrients 2020; 12(5): 1466.
64. *Monnier L, Mas E, Ginet C, Michel F, Villon L, Cristol JP*, et al. Activation of oxidative stress by acute glucose fluctuations compared in patients with type 2 diabetes. JAMA 2006; 295(14): 1681–7.
65. *Singh RK, Chang HW, Yan D, Lee KM, Ucmak D, Wong K,* et al. Influence of diet on the gut microbiome and implications for human health. J Transl Med 2017; 15(1): 73.
66. *Barrea L, Muscogiuri G, Frias-Toral E, Laudisio D, Pugliese G, Castellucci B,* et al. Nutrition and immune system: from the Mediterranean diet to dietary supplementary through the microbiota. Crit Rev Food Sci Nutr 2021; 61(18): 3066–90.
67. *Institute of Medicine*. Dietary Reference Intakes for Water, Potassium, Sodium, Chloride, and Sulfate. Washington, DC: The National Academies Press; 2005. 638 p.
68. *El Khoury CN, Julien SG*. Inverse Association Between the Mediterranean Diet and COVID-19 Risk in Lebanon: A Case-Control Study. Front Nutr 2021; 8: 707359.
69. *Greene MW, Roberts AP, Frugé AD*. Negative Association Between Mediterranean Diet Adherence and COVID-19 Cases and Related Deaths in Spain and 23 OECD Countries: An Ecological Study. Front Nutr 2021; 8: 591964.
70. *Ponzo V, Pellegrini M, D'Eusebio C, Bioletto F, Goitre I, Buscemi S*, et al. Mediterranean Diet and SARS-COV-2 Infection: Is There Any Association? A Proof-of-Concept Study. Nutrients 2021; 13(5): 1721.
71. *Suardi C, Cazzaniga E, Graci S, Dongo D, Palestini P*. Link between Viral Infections, Immune System, Inflammation and Diet. Int J Environ Res Public Health 2021; 18(5): 2455.
72. *Shanbehzadeh S, Tavahomi M, Zanjari N, Ebrahimi-Takamjani I, Amiri-Arimi S*. Physical and mental health complications post-COVID-19: Scoping review. J Psychosom Res 2021; 147: 110525.
73. *Lassale C, Batty GD, Baghdadli A, Jacka F, Sánchez-Villegas A, Kivimäki M*, et al. Healthy dietary indices and risk of depressive outcomes: a systematic review and meta-analysis of observational studies. Mol Psychiatry 2019; 24(7): 965–86. Erratum in: Mol Psychiatry 2021; 26(7): 3657.
74. *Kim H, Rebholz CM, Hegde S, LaFiura C, Raghavan M, Lloyd JF*, et al. Plant-based diets, pescatarian diets and COVID-19 severity: a population-based case–control study in six countries. BMJ Nutr Prev Health 2021; 4(1): 257–66.
75. *Towery P, Guffey JS, Doerflein C, Stroup K, Saucedo S, Taylor J*. Chronic musculoskeletal pain and function improve with a plant-based diet. Complement Ther Med 2018; 40: 64–9.
76. *Shen YC, Chang CE, Lin MN, Lin CL*. Vegetarian Diet Is Associated with Lower Risk of Depression in Taiwan. Nutrients 2021; 13(4): 1059.
77. *Craddock JC, Neale EP, Peoples GE, Probst YC*. Vegetarian-Based Dietary Patterns and their Relation with Inflammatory and Immune Biomarkers: A Systematic Review and Meta-Analysis. Adv Nutr 2019; 10(3): 433–51.

Received on May 12, 2023
Accepted on July 20, 2023
Online First August 2023

ORIGINAL ARTICLES

UDC: 616.832-004:616-073.763.5-06
DOI: https://doi.org/10.2298/VSP220314018K

Gadolinium deposition in the brain of patients with relapsing-remitting multiple sclerosis after 10 years of follow-up

Taloženje gadolinijuma u mozgu bolesnika sa relapsno-remitentnom multiplom sklerozom nakon 10 godina praćenja

[1]Dejan Kostić*[†], [1]Miroslav Mišović*[†], Filip Vučković[†], Djuro Crevar[†], Igor Sekulić*[†], Biljana Georgievski-Brkić[‡], Smiljana Kostić[†§], Evica Dinčić[†§]

Military Medical Academy, *Institute of Radiology, [§]Clinic of Neurology, Belgrade, Serbia; [†]University of Defence, Faculty of Medicine of the Military Medical Academy, Belgrade, Serbia; [‡]Special Hospital for Cerebrovascular Diseases "Sveti Sava", Department of Radiology Diagnostics, Belgrade, Serbia

[1]Contributed equally

Abstract

Background/Aim. Since 2014 and the publication of the results of the first study on the accumulation of gadolinium contrast, we have witnessed a growing body of evidence on the deposition and retention of gadolinium in the brain after the use of gadolinium-based contrast agents (GBCAs). However, there is still no strong clinical evidence of the adverse effects of GBCAs on the brain parenchyma. The aim of the study was to determine the existence of gadolinium deposits in the brain of patients with relapsing-remitting multiple sclerosis after a ten-year follow-up period. During this period, the patients have regularly, each year, undergone magnetic resonance imaging (MRI) with the administration of gadolinium contrast (gadopentetate dimeglumine – Magnevist®) in order to follow the course of the disease. **Methods.** A cohort of 20 patients was formed for the purpose of this study. The ratio of the values of the signal intensity (SI) of different regions of the brain-to-cerebrospinal fluid (CSF) was compared for each patient on the initial MRI examination and the MRI examination ten years later. **Results.** Frontal cortex-to-CSF ($p < 0.01$), occipital cortex-to-CSF ($p < 0.01$), the white matter of the *corona radiata*-to-CSF ($p < 0.01$), parietal cortex-to-CSF ($p < 0.05$), thalamus-to-CSF ($p = 0.051$), putamen-to-CSF ($p = 0.06$), and anterior and posterior limb of the *capsula interna*-to-CSF ($p = 0.062$) SI ratios increased after multiple gadopentetate administrations. An increase in the absolute values of the T1-weighted (T1W) signal in three-quarters of patients was registered in the frontal and occipital cortex and cerebellar hemispheres. A slightly smaller increase in SI, but still greater than 55–65%, was registered in structures of the parietal cortex, putamen, *cornu* anterior and posterior of the *capsula interna*, *corpus callosum* (CC) *splenium*, *pons*, thalamus, *nucleus caudatus*, *substantia nigra*, CC *genu*, and temporal cortex. **Conclusion.** In the cohort of 20 patients, there was a statistically significant increase in SI in the pre-contrast T1W sequence in the following structures: frontal, parietal, and occipital cortex, as well as supratentorial white matter. This result speaks in favor of the existence of chronic accumulation of gadolinium contrast agent gadopentetate dimeglumine in brain structures.

Key words:
gadolinium dtpa; long term adverse effects; magnetic resonance imaging; multiple sclerosis, relapsing-remitting.

Apstrakt

Uvod/Cilj. Od 2014. godine kao i od objavljivanja rezultata prve studije o akumulaciji kontrastnih sredstava na bazi gadolinijuma (*gadolinium-based contrast agents* – GBCAs), svedoci smo sve većeg broja dokaza o taloženju i zadržavanju gadolinijuma u mozgu nakon primene ovih sredstava. Međutim, još uvek nema jakih kliničkih dokaza o štetnim efektima GBCAs na moždani parenhim. Cilj rada bio je da se utvrdi postojanje naslaga gadolinijuma u mozgu kod bolesnika sa relapsno-remitentnom multiplom sklerozom nakon desetogodišnjeg perioda praćenja. Tokom ovog perioda, bolesnici su redovno, svake godine, bili podvrgnuti pregledu magnetnom rezonancom (MR) koji je uključivao davanje linearnog kontrastnog sredstva (gadopentetat dimeglumin – Magnevist®) kako bi se pratio tok bolesti. **Metode.** Za potrebe ove studije formirana je kohorta od 20 bolesnika. Za svakog bolesnika je upoređivan

Correspondence to: Dejan Kostić, Military Medical Academy, Institute of Radiology, Crnotravska 17, 11 000 Belgrade, Serbia.
E-mail: drdkostic@gmail.com

odnos vrednosti intenziteta signala (IS) u različitim regionima mozga i IS cerebrospinalnog likvora (CSL) na inicijalnom pregledu primenom MR i na pregledu deset godina kasnije primenom iste metode. **Rezultati.** Odnosi IS frontalnog korteksa i CSL-a ($p < 0,01$), okcipitalnog korteksa i CSL-a ($p < 0,01$), bele mase *corona radiata* i CSL-a ($p < 0,01$), parijetalnog korteksa i CSL-a ($p < 0,05$), talamusa i CSL-a ($p = 0,051$), putamena i CSL-a ($p = 0,06$) i *cornu anterior* i *posterior capsula interna* i CSL-a ($p = 0,062$) povećali su se nakon višestruke primene gadopentetata. Porast apsolutnih vrednosti *T1-weighted* (T1W) signala kod tri četvrtine bolesnika registrovan je u frontalnom i okcipitalnom korteksu i hemisferi malog mozga. Nešto manje povećanje IS, ali ipak veće od 55–65%, registrovano je u strukturama kao što su: parijetalni korteks, putamen, *cornu anterior* i *posterior capsula interna*, *corpus callosum* (CC) *splenium*, *pons*, talamus, *nucleus caudatus*, *substantia nigra*, CC *genu* i temporalni korteks. **Zaključak.** U kohorti od 20 bolesnika pokazano je statistički značajno povećanje IS u prekontrastnoj T1W sekvenci u sledećim strukturama: frontalnom, parijetalnom i okcipitalnom korteksu, kao i beloj masi *corona radiata*. Rezultati govore u prilog tome da postoji hronično deponovanje gadolinijumskog kontrastnog sredstva, gadopentetat dimeglumina, u moždanim strukturama.

Ključne reči:
gadolinijum dtpa; neželjeni efekti, dugoročni; magnetska rezonanca, snimanje; multipla skleroza, relapsno-remitentna.

Introduction

Since 1988, after being approved by the Food and Drug Administration (FDA), gadolinium-based contrast agents (GBCAs) have been widely used in magnetic resonance imaging (MRI) [1]. Today they are used in about 30% of MRI diagnostics [2].

They have long been considered safe to use, and in 2006, cases of potentially lethal nephrogenic systemic fibrosis (NSF) caused by the use of GBCAs were described in patients with renal insufficiency [3, 4].

After the initial report in 2014, gadolinium depositions in the brain have mainly been found in the *nucleus dentatus* (ND) and *globus pallidus* (GP), mostly associated with linear GBCAs [5, 6]. Many studies have indicated the occurrence of gadolinium uptake in the grey matter, thalamus, *pons*, and white matter [6, 7]. Since 2014, studies on gadolinium depositions in the brain have focused on detection, distribution, potential toxicity, and clinical consequences [8].

In addition to deposition in these regions, deposition in other regions of the brain but of lower intensity has also been proven. Furthermore, several studies have found that GBCAs can be deposited in other organs, including the skin, bones, and liver, despite normal renal function [9–11]. This study aimed to determine the existence of contrast deposition in different areas of the brain in patients with relapsing-remitting (RR) multiple sclerosis (MS).

Methods

Subject population

The study was conducted as a retrospective study of a series of observational cases. It included 20 patients with RR MS treated with a unique immunomodulatory protocol (interferon beta 1b) for ten years after the diagnosis of MS at the Clinic of Neurology of the Military Medical Academy (MMA), Belgrade, Serbia. The study protocol followed the Declaration of Helsinki and was approved by the Ethics Committee of the MMA on January 21, 2016. Informed consent was obtained from each patient.

Inclusion criteria were: both genders aged 24 to 51 years with RR MS (according to the revised McDonald criteria); neurologically determined functional disability (Extended Disability Status Scale – EDSS ≤ 6); clinically and/or radiologically active MS in the previous year (the review was performed for reasons other than MS). All patients signed informed consent.

Exclusion criteria were: other central nervous system diseases; head trauma; renal or hepatic insufficiency; psychiatric diseases; malignancy; use of psychoactive substances; pregnancy.

In 20 patients, 8 (40%) men and 12 (60%) women, with an average age of 38.9 ± 6.6 years and a mean disease duration of 5.8 ± 7.0 years, after neurological examination, at the Institute of Radiology of the MMA, Belgrade, Serbia, a standard MRI of the brain was performed with one initial and at least one follow-up examination *per* year over a 10-year follow-up period, which included the administration of a linear contrast agent (gadopentetate dimeglumine – Magnevist®), in the amount of 0.2 mL/kg of body weight (Table 1).

Table 1

Demographic characteristics of the patients

Parameter	Male	Female
Gender, n (%)	8 (40)	12 (60)
Age, mean ± SD	33.2 ± 6.6	37.8 ± 6.3
Phenotype	RR MS	RR MS

RR MS – relapsing-remitting multiple sclerosis; SD – standard deviation.

Image acquisition

The brain MRI examinations were performed with a 3T magnet (General Electric, Signa HDxt 3T, Milwaukee, WI, USA) with a standard 8HR head-coil. The MRI protocol included the following sequences: (1) T1-weighted (T1W) images with a repetition time (TR) of 30 ms and an echo time (TE) of 6 ms, a field of view of 250 mm, and a flip angle of 27°; (2) T2-weighted (T2W) Fluid-Attenuated Inversion Recovery (FLAIR) images with a TR of 9,000 ms and a TE of

83 ms, the field of view of 250 mm, and flip angle of 90°; (3) T2W images with a TR of 5,300 ms and a TE of 85 ms, field of view of 250 mm, and flip angle of 90°. Three-millimeter-thick contiguous slices were obtained. MRI scan was performed before and after the injection of linear gadolinium contrast agent (gadopentetate dimeglumine – Magnevist®) at 0.2 mL/kg of body weight.

Image analysis

Pre-contrast T1W MRI from the initial scan, and a scan ten years later, after follow-up, were used for analysis.

Analysis of pre-contrast T1W images was first utilized to define regions of interest (ROIs). ROIs included 16 anatomical regions of the brain: cortex of the frontal, temporal, parietal, and occipital lobes, *nucleus caudatus* (NC), *putamen*, thalamus, anterior and posterior horn of the internal capsule, *genu* and *splenium* of the *corpus callosum* (CC), *substantia nigra* (SN), *pons*, white matter of *centrum semiovale* (CSO), the white matter of *corona radiata* (CR), and cerebellar hemisphere (Figure 1).

The selection of voxels representative of cerebrospinal fluid (CSF) signal intensity (SI) consisted of starting inferiorly and moving superiorly on axial slices until the initial appearance of both anterior horns of the lateral ventricles and was used to determine the "CSF intensity" for CSF for that scan (Figure 2).

Two radiologists, with ten and nine years of experience in MS neuroimaging, respectively, conducted the quantitative analysis using a software package Carestream Vue PACS v 11.04.0 (Carestream Health, Inc., Rochester, NY). They were both blinded to the data. Both of them used the T1W images with previously defined ROIs and CSF to measure SI value. The SI value within any particular area was divided by the mean SI within the CSF to calculate the area-to-CSF SI ratio (Figures 1 and 2). In the event of disagreement in evaluating data, the radiologists reached a final consensus together.

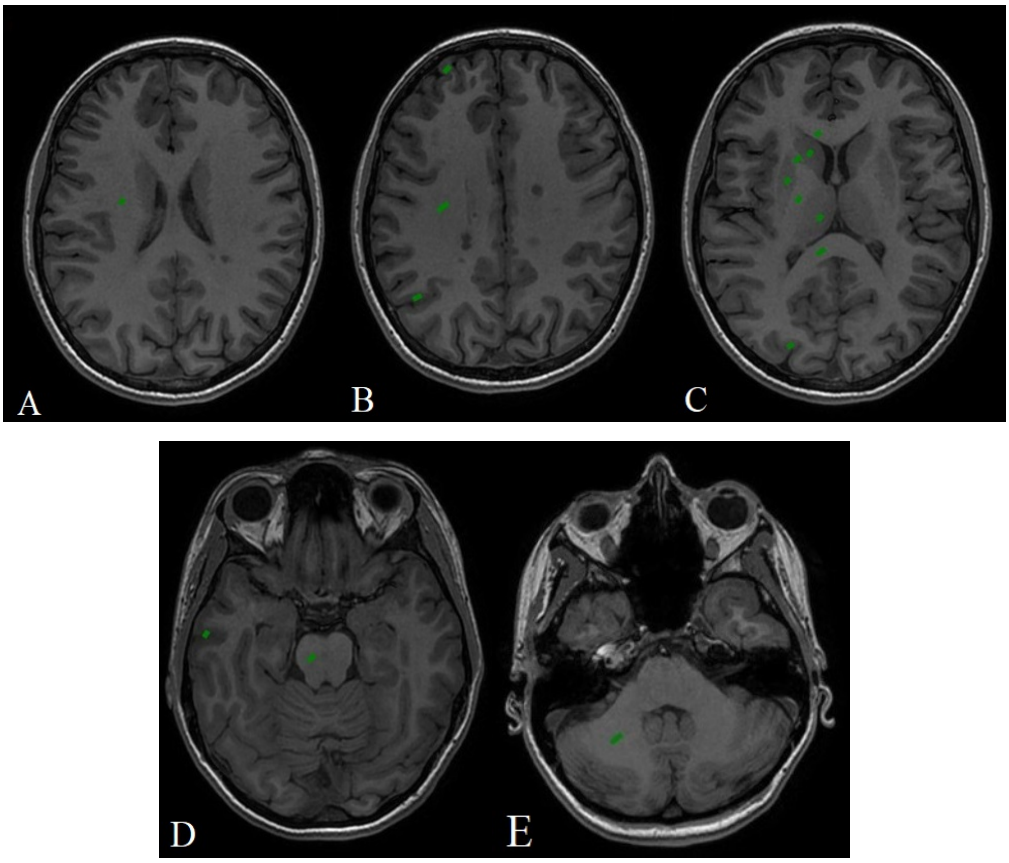

Fig. 1– Pre-contrast T1-weighted magnetic resonance images in a 50-year-old man with multiple sclerosis at the initial scan. Standard regions of interest were set in 16 different anatomical regions of the brain: the white matter of *corona radiata* (A), cortex of the frontal and the parietal lobes, white matter of *centrum semiovale* (B), cortex of the occipital lobes, *nucleus caudatus*, putamen, thalamus, anterior and posterior horn of the *capsula interna*, *genu* and *splenium* of the *corpus callosum* (C), cortex of the temporal lobes, *substantia nigra*, *pons* (D), and cerebellar hemisphere (E).

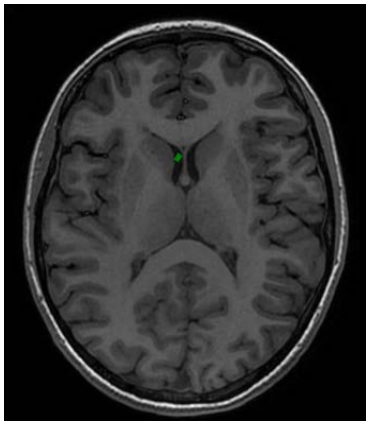

Fig. 2 – The signal intensity (SI) value in any given area is divided by the SI value of cerebrospinal fluid (CSF) within the anterior horns of the lateral ventricle to calculate the SI area-to-CSF ratio.

Statistical analysis

Statistical analysis was performed using the statistical software package PASW Statistics 18® [SPSS (Hong Kong) Ltd., Hong Kong]. All variables were presented as frequencies of certain categories. Continuous variables were presented as mean ± standard deviation and compared using paired *t*-tests.

Results

In the initial pre-contrast T1 images, the white matter of the CSO (1.744 ± 0.089), CC *genu* (1.734 ± 0.124), the anterior limb (1.765 ± 0.102), and posterior limb (1.723 ± 0.141) of the *capsula interna* (CI) had the highest values of the area-to-CSF SI ratio, and the lowest values of the area-to-CSF SI ratio were in SN, parietal cortex, temporal cortex, *pons*, and white matter of CR. After ten years, the anterior and posterior limb of the CI, CC *genu*, frontal cortex, and white matter of the CSO had the highest value of area-to-CSF SI ratio, while SN (1.399 ± 0.159), parietal cortex (1.496 ± 0.107), *pons* (1.505 ± 0.156), and temporal cortex (1.512 ± 0.141) had the lowest values. Comparing the value area-to-CSF SI ratio relationship from the initial and final MRI examination, there was a statistically significant difference in the frontal cortex ($p < 0.01$), occipital cortex ($p < 0.01$), and the white matter of the CR ($p < 0.01$) while parietal cortex ($p < 0.05$), thalamus ($p = 0.051$), *putamen* ($p = 0.06$), and anterior and posterior limb of the CI ($p = 0.062$) were close to statistical significance (Table 2).

Table 2

Comparison of the value of brain region-to-cerebrospinal fluid signal intensity ratio relationship from the initial and final magnetic resonance imaging (MRI) examination

Region of the brain	Initial MRI scan	Final MRI scan	*p*-value
Frontal cortex	1.674 ± 0.096	1.768 ± 0.142	<0.01
Parietal cortex	1.496 ± 0.107	1.559 ± 0.142	<0.05
Temporal cortex	1.512 ± 0.141	1.545 ± 0.143	0.375
Occipital cortex	1.601 ± 0.136	1.718 ± 0.188	<0.01
Putamen	1.674 ± 0.105	1.738 ± 0.086	0.06
Thalamus	1.595 ± 0.118	1.678 ± 0.102	0.051
Nucleus caudatus	1.605 ± 0.113	1.668 ± 0.098	0.091
Anterior limb of *capsula interna*	1.765 ± 0.102	1.837 ± 0.112	0.062
Posterior limb of *capsula interna*	1.723 ± 0.141	1.809 ± 0.110	0.062
Corpus callosum genu	1.734 ± 0.124	1.782 ± 0.112	0.241
Corpus callosum splenium	1.579 ± 0.176	1.644 ± 0.106	0.158
White matter of *centrum semiovale*	1.744 ± 0.089	1.763 ± 0.098	0.444
White matter of *corona radiata*	1.535 ± 0.129	1.627 ± 0.106	0.01
Pons	1.505 ± 0.156	1.560 ± 0.124	0.163
Substantia nigra	1.399 ± 0.159	1.472 ± 0.106	0.73
Cerebellar hemisphere	1.674 ± 0.111	1.694 ± 0.115	0.556

All values are expressed as mean ± standard deviation.

Table 3
The number of patients that had an increase in the value of brain region-to-cerebrospinal fluid signal intensity ratio at the initial and final magnetic resonance imaging scan

Region of the brain	Patient
Frontal cortex	15 (75)
Parietal cortex	13 (65)
Temporal cortex	11 (55)
Occipital cortex	15 (75)
Putamen	13 (65)
Thalamus	12 (60)
Nucleus caudatus	12 (60)
Anterior limb of *capsula interna*	13 (65)
Posterior limb of *capsula interna*	12 (60)
Corpus callosum genu	11 (55)
Corpus callosum splenium	13 (65)
White matter of centrum semiovale	10 (50)
White matter of *corona radiata*	9 (45)
Pons	13 (65)
Substantia nigra	12 (60)
Cerebellum hemisphere	15 (75)

All values are expressed as numbers (percentages).

By comparing the initial and final values of the SI ratio in each subject for each of the previously defined areas, we registered an increase in the value of the SI ratio in all subjects. The lowest (45%) percentage of respondents had an increase in the SI ratio of the white matter of CR and white matter of CSO (50%); the largest (75%) percentage of respondents had an increase in the SI ratio in the frontal cortex, occipital cortex, and cerebellar hemisphere (Table 3).

Discussion

GBCAs are widely used in MRI. They were first applied in 1988, and today, they are used in about 30% of MRI diagnostics [2].

They have long been considered safe to use; however, in 2006, cases of potentially lethal NSF caused by using GBCAs in patients with renal insufficiency were described [12, 13]. Then in 2014, Kanda et al. [5] published a paper on the intracranial accumulation of gadolinium, based on observations of the increased intensity of T1W signals in the ND and GP. Subjects receiving gadopentetate dimeglumine or gadodiamide had a statistically significant increase in SI in these structures. This study was subsequently confirmed through independent studies, in which an increase in T1W signal was also observed after intravenous administration of linear GBCAs. Namely, according to the structure of chelated ligands, GBCAs were divided into two groups, linear and macrocyclic [14, 15]. Since gadolinium itself is toxic, GBCAs were used in the form of chelating compounds bound to different ligands [15].

It is generally accepted that, due to their structure, macrocyclic GBCAs are more stable than linear GBCAs; therefore, there is none of the so-called degeneration of gadolinium, which can result in toxic effects, primarily on the kidneys, through which gadolinium is metabolized [16]. In the study by Ramalho et al. [8], gadolinium deposition in NC and GP after using linear GBCAs was confirmed.

However, the high SI in GP and NC in the T1W sequence can be observed in several diseases and conditions. Thus, for instance, the hyperintensity of T1W in NC is found in conditions such as calcifications of the basal ganglia after radiotherapy, Langerhans' histiocytosis, and MS. On the other hand, hyperintense GP in T1W is associated with liver dysfunction, Wilson's disease, exclusively parenteral nutrition, neurofibromatosis type 1, manganese toxicity, Randu-Osler-Weber disease, hemodialysis, and other health conditions that can cause calcification of GP, which should be kept in mind when interpreting the results of the study [5, 17–20].

In addition to gadolinium deposition in these two regions, deposition in other regions of the brain but of lower intensity has also been proven [21]. Among others, Zhang et al. [22] analyzed patients, each of whom had more than 35 applications of linear GBCAs. They found T1 hyperintensity not only in the ND (100%) and GP (100%) but also in SN (100%), the latter part of the thalamus (92%), *nucleus ruber* (77%), *colliculus* (77%), upper cerebellar peduncle (54%), NC (31%), whole thalamus (23%), and *putamen* (15%).

The results of our retrospective study on 20 patients with a diagnosis of MS were homogenized according to the therapeutic protocol and to the fact that all patients underwent MRI on the same machine with a magnetic field strength of 3T, which included the administration of a linear contrast agent (gadopentetate dimeglumine – Magnevist®), from 2010 to 2019, once a year on average. The pre-contrast T1W SI was measured by the anatomical structures, which were then divided by the SI of the right lateral ventricle to normalize the results, obtaining the SI ratio. The same methodology was used in similar research [5, 20, 23–25].

A statistically significant increase in signals was obtained in the structures: frontal, parietal, and occipital cortex, as well as supratentorial white matter. We should not neglect the results that are very close to statistical significance, such as the case of the thalamus $p = 0.051$, *putamen* $p = 0.06$, and CI $p = 0.062$.

We also analyzed the absolute increase in the value of SI in each patient. Thus, an increase in T1W SI was detected in 75% of patients in the frontal and occipital cortex and in the infratentorial white matter. In 65% of patients, an increase in the intensity of T1W signals was also observed in the parietal cortex, *putamen*, anterior limb of the CI, *splenium* of the CC, and *pons*. An increase in T1W SI was found in 60% of patients in the following regions: thalamus, NC, posterior limb of the CI, and SN. In 55% of patients, we detected signal enhancement in both the temporal cortex and the *genu* of the CC. In half of the patients, the signal amplification was registered in the white matter-CS and in 45% in the supratentorial white matter. In our study, the following structures were not examined: NC, *colliculi*, and *pedunculus cerebellaris* superior, while the thalamus was examined as a whole.

If we observed the increase of the signal in absolute values of the T1W signal, we might notice that it was increased in the frontal and occipital cortex and infratentorial white matter in three-quarters of patients. A slightly smaller increase in SI, but still greater than 55–65%, was registered in structures such as the parietal cortex, *putamen*, anterior and posterior limb of the CI, *splenium* of the CC, *pons*, thalamus, NC, SN, and the temporal cortex.

Thus, it has been shown that after long-term use of gadolinium in patients diagnosed with MS, the absolute values of the T1W signal are registered not only in the basal ganglia but also in other areas. However, things can be viewed from another angle. Since MS is a diffuse disease that predominantly affects white matter, contrast deposition in these zones was registered in 55% and 45% of respondents, which may suggest that these brain regions are most affected by the underlying disease, unlike cortical structures that are less affected by MS. Research has shown that gadolinium deposition occurs in other diseases and in patients who do not have intracranial diseases [5, 17–20, 26].

In this study, the linear GBCA was used. In retrospective studies involving patients with recurrent linear GBCAs, changes in T1 signaling in the basal ganglia correlated with the number of linear GBCAs such as gadodiamide and gadopentetate [27, 28]. Subjects received gadopentetate dimeglumine (Magnevist®), a linear GBCA, for the duration of the study. On the other hand, some studies focused on examining changes in SI in patients who received multiple macrocyclic GBCA gadobutrol (Gadovist®), gadoterate meglumine, and gadoteridol, which were more stable, and found that macrocyclic GBCA was not associated with significant changes in SI in GP and NC [26, 27]. Studies comparing linear (gadopentetate) and macrocyclic (gadoteridol or gadoterate meglumine) agents have confirmed that changes in SI are significantly and exclusively associated with the use of linear agents [28].

What the results of our study, as well as many other studies, open as a topic for new research, is whether the intracranial deposition of gadolinium in different structures is proven since its toxicity is known and which implications that may have. Little is known about the clinical consequences of intracranial gadolinium deposition.

Thus, one study dealt with parkinsonism as a possible consequence of gadolinium deposition, taking into account that a significant percentage showed gadolinium deposition in GP, from which it could be concluded that gadolinium deposition should be associated with extrapyramidal dysfunction and with parkinsonism.

In a population study (n = 246,557) of two groups, who underwent MRI, between 2003 and 2013 (one group exposed to at least one dose of GBCA and the other without exposure), the authors did not find a significant difference in the presence of accidental parkinsonism and concluded that their results contradict the hypothesis that gadolinium deposits in GP lead to neuronal damage that manifests as parkinsonism [29, 30].

Semelka et al. [6] proposed a new category of disease – gadolinium deposition disease, based on an observational study of 42 patients who had previously undergone MRI with GBCA. In the acute phase of gadolinium exposure, patients complained of central and peripheral pain, headache, bone pain, and skin thickening. In the chronic phase, 29 of 42 patients had problems with concentration and headaches. Of course, all this could and should be the subject of further research.

MRI diagnostics are getting more and more common; however, ultrasound diagnostics is the safest and least harmful compared to other radiological procedures. Until recently, using gadolinium contrast agents was considered safe, but today, as the number of procedures increases, certain questions, which will certainly capture the attention of the professional public and deserve an answer, arise.

Retrospective analysis and a small number of patients are significant study limitations. Additional studies with a larger number of patients are necessary to validate our findings further.

Conclusion

The study showed that in a cohort of 20 patients, there was a statistically significant increase in SI in the T1W sequence in the following structures: frontal, parietal, and occipital cortex, as well as supratentorial white matter.

An increase in the absolute values of the T1W signal in three-quarters of patients was registered in the frontal and occipital cortex and cerebellar hemispheres. A slightly smaller increase in SI, but still greater than half (55–65%), was registered in structures such as the parietal cortex, *putamen*, *cornu* anterior and posterior of the CI, *splenium* of the CC posterior, *pons*, thalamus, NC, SN, *genu* of the CC, and temporal cortex.

This result speaks in favor of the existence of chronic accumulation of gadolinium contrast agent gadopentetate dimeglumine. We can also conclude from the research that the white brain matter of the CR and the CSO are most affected by the disease itself.

Since all subjects in our study suffered from an RR form of MS, we cannot distinguish with certainty the effects of the underlying disease from the potentially harmful effects of contrast agent accumulation.

R E F E R E N C E S

1. *Matsumura T, Hayakawa M, Shimada F, Yabuki M, Dohanish S, Palkowitsch P,* et al. Safety of gadopentetate dimeglumine after 120 million administrations over 25 years of clinical use. Magn Reson Med Sci 2013; 12(4): 297–304.
2. *Lohrke J, Frenzel T, Endrikat J, Alves FC, Grist TM, Law M,* et al. 25 years of contrast-enhanced MRI: developments, current challenges, and future perspectives. Adv Ther 2016; 33(1): 1–28.
3. *Grobner T*. Gadolinium- a specific trigger for the development of nephrogenic fibrosing dermopathy and nephrogenic systemic fibrosis? Nephrol Dial Transplant 2006; 21(4): 1104–8.
4. *Xia D, Davis RL, Crawford JA, Abraham JL*. Gadolinium released from MR contrast agents is deposited in brain tumors: in situ demonstration using scanning electron microscopy with energy-dispersive X-ray spectroscopy. Acta Radiol 2010; 51(10): 1126–36.
5. *Kanda T, Ishii K, Kawaguchi H, Kitajima K, Takenaka D*. High signal intensity in the dentate nucleus and globus pallidus on unenhanced T1-weighted MR images: relationship with an increasing cumulative dose of gadolinium-based contrast material. Radiology 2014; 270(3): 834–41.
6. *Semelka RC, Ramalho J, Vakharia A, AlObaidy M, Burke LM, Jay M,* et al. Gadolinium deposition disease: initial description of a disease that has been around for a while. Magn Reson Imaging 2016; 34(10): 1383–90.
7. *Kuno H, Jara H, Buch K, Qureshi MM, Chapman MN, Sakai O*. Global and regional brain assessment with quantitative MR imaging in patients with prior exposure to linear gadolinium-based contrast agents. Radiology 2017; 283(1): 195–204.
8. *Ramalho M, Ramalho J, Burke LM, Semelka RC*. Gadolinium Retention and Toxicity-An Update. Adv Chronic Kidney Dis 2017; 24(3): 138–46.
9. *Lord ML, Chettle DR, Gräfe JL, Noseworthy MD, McNeill FE*. Observed deposition of gadolinium in bone using a new noninvasive in vivo biomedical device: Results of a small pilot feasibility study. Radiology 2018; 287(1): 96–103.
10. *White GW, Gibby WA, Tweedle MF*. Comparison of Gd (DTPA-BMA) (Omniscan) versus Gd (HP-DO3A) (ProHance) relative to gadolinium retention in human bone tissue by inductively coupled plasma mass spectroscopy. Invest Radiol 2006; 41(3): 272–8.
11. *Darrah TH, Prutsman-Pfeiffer JJ, Poreda RJ, Ellen Campbell M, Hauschka PV, Hannigan RE*. Incorporation of excess gadolinium into human bone from medical contrast agents. Metallomics 2009; 1(6): 479–88.
12. *Marckmann P, Skov L, Rossen K, Dupont A, Damholt MB, Heaf JG,* et al. Nephrogenic systemic fibrosis: suspected causative role of gadodiamide used for contrast-enhanced magnetic resonance imaging. J Am Soc Nephrol 2006; 17(9): 2359–62.
13. *Grobner T, Prischl FC*. Gadolinium and nephrogenic systemic fibrosis. Kidney Int 2007; 72(3): 260–4.
14. *Frenzel T, Lengsfeld P, Schirmer H, Hütter J, Weinmann HJ*. Stability of gadolinium-based magnetic resonance imaging contrast agents in human serum at 37 degrees C. Invest Radiol 2008; 43(12): 817–28.
15. *Pałasz A, Czekaj P*. Toxicological and cytophysiological aspects of lanthanides action. Acta Biochim Pol 2000; 47(4): 1107–14.
16. *Idée JM, Port M, Robic C, Medina C, Sabatou M, Corot C*. Role of thermodynamic and kinetic parameters in gadolinium chelate stability. J Magn Reson Imaging 2009; 30(6): 1249–58.
17. *Roccatagliata L, Vuolo L, Bonzano L, Pichiecchio A, Mancardi GL*. Multiple sclerosis: hyperintense dentate nucleus on unenhanced T1-weighted MR images is associated with the secondary progressive subtype. Radiology 2009; 251(2): 503–10.
18. *Lai PH, Chen C, Liang HL, Pan HB*. Hyperintense basal ganglia on T1-weighted MR imaging. AJR Am J Roentgenol 1999; 172(4): 1109–15.
19. *Lai PH, Tien RD, Chang MH, Teng MM, Yang CF, Pan HB,* et al. Chorea-ballismus with nonketotic hyperglycemia in primary diabetes mellitus. AJNR Am J Neuroradiol 1996; 17(6): 1057–64.
20. *Kanda T, Osawa M, Oba H, Toyoda K, Kotoku J, Haruyama T,* et al. High Signal Intensity in Dentate Nucleus on Unenhanced T1-weighted MR Images: Association with Linear versus Macrocyclic Gadolinium Chelate Administration. Radiology 2015; 275(3): 803–9.
21. *Kanda T, Fukusato T, Matsuda M, Toyoda K, Oba H, Kotoku J,* et al. Gadolinium-based Contrast Agent Accumulates in the Brain Even in Subjects without Severe Renal Dysfunction: Evaluation of Autopsy Brain Specimens with Inductively Coupled Plasma Mass Spectroscopy. Radiology 2015; 276(1): 228–32.
22. *Zhang Y, Cao Y, Shih GL, Hecht EM, Prince MR*. Extent of Signal Hyperintensity on Unenhanced T1-weighted Brain MR Images after More than 35 Administrations of Linear Gadolinium-based Contrast Agents. Radiology 2017; 282(2): 516–25.
23. *Radbruch A, Weberling LD, Kieslich PJ, Hepp J, Kickingereder P, Wick W,* et al. High-Signal Intensity in the Dentate Nucleus and Globus Pallidus on Unenhanced T1-Weighted Images: Evaluation of the Macrocyclic Gadolinium-Based Contrast Agent Gadobutrol. Invest Radiol 2015; 50(12): 805–10.
24. *Eisele P, Alonso A, Szabo K, Ebert A, Ong M, Schoenberg SO,* et al. Lack of increased signal intensity in the dentate nucleus after repeated administration of a macrocyclic contrast agent in multiple sclerosis: An observational study. Medicine (Baltimore) 2016; 95(39): e4624.
25. *Cao Y, Huang DQ, Shih G, Prince MR*. Signal Change in the Dentate Nucleus on T1-Weighted MR Images After Multiple Administrations of Gadopentetate Dimeglumine Versus Gadobutrol. AJR Am J Roentgenol 2016; 206(2): 414–9.
26. *McDonald RJ, McDonald JS, Kallmes DF, Jentoft ME, Paolini MA, Murray DL,* et al. Gadolinium Deposition in Human Brain Tissues after Contrast-enhanced MR Imaging in Adult Patients without Intracranial Abnormalities. Radiology 2017; 285(2): 546–54.
27. *McDonald RJ, Levine D, Weinreb J, Kanal E, Davenport MS, Ellis JH,* et al. Gadolinium Retention: A Research Roadmap from the 2018 NIH/ACR/RSNA Workshop on Gadolinium Chelates. Radiology 2018; 289(2): 517–34.
28. *Adin ME, Kleinberg L, Vaidya D, Zan E, Mirbagheri S, Yousem DM*. Hyperintense Dentate Nuclei on T1-Weighted MRI: Relation to Repeat Gadolinium Administration. AJNR Am J Neuroradiol 2015; 36(10): 1859–65.
29. *Choi JW, Moon WJ*. Gadolinium Deposition in the Brain: Current Updates. Korean J Radiol 2019; 20(1): 134–47.
30. *Welk B, McArthur E, Morrow SA, MacDonald P, Hayward J, Leung A,* et al. Association Between Gadolinium Contrast Exposure and the Risk of Parkinsonism. JAMA 2016; 316(1): 96–8.

Received on March 14, 2022
Revised on March 21, 2023
Accepted on March 21, 2023
Online First April 2023

ORIGINAL ARTICLE

UDC: 615.465::616.314]:616.311.2
DOI: https://doi.org/10.2298/VSP221203012R

The connection between discolored gingiva of abutment teeth and the presence of cast post

Povezanost prebojene gingive pored zuba nosača sa prisustvom livene nadogradnje

Ljubiša Ristić*, Vojkan Lazić†, Srdjan Postić†, Nenad Jelić*, Igor Djordjević†, Raša Mladenović‡

***Military Medical Academy, Dental Clinic, Belgrade, Serbia; †University of Belgrade, Faculty of Dental Medicine, Department of Prosthodontics, Belgrade, Serbia; ‡University of Kragujevac, Faculty of Medical Sciences, Department of Dentistry, Kragujevac, Serbia**

Abstract

Background/Aim. The cause of discolored gingiva (DG) is the presence of metal in the gingival tissue. DG is a relatively common case and is caused by the deposition of amalgam material in the gingival tissue during dental application or oral surgery. The aim of this study was to determine the significance of the presence of a cast post for the appearance of DG of abutment teeth (AT) in relation to the type of alloy used to make the fixed dental prosthesis (FDP). **Methods.** The study included 327 subjects with FDP. A total of 1,585 AT were examined. The subjects were classified into four groups depending on the type of alloy used to fabricate their FDPs (silver-palladium, gold, nickel-chromium alloy, or a combination of them). The presence of a cast post was confirmed by X-ray or by inspection of the dental chart. The study was conducted over the course of one year. **Results.** DG was observed in more than one-third (37.7%) of the subjects, of which 57.3% had a cast post. In the case of AT, discoloration occurred in 14.6%. Cast post was present in 92.7% of AT with DG. **Conclusion.** DG occurred in all groups of subjects regardless of the type of alloy from which the FDP was fabricated. The presence of a cast post is of great significance for the appearance of gray-bluish discoloration of the gingiva.

Key words:
dental alloys; dental amalgam; denture, partial, fixed; gingiva.

Apstrakt

Uvod/Cilj. Uzrok promene boje gingive (*discolored gingiva* – DG) je prisustvo metala u gingivalnom tkivu. DG je relativno česta pojava, a izazvana je taloženjem amalgamskog materijala u gingivalnom tkivu tokom stomatološke primene ili oralne hirurgije. Cilj rada bio je da se utvrdi značaj prisustva livene nadogradnje za pojavu DG kod zuba nosača u odnosu na vrstu legure od koje su proizvedene fiksne zubne nadoknade (FZN). **Metode.** U studiju je bilo uključeno 327 ispitanika sa ugrađenim FZN. Ispitivano je ukupno 1 585 zuba nosača FZN. U zavisnosti od vrste legure od kojih su bile izrađene FZN (srebro-paladijum, zlato, metal-keramika ili njihova kombinacija), ispitanici su bili razvrstani u četiri grupe. Prisustvo livene nadogradnje potvrđivano je rendgenskim snimkom ili uvidom u stomatološki karton. Ispitivanje je vršeno u periodu od jedne godine. **Rezultati.** Kod više od trećine (37,7%) ispitanika uočena je DG, od kojih je 57,3% imalo izrađenu livenu nadogradnju. Kod zuba nosača, FZN prebojenost se javila kod 14,6% ispitanika. Livena nadogradnja bila je prisutna kod 92,7% zuba nosača kod kojih se javila DG. **Zaključak.** Prebojena gingiva pojavila se u svim grupama ispitanika, bez obzira na vrstu legure od koje je FZN bila izrađena. Prisustvo livene nadogradnje je od velikog značaja za pojavu sivo-plavičaste prebojenosti gingive.

Ključne reči:
legure, stomatološke; amalgam, stomatološki; zubna proteza, parcijalna, fiksna; gingiva.

Introduction

"Amalgam tattoo" is a term that refers to gray-bluish discoloration of the gingiva that has been retained due to the centuries-old use of silver amalgam as a restorative material in dentistry. The cause of discolored gingiva (DG) or "amalgam tattoo" is the presence of metal in the gingival tissue. Oral amalgam pigmentation is a relatively common clinical

Correspondence to: Raša Mladenović, University of Kragujevac, Faculty of Medical Sciences, Department of Dentistry, Svetozara Markovića 69, 34 000 Kragujevac, Serbia. E-mail: rasa.mladenovic@med.pr.ac.rs

lesion in about 12% of patients and is caused by the deposition of amalgam material in the gingival tissue during the dental application or oral surgery [1].

Numerous *in vitro* and *in vivo* studies (case reports, animal models) have examined the frequency of "amalgam tattoo" [1–3]; however, there are practically no papers concerning the reasons for the appearance of DG of the abutment teeth (AT). According to some authors, DG is a consequence of the "dissolution" of amalgam as a result of galvanic corrosion. Due to the difference in the potential between different metals in the presence of saliva as an electrolyte, a galvanic current leads to corrosion, and the released metal ions can be deposited in the surrounding tissues [4]. However, some studies have shown that patients with various metal restorations do not have galvanic current and side effects, like periodontal and mucosal diseases, caries lesions, or increased concentration of metal ions in their saliva [5, 6].

Through our clinical practice, we have noticed that DG also occurs in teeth that do not have amalgam filling, such as incisors or canines (Figures 1 and 2). We also observed that, in a large number of cases, these teeth were restored by cast post, a type of dental restoration required in cases of reduced remaining tooth structure to retain the core [7]. The cast post can be made of gold, silver and palladium alloys, or base metal alloys [8].

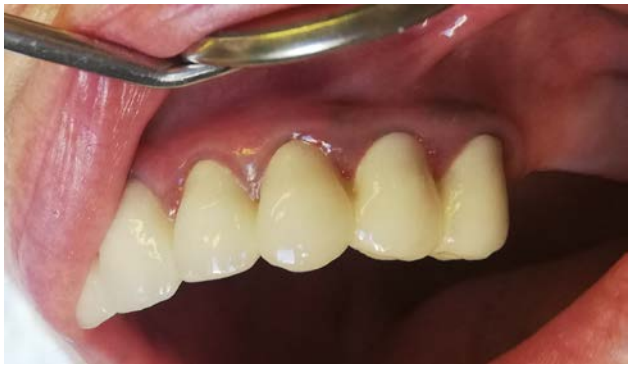

Fig. 1 – Discolored gingiva at the metal-ceramic bridge made of nickel-chromium alloy.

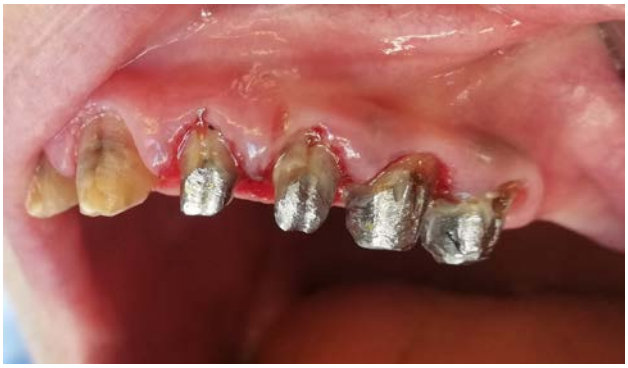

Fig. 2 – Discolored gingiva and cast post after removal of the metal-ceramic bridge made of nickel-chromium alloy.

The aim of this study was to determine the significance of cast post presence on the appearance of DG of AT.

Methods

The observational study included 327 subjects of both genders with an average age of 52 ± 11.4 years, treated at the Dental Clinic, Military Medical Academy, Belgrade, Serbia. Examinees with a fixed dental prosthesis (FDP) were included in the study. Exclusion criteria were severe periodontal and other oral diseases. All study participants provided written informed consent for participating in this study. The protocol of this study was approved by the Ethics Committee of the Military Medical Academy on May 21, 2009. The data were collected within one year.

Subjects were divided into four groups according to the type of alloy from which their FDP was fabricated: group 1 – subjects with metal-acrylate FDP made of gold (Au) alloy (n = 70); group 2 – subjects with metal-acrylate FDP made of silver-palladium (Ag-Pd) alloy (n = 94); group 3 – subjects with metal-ceramic FDP made of nickel-chromium (Ni-Cr) alloy (n = 85); group 4 – subjects with two or more FDPs made of different alloys (Au or Ag-Pd or Ni-Cr) (n = 78).

The following data were recorded: type of dental restoration (type of alloy used, date of manufacture, and possible changes in the restoration); presence of cast dowels (confirmed by inspection of dental chart or X-ray imaging).

Two dentists had to confirm the presence and characteristics of DG (localization, shape, size). AT without DG were marked as non-DG (NDG).

We compared the number of subjects and AT with DG with those without DG. The number of subjects and AT with cast post were compared to those without DG as well.

All parameters are presented as percentages. Statistical processing of the results was performed using the Chi-squared (χ^2) test on the commercial statistical software SPSS-18 (USA).

Results

The percentage of the subjects with DG in relation to the type of alloy that the FDP was fabricated from is shown in Table 1. A statistically significant difference in the presence of DG among the compared examined groups was not found.

The percentage of AT with the appearance of DG in relation to the type of alloy from which the FDP was fabricated is shown in Table 2. A statistically significant difference in the presence of AT with DG among the compared examined groups was not found. The analysis of the group of examinees developing DG showed that most of them had FDPs fabricated from the combination of alloys. DG appeared in 68 subjects whose FDPs were fabricated from Ni-Cr, while 48 and 39 patients had their FDPs fabricated from Ag-Pd and Au, respectively.

The percentage of the subjects with the cast post and the presence of DG in relation to the type of FDP alloy is shown in Table 3. A statistically significant difference in the presence of DG among the compared examined groups was not found. However, it was shown that more than half of the subjects with a cast post had DG, mainly the ones whose

FDPs were fabricated using a combination of two alloys, while the smallest percentage was among those whose FDPs were fabricated from Au.

Additional analysis of the subjects with cast post and DG showed that DG occurs in 92.7% of these subjects and in a significantly smaller number of subjects without the cast post (Table 4).

The percentage of AT with cast post and the presence of DG in relation to the type of FDP alloy is shown in Table 5, showing the same trend as has been previously described. Namely, the number of AT with DG was higher in the AT group with cast post (n = 171) when compared with AT without cast post. The highest number of AT with DG was detected in the group whose FDPs were fabricated from the combination of different alloys, and the least was in the group whose FDPs were fabricated from Au. A statistically significant difference in the presence of DG between the examined groups (depending on the type of the FDP alloy) was not found.

Table 1

Percentage of subjects with discolored gingiva in relation to the type of alloy used to fabricate the fixed dental prosthesis

Group	Type of alloy	Subjects with FDP (n)		Percentage
		DG	NDG	
1 (n = 70)	Au	23	47	32.9
2 (n = 94)	Ag-Pd	30	64	31.9
3 (n = 85)	Ni-Cr	34	51	40.0
4 (n = 78)	different alloys[#]	36	42	46.2
Total (n = 327)		123	204	37.7

DG – discolored gingiva; NDG – non-discolored gingiva; FDP – fixed dental prosthesis; Au – gold; Ag – silver; PD – palladium; Ni – nickel; Cr – chromium; n – number. [#]Au and/or Ag-Pd and/or Ni-Cr.

Table 2

Presence of abutment teeth (AT) with discolored gingiva in relation to the type of alloy used to fabricate the fixed dental prosthesis

Group	Type of alloy	AT (n)		AT with DG
		DG	NDG	%
1 (n = 263)	Au	39	224	14.8
2 (n = 370)	Ag-Pd	49	321	13.2
3 (n = 440)	Ni-Cr	68	372	15.5
4 (n = 512)	different alloys[#]	76	436	14.8
Total (n = 1,585)		232	1353	14.6

For abbreviations, see Table 1. [#]Au and/or Ag-Pd and/or Ni-Cr.

Table 3

Presence of discolored gingiva in subjects with a cast post in relation to the type of alloy used to fabricate the fixed dental prosthesis

Group	Type of alloy	Subjects with cast post (n)		Percentage
		DG	NDG	
1 (n = 28)	Au	19	9	67.8
2 (n = 51)	Ag-Pd	28	23	54.9
3 (n = 61)	Ni-Cr	31	30	50.8
4 (n = 59)	different alloys[#]	36	23	61.0
Total (n = 199)		114	85	57.3

For abbreviations, see Table 1. [#]Au and/or Ag-Pd and/or Ni-Cr.

Table 4

Frequency of subjects with a cast post in the group of subjects experiencing discolored gingiva

Group	Type of alloy	Subjects with cast post	Subjects without cast post
1	Au	19 (82.6)	4 (17.4)
2	Ag-Pd	28 (93.3)	2 (6.7)
3	Ni-Cr	31 (91.2)	3 (8.8)
4	different alloys[#]	36 (100)	0 (0)
Total		114	9***

For abbreviations, see Table 1. All values are expressed as numbers (percentages). [#]Au and/or Ag-Pd and/or Ni-Cr; ***$p < 0.005$ compared to subjects with cast post.

Table 5

Presence of discolored gingiva in abutment teeth (AT) with a cast post in relation to the type of alloy used to fabricate the fixed dental prosthesis

Group	Type of alloy	AT with DG (n)		AT with cast post %
		with cast post	without cast post	
1 (n = 39)	Au	29	10	74.4
2 (n = 49)	Ag-Pd	38	11	77.6
3 (n = 68)	Ni-Cr	47	21	69.1
4 (n = 76)	different alloys[#]	57	19	75.0
Total (n = 232)		171	61	73.7

For abbreviations, see Table 1. [#]Au and/or Ag-Pd and/or Ni-Cr.

The size, shape, and intensity of coloring were very inconsistent, even in the same subject/tooth, with no connection between these characteristics and the type of alloy used to fabricate the FDP. Discoloration occurred on the free and attached gingiva as well as the interdental gingiva. It was of various sizes (1–12 mm^2), and in some instances, it included a 3 mm wide gingiva around the tooth. The DG was present in the form of one or more dots but most often in the form of lines that followed the shape of the free gingiva.

Subjects with FDP made of Au alloy (the oldest one created) had the lowest percentage of DG in the presence of cast post. Moreover, DG was observed in subjects whose FDP was cemented just before this research.

Discussion

Regardless of the carefully made FDP, side effects can occur, most often on soft tissues. They can appear in the form of inflammation, recession, or DG. In contrast to the red coloration of the gingiva, which develops as a consequence of inflammation, characteristic grey-bluish discoloration that frequently appears is not a consequence of inflammation [9, 10].

That can compromise the entire dental prosthetic work. The gray-blue discoloration is in great contrast with the color of the teeth and the coral-pink color of the gingiva. It significantly reduces the aesthetic appearance of the patient. Such DG raises suspicion in both the patient and the dentist that more serious pathological changes are occurring in the tissue. If the indication for making an artificial crown was aesthetic, then the goal of therapy is completely unfulfilled, with high costs and wasted time. In addition, it has been noticed that DG is a long-standing problem, and no noninvasive therapy could remove it [11].

According to some theories, DG is a consequence of the "dissolution" of the dental amalgam, cast post, and crown made of Ag alloy due to the occurrence of galvanic corrosion between all groups of materials and Ag-Pd alloys [12]. This theoretical explanation of the appearance of DG is not acceptable for several reasons. Firstly, the cast post on which the FDP is made is practically covered and protected in the mouth from the influence of the external environment. Secondly, if DG is caused by ion release, this discoloration will appear gradually and increase with time. Thirdly, if that is the case, there would be cases of DG around the teeth with the cast post before grinding.

In our study, the lowest incidence of DG was observed in patients with fixed Ag-Pd alloy restorations (31.9%) and only one percent more in Au alloys (32.9%). These results and the absence of a statistically significant difference in the occurrence of DG in relation to the type of alloy that the FDPs were fabricated from suggested that galvanic corrosion, which can occur between cast post and FDP, has no big effect on gingival discoloration.

We could not determine the composition of each cast post; however, based on the time of their creation, we concluded that in that period, in our department, the cast posts and FDPs were made mainly of Ag-Pd alloy.

In previous *in vitro* studies, Ag-Pd alloys showed higher ion release and stronger biological interaction due to poor corrosion resistance [13]. In contrast, we found the lowest incidence of DG in teeth with Ag-Pd restorations. That indicates that the increased release of ions from Ag-Pd alloys caused by corrosion does not significantly affect the appearance of DG. The small influence of galvanic corrosion on the occurrence of DG is also shown by our results which showed that the largest number of AT with DG was in the group of subjects with restorations made of Ni-Cr alloy (15.5%). In metal-ceramic restorations, the metal alloy is completely covered with a ceramic that is resistant to corrosion and thus protects the metal core. However, the use of metal-ceramic systems requires more extensive grinding of the AT with and without cast post than other tested materials (Au and Ag-Pd) [14].

The highest percentage (100%) of patients with cast post and DG in group 4 could be explained by perennial therapy and a large number of different dental restorations carried out in these patients. Over time, a greater number of indications (secondary caries, devitalization of teeth) and repeated therapy with various restorations (crown, bridge, combined prosthesis) may lead to a greater need for making a cast post [7].

The observed high frequency of DG during our examinations is not in line with the findings of other researchers. Garhammer et al. [15] analyzed 86 out of 250 patients with possible side effects caused by dental alloys, selected from a population of one million citizens, and reported that 12% of research subjects had DG. The authors attributed it to a non-irritating "amalgam tattoo" based on earlier descriptions of such changes in the literature. None of the patients had other subjective problems; apparently, DG was the only reason to be included in the research. It was not noted which teeth DG occurred on (anterior or lateral), which alloys were used for the dental restorations, and whether a cast post had been present.

Therefore, the reason for a high frequency (37.7%) of DG in our subjects could be the consequence of frequent caries destruction of the teeth with an indication for making a cast post. The appearance of discoloration can also be a consequence of inadequate modeling of the cast post by acrylate, additional preparation of cast post after cementation, and the use of feather edge demarcation, which often leads to injury of the gingiva [16, 17].

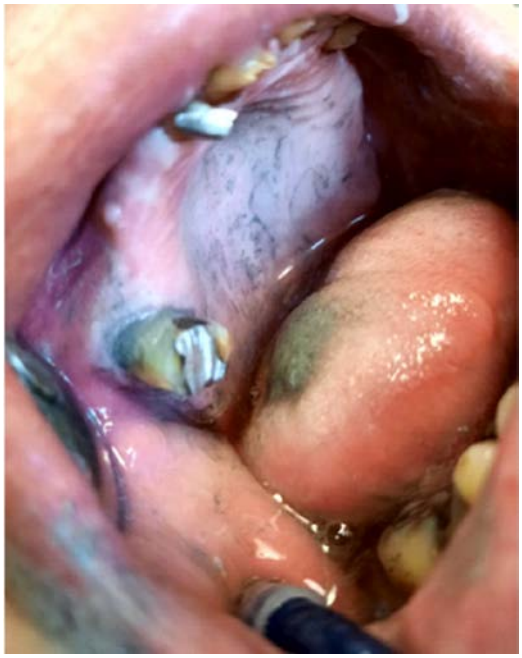

Fig. 3 – Metal powder on oral mucosa during the preparation of tooth with amalgam filling for fixed dental prosthesis.

Among our subjects with DG, 92.7% had a cast post. Furthermore, our results show that a large number (73.7%) of AT with cast post had DG. The presence of a cast post in a high percentage of AT with DG clearly shows its significant role in the appearance of DG. It should be emphasized that we were unable to find a similar study in the literature. All other AT with DG, without cast post, are premolars and molars, except one. In our population, these teeth are often treated with amalgam filling, and its preparation creates a large amount of metal powder (Figure 3). Most powders can be washed out easily, whereas metal powder could adhere to the injured gingiva. As the gingiva heals, the powder remains in the tissue and, with its gray color, causes a change in the color of the gingiva.

A significant limitation of this study was the fact that the patients did not undergo sampling for histological examination of DG. In our future work, we shall focus on identifying the pathohistological characteristics of DG.

Conclusion

Cast post was present in 123 (37.7%) subjects and 232 (14.6%) AT with DG. If the artificial crown is not left with sufficient space during the modeling, the reduction of the volume of the cast post in the mouth leads to the creation of a large amount of metal powder that can be adhered to the injured gingiva. It is necessary to perform periodontal treatment, appropriate modeling of the cast post, and careful preparation of the cast post to avoid the appearance of discolored gingiva.

REFERENCES

1. *McCullough MJ, Tyas MJ*. Local adverse effects of amalgam restorations. Int Dent J 2008; 58(1): 3–9.
2. *Martín JM, Nagore E, Cremades A, Botella-Estrada R, Sanmartín O, Sevila A,* et al. An amalgam tattoo on the oral mucosa related to a dental prosthesis. J Eur Acad Dermatol Venereol 2005; 19(1): 90–2.
3. *Hassona Y, Sawair F, Al-Karadsheh O, Scully C*. Prevalence and clinical features of pigmented oral lesions. Int J Dermatol 2016; 55(9): 1005–13.
4. *Pigatto PD, Brambilla L, Guzzi G*. Amalgam tattoo: a close-up view. J Eur Acad Dermatol Venereol 2006; 20(10): 1352–3.
5. *Nilner K*. Studies of electrochemical action in the oral cavity. Swed Dent J Suppl 1981; (9): 1–42.
6. *Johansson BI, Stenman E, Bergman M*. Clinical registration of charge transfer between dental metallic materials in patients with disorders and/or discomfort allegedly caused by corrosion. Scand J Dent Res 1986; 94(4): 357–63.
7. *Dangra Z, Gandhewar M*. All about Dowels - A Review Part I. Considerations before Cementation. J Clin Diagn Res 2017; 11(8): ZG06–11.
8. *Hayashi M, Takahashi Y, Imazato S, Ebisu S*. Fracture resistance of pulpless teeth restored with post-cores and crowns. Dent Mater 2006; 22(5): 477–85.
9. *Knoernschild KL, Campbell SD*. Periodontal tissue responses after insertion of artificial crowns and fixed partial dentures. J Prosthet Dent 2000; 84(5): 492–8.
10. *Ristic Lj, Dakovic D, Postic S, Lazic Z, Bacevic M, Vucevic D*. Clinical characteristics of abutment teeth with gingival discoloration. J Prosthodont 2019; 28(1): e45–50.
11. *Aguirre-Zorzano LA, García-De-La-Fuente AM, Estefanía-Fresco R*. Treatment of amalgam tattoo with a new technique: mucoabrasion and free connective tissue graft. Clin Adv Periodontics 2019; 9(3): 120–4.
12. *Joska L, Venclikova Z, Poddana M, Benada O*. The mechanism of gingiva metallic pigmentations formation. Clin Oral Investig 2009; 13(1): 1–7.
13. *Wataha JC, Lockwood PE, Nelson SK*. Initial versus subsequent release of elements from dental casting alloys. J Oral Rehabil 1999; 26(10): 798–803.
14. *Goodacre CJ*. Designing tooth preparations for optimal success. Dent Clin North Am 2004; 48(2): 359–85.
15. *Garhammer P, Schmalz G, Hiller KA, Reitinger T, Stolz W*. Patients with local adverse effects from dental alloys: frequency, complaints, symptoms, allergy. Clin Oral Investig 2001; 5(4): 240–9.
16. *Cagidiaco EF, Discepoli N, Goracci C, Carboncini F, Vigolo P, Ferrari M*. Randomized Clinical Trial on Single Zirconia Crowns with Feather-Edge vs Chamfer Finish Lines: Four-Year Results. Int J Periodontics Restorative Dent 2019; 39(6): 817–26.
17. *Dangra Z, Gandhewar M*. All About Dowels - A Review Part II Considerations After Cementation. J Clin Diagn Res 2017; 11(10): ZE06–11.

Received on December 03, 2022
Revised on February 8, 2023
Accepted on February 21, 2023
Online First March 2023

ORIGINAL ARTICLE

UDC: 616.718.7/.9-089:617.585/.587
DOI: https://doi.org/10.2298/VSP221226015G

Clinical results of scarf osteotomy

Klinički rezultati *scarf* osteotomije

Boris Gluščević*†, Aleksandar Stanojković*, Dragica Bukumirić‡, Danilo Jeremić*†

***Institute for Orthopedic Surgery "Banjica", Belgrade, Serbia; †University of Belgrade, Faculty of Medicine, Belgrade, Serbia; ‡Institute of Public Health of Serbia "Dr. Milan Jovanović Batut", Belgrade, Serbia**

Abstract

Background/Aim. There are a few research papers in Serbia that report on the clinical results of scarf osteotomy (SO) and its long-term effects. The aim of this retrospective study was to evaluate the efficacy of SO in hallux valgus (HV) deformity correction, as well as the degree of recurrence and its possible causes. **Methods.** The study included 48 patients (52 feet) who underwent SO. The average follow-up time was 103.9 (63–156) months. In order to clinically evaluate the results, the American Orthopedic Foot and Ankle Society (AOFAS) scale and the Visual Analog Scale (VAS) of pain were used. In order to radiographically determine the degree of deformity, preoperative and postoperative radiographs of the feet were taken in the standing position, and the following parameters were determined: HV angle (HVA), intermetatarsal angle, distal metatarsal articular angle, and sesamoid position. **Results.** The AOFAS scores increased from 19 (5–45) points preoperatively to 92 (54–100) points at the time of the latest follow-up examination ($p < 0.001$). The VAS values significantly improved from 10 (8–10) preoperatively to 0 (0–6). The average HVA correction was 24.8°. The recurrence rate in patients in whom the HVA was greater than 20° was 26.9%. **Conclusion.** Although SO is a proven procedure for the correction of HV, long-term results still show a relatively high rate of recurrence.

Key words:
hallux valgus; orthopedic procedures; osteotomy; recurrence; serbia; treatment outcome.

Apstrakt

Uvod/Cilj. U Srbiji ima vrlo malo radova u kojima se opisuju klinički rezultati i dugoročni efekti *scarf* osteotomije (SO). Cilj ove retrospektivne studije bio je da se utvrdi efikasnost SO kod *hallux valgus* (HV) deformiteta, kao i stepen recidiva i njihovi mogući uzroci. **Metode.** Studijom su bila obuhvaćena 48 bolesnika (52 stopala) kod kojih je izvršena SO. Prosečno vreme praćenja bilo je 103,9 (63–156) meseci. U cilju kliničke procene rezultata korišćena je skala američkog ortopedskog udruženja za skočni zglob i stopalo (*American Orthopedic Foot and Ankle Society* – AOFAS) i Vizuelna analogna skala (VAS) bola. U cilju radiografskog utvrđivanja stepena deformiteta, preoperativno i postoperativno su rađene radiografije stopala u stojećoj poziciji i određivani su sledeći parametri: HV ugao (HVU), intermetatarzalni ugao, distalni metatarzalni artikularni ugao i pozicija sezamoida. **Rezultati.** Vrednosti skora AOFAS povećane su sa 19 (5–45) poena preoperativno na 92 (54–100) poena u trenutku poslednjeg kontrolnog pregleda ($p < 0,001$). Vrednosti VAS su se značajno poboljšale sa preoperativnih vrednosti 10 (8–10) na 0 (0–6). Prosečna korekcija HVU bila je 24,8°. Stepen recidiva kod bolesnika gde je HVU bio veći od 20° iznosio je 26,9%. **Zaključak.** Iako je SO dokazana procedura za korekciju HV, ipak dugotrajni rezultati govore u prilog relativno visokog stepena recidiva.

Ključne reči:
haluks valgus; ortopedske procedure; osteotomija; recidiv; srbija; lečenje, ishod.

Introduction

Hallux valgus (HV) is a progressive deformity of the foot characterized by the abduction and/or pronation of the proximal phalanx of the big toe, as well as by the adduction, pronation, and elevation of the first metatarsal (MT) bone, with the increase of the intermetatarsal angle (IMTA) and with capsular and ligamentous derangement of the first metatarsophalangeal (MTP) joint, accompanied by painful bunions. More than a hundred different surgical procedures for the correction of HV have been described; however, the scarf procedure is one of the most commonly applied

Correspondence to: Boris Gluščević, Institute for Orthopedic Surgery "Banjica", Mihaila Avramovića 28, 11 000 Belgrade, Serbia.
E-mail: glborismmm@gmail.com

techniques. Scarf osteotomy (SO) was first described by Meyer [1] in 1926 and then applied by Burutaran [2] in 1976. After that, osteotomy was popularized and modified by Borrelli and Weil [3] in the United States and by Barouk [4] in Europe.

SO is a horizontally positioned Z dislocation osteotomy of the diaphysis of the first MT bone fixed by two screws. In relation to the anatomical position of correction, it is categorized as a midshaft osteotomy [5].

The most common indication for performing SO is a painful HV deformity of a variable medium to a severe degree. In addition, this procedure can also be used in cases where revision surgery of this deformity is necessary [6]. An absolute contraindication for performing SO is an active infection. Other contraindications are severe neuropathic changes in the foot as well as vascular compromise and severe arthrosis of the first MTP joint. Relative contraindications include hypermobility of the first tarsometatarsal joint [7].

With osteotomy, it is possible not only to correct IMTA but also to dictate the shortening or lengthening of the first MT bone.

Additionally, by a lateral translation and medial rotation of the plantar fragment, the correction of the distal MT angle is also made possible in SO [8].

The advantages of SO are the following: reliability, the possibility of correcting more severe deformities, good healing, stable osteotomy, and immediate postoperative walking without immobilization.

Different types of complications of this procedure have been described. The most common long-term complication is the recurrence of the deformity. Bock et al. [9] reported on recurrence of HV in 30% of patients after a 10-year follow-up.

The aim of the study was to evaluate the efficiency of the SO procedure in HV deformity corrections, its long-term results, as well as the risk factors for the recurrence of the deformity.

Methods

The indication for SO was a painful HV deformity greater than 20°. Patients with systemic diseases such as rheumatoid arthritis, as well as those with a complex deformity or severe osteoporosis, were not considered. No patient had hypermobility of the first tarsometatarsal joint.

Clinical and radiographic evaluation of the results was performed preoperatively, six weeks after surgery, and then once a year. The American Orthopedic Foot and Ankle Society (AOFAS) scale and Visual Analog Scale (VAS) were used. Radiographs were taken in two standard planes. A four-stage system was used to determine the degree of sesamoid lateral migration.

Surgical technique

The patient was lying on his back. A tourniquet was placed on the middle of the upper leg after exsanguination. A medial longitudinal incision was made over the first MTP (I MTP) joint, distally extending about 1 cm from the joint (extended if AO is required) and proximally extending to the middle of the diaphysis of the first MT (I MT) bone (if greater deformity, the incision extends more, to 1 cm proximal to the first metatarsocuneiform joint). Subcutaneous tissue and capsule of the I MTP joint were cut and peeled off subperiosteally to free the joint and the shaft (except for the plantar side to avoid damage of the I MT bone head vascularization). After approaching the joint and shaft, a longitudinal cut of the I MT bone was made. The cutting angle in the frontal plane was inclined towards the plantar. Longitudinal resection ended proximally 1.5 cm from the metatarsocuneiform joint and distally 6–8 mm from the I MTP joint line. After that, transversal cuts were made, which must be parallel and at an angle of 60° to the longitudinal axis. The correction is then achieved by moving the plantar fragment laterally for 65–75% of the shaft diameter, and the osteotomy is fixed with two cortical screws. By reverse rotation of the I MT bone head after described osteotomy, the distal MT articular angle can be corrected. After correction, the medial bony prominence was removed, and a capsulorrhaphy was performed. If the deformity is larger, soft tissue release of the lateral side of the I MTP joint was performed before this osteotomy. This release is done through a special dorsal approach to the first MT space or if there is a residual HV after correction, an additional AO was performed.

Postoperative wound control was performed on the third day, and the sutures were removed on the 14th day after surgery. Postoperatively, all patients walked without weight bearing on the forefoot. A specially designed orthosis was used. After six weeks, weight-bearing was allowed on the operated foot at the time when the radiographic and clinical evaluations were performed again. Clinical and radiographic assessments were then performed at 6 months, 12 months, and once a year thereafter. In this study, it was considered that recurrence of the deformity occurred if the HV angle (HVA) exceeded 20°. There were possible risk factors for the recurrence of HV analyzed in this study: age, gender, body mass index, side of surgically treated feet, bilaterality, the preoperative AOFAS score, as well as the preoperative values of HVA, IMTA, and the sesamoid position.

The study was approved by the Ethical Committee of the Institute for Orthopedics “Banjica” (No. I–97/30, from December 16, 2022).

Statistical analysis

All data were processed using the IBM SPSS Statistics 22 software (SPSS Inc., Chicago, IL, USA) or in the R Programming Environment (R Core Team, 2019). Depending on the type of variables and the normality of distribution, the Wilcoxon and Friedman tests were used. Logistic regression was used to analyze potential predictors on binary variables (the existence of recurrence) and potential predictors. Due to the unfavorable number of outcomes, multivariate analysis was not performed. The level of significance was set at 0.05.

Results

We evaluated 48 (52 feet) patients who underwent SO between February 2009 and December 2016. There were 40 female and 8 male patients (Table 1). The average age of the patients was 51.2 years, and the average follow-up time was 103.9 months. As an additional procedure, when necessary, an Akin osteotomy (AO) was performed in nine (18.7%) patients.

Clinical assessment

According to HVA criteria (normal if the angle was < 15°, mild if HVA was 15–20°, moderate if HVA was 20–39°, and severe if HVA was > 40°), 25 feet had a moderate deformity, while 27 had a severe deformity.

The median preoperative AOFAS score was 19 (5–45), while it was 92 (54–100) at the latest follow-up examination ($p < 0.001$) (Figure 1).

All the AOFAS subscores (pain, function, and alignment) improved significantly (Table 2).

The median scores on the VAS were 10 (8–10) preoperatively, decreasing to 0 (0–6) after surgery ($p < 0.001$) (Figure 2). The average HVA correction was 24.8°.

Radiological assessment

According to the radiographic assessment, a significant improvement ($p < 0.001$) occurred regarding the HVA, IMTA, and the position of the sesamoid (Table 3).

Table 1

Demographic and baseline characteristics of patients who underwent scarf osteotomy

Parameter	Values
Gender	
female	40 (83)
male	8 (17)
Foot side	
left	27 (52)
right	25 (48)
Age at the time of surgery, years	51.2 ±10.3
Clinical follow-up, months	103.9 (63–156)

Values are expressed as numbers (percentages), average ± standard deviation, or average (minimum – maximum).

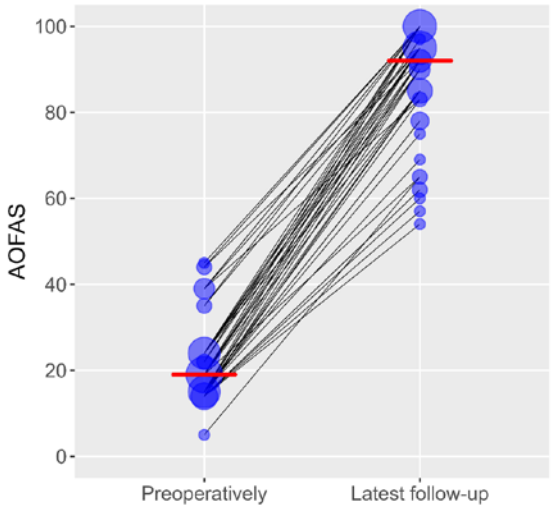

Fig. 1 – Frequencies of individual values and median values of the hallux valgus angle, preoperatively and at the latest follow-up. AOFAS – American Orthopedic Foot and Ankle Society.

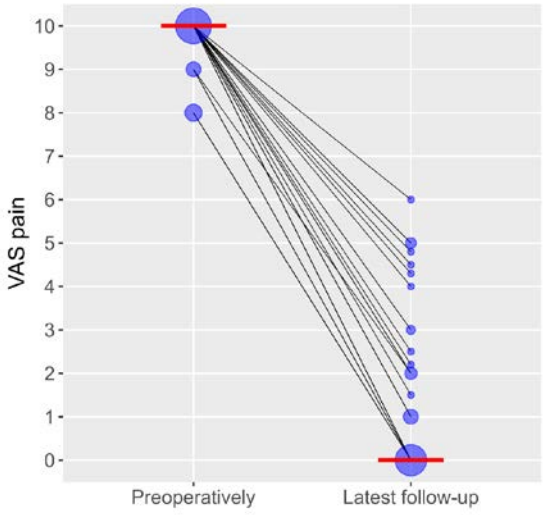

Fig. 2 – Frequencies of individual values and median scores on the Visual Analog Scale (VAS) for measuring pain preoperatively and at the latest follow-up.

Table 2

AOFAS subscores in patients who underwent scarf osteotomy

AOFAS categories	Preoperatively	Latest follow-up	*p*-value*
Pain	0 (0–20)	40 (20–40)	< 0.001
Function	19 (5–24)	40 (34–45)	< 0.001
Alignment	0 (0–0)	15 (0–15)	< 0.001

AOFAS – American Orthopedic Foot and Ankle Society; * Wilcoxon test.
All values are expressed as median (minimum–maximum).

Recurrence

Radiographic recurrence of HV occurred in 14 (26.9%) out of 52 feet at the latest follow-up examination. During the early postoperative period, recurrence was not registered. Recurrence occurred in two (8.0%) feet with primary moderate deformity and in 12 (44.4%) feet with severe deformity (Table 4). The results of the risk factor analysis are presented in Table 5. The results show that preoperative values of HVA, IMTA, and AOFAS, as well as the sesamoid position, were presented as risk factors for the recurrence of HV.

Complications

In addition to the recurrence of HV, other complications were registered. In four (7.7%) cases, the wound took longer to heal. In one (1.9%) case there was a superficial infection, which was resolved with an antibiotic. In one (1.9%) case, the screw impeded movement that was resolved by the removal of the screw. In two (3.8%) cases, limitation in plantar flexion was present.

Discussion

It has been approved that SO is a reliable procedure for correcting a moderate to severe HV deformity of the foot [10]. However, there is a relatively small number of studies reporting on long-term results [6].

Significant improvement after surgery to HVA, AOFAS score, and IMTA, as well as reduction of pain, was presented in our study, and it is in accordance with other studies from the literature [3, 6, 10, 11].

With SO, the positional correction can be made in all three planes, although it is technically demanding and requires a lot of time to learn and perfect. Due to its complexity, significant complications can be possible [12, 13].

Table 3

Comparison of preoperative and postoperative radiographic results

Parameters	Preoperative	Six weeks after surgery	Latest follow-up	*p*-value*
HVA (degrees)	40 (29–62)	9 (6–13)	13 (8–35)	< 0.001
IMTA (degrees)	14 (11–17)	8 (6–10)	9 (7–13)	< 0.001
Sesamoid lateral migration grade	3 (2–3)	0 (0–1)	1 (0–3)	< 0.001

HVA – hallux valgus angle; IMTA – intermetatarsal angle; *Friedman test.
All values are expressed as median (minimum–maximum).

Table 4

Recurrence of different grades of deformity after scarf osteotomy performed

Grade	Recurrence	Without recurrence
Mild	0 (0)	0 (0)
Moderate	2 (8)	23 (92)
Severe	12 (44)	15 (56)
Total	14 (27)	38 (73)

All values are expressed as numbers (percentages).

Table 5

Possible risk factors for recurrence of deformity after scarf osteotomy performed

Variable	Recurrence (n = 14)	Without recurrence (n = 38)	*p*-value*
Age (years)	51.4 ± 12.3	49.1 ± 11.0	0.522
Gender			
male	1 (7.1)	7 (18.4)	0.336
female	13 (92.9)	31 (81.6)	
Body mass index, kg/m^2	26.8 ± 3.5	26.0 ± 2.8	0.415
Side			
left	7 (50)	20 (52.6)	0.866
right	7 (50)	18 (47.4)	
Bilateral	2 (14.3)	6 (15.8)	0.894
AOFAS preoperatively	14.5 (5–39)	22 (14–45)	0.013
HVA degrees preoperatively	47.5 (35–62)	38.5 (29–52)	0.001
IMTA degrees preoperatively	16 (13–17)	13.5 (11–17)	0.002
Sesamoid lateral migration grade preoperatively			
2	0 (0)	13 (34.2)	0.008
3	14 (100)	25 (65.8)	

HVA – hallux valgus angle; IMTA – intermetatarsal angle; AOFAS – American Orthopedic Foot and Ankle Society; *logistic regression.

All values are expressed as mean ± standard deviation, numbers (percentages), or median (minimum–maximum).

Although this study reports on significant clinical and radiographic improvement, the fact that it also reports on a relatively high recurrence rate has to be noted. On the other hand, although the recurrence rate is relatively high, it seems to be at a degree that does not cause difficulty to most patients. In the group of patients with recurrence of the deformity, eight (57.1%) patients were symptomatic, while only one (7.1%) patient required a secondary surgical procedure [14]. The most common surgical treatment of an HV deformity relies mostly on the correction of the deformity in the transverse plane [15]. However, an HV deformity is characterized by changes in all three planes. Therefore, it is better to correct the deformity not only in the transverse plane but also to take into account the pronation of the first MT bone as well as the position of the sesamoid bones [16, 17]. Inadequate pronation of the first MT bone and insufficient reduction of the sesamoid bones can be significant risk factors for a recurrence [17–20].

A high recurrence rate of the deformity following SO [9] may be the reason for performing an AO. In this study, we considered an additional AO necessary in 17.3% of cases. Although some authors consider an AO mandatory when performing an HV correction [21, 22] clear guidelines about adding an AO are not yet defined.

Some complications, such as nonunion, unsuccessful osteosynthesis, and clawing of the big toe, are mostly associated with inadequate following of the surgical technique and lack of surgeon experience. Other possible complications, followed by very low incidence, are as follows: infection, fracture of the first MT bone due to weight bearing, deep vein thrombosis, complex regional pain syndrome, and osteonecrosis of the first MT head [23]. A stiff I MTP joint remains the most frequent complication. In our study, only two (3.8%) feet had this type of complication, while superficial infection was more frequent.

Based on our study, factors including preoperative HVA, IMTA, AOFAS, and the position of the sesamoid bones have a significant impact on the recurrence of the deformity in long-term follow-up. Whether additional AO was performed or not, it did not affect the recurrence.

Study limitations

There were difficulties in calling each patient individually to come for follow-up, especially those whose surgery was performed a long time ago. Some patients did not report for check-ups regularly, which is why they were called to come in after the time for follow-up had passed, which caused problems in accurately determining the time of recurrence of the deformity.

Conclusion

In general, moderate to severe HV foot deformities can be resolved quite successfully with SO. However, there is a significant degree of deformity recurrence. Patients with a case of recurrence rarely have symptoms requiring revision surgery. Large HVA and IMTA angles preoperatively, along with preoperative AOFAS and significant subluxation of the sesamoids, are considered risk factors for the recurrence of the deformity.

R E F E R E N C E S

1. *Meyer M.* Eine neue modifikation der hallux valgus operation. Zbl Chir 1926; 53: 3265–8. (German)
2. *Burutaran JM.* Hallux valgus y cortedad anatomica del primer metatarsano (correction quinrusica). Actual Med Chir Pied 1976; 13: 261–6. (Spanish)
3. *Borelli AN, Weil LS.* Modified Scarf bunionectomy: Our experience in more than 1000 cases. J Foot Surg 1991; 30: 609–22.
4. *Barouk LS.* Scarf osteotomy for hallux valgus correction. Local anatomy, surgical technique, and combination with other forefoot procedures. Foot Ankle Clin 2000; 5(3): 525–58.
5. *Lipscombe S, Molloy A, Sirikonda S, Hennessy MS.* Scarf osteotomy for the correction of hallux valgus: midterm clinical outcome. J Foot Ankle Surg 2008; 47(4): 273–7.
6. *Bock P, Lanz U, Kröner A, Grabmeier G, Engel A.* The scarf osteotomy: a salvage procedure for recurrent hallux valgus in selected cases. Clin Orthop Relat Res 2010; 468(8): 2177–87.
7. *Doty JF, Coughlin MJ.* Hallux valgus and hypermobility of the first ray: facts and fiction. Int Orthop 2013; 37(9): 1655–60.
8. *Swanton E, Mason L, Molloy A.* How do I use the scarf osteotomy to rotate the metatarsal and correct the deformity in three dimensions? Foot Ankle Clin 2018; 23(2): 239–46.
9. *Bock P, Kluger R, Kristen KH, Mittlböck M, Schuh R, Trnka HJ.* The Scarf Osteotomy with Minimally Invasive Lateral Release for Treatment of Hallux Valgus Deformity: Intermediate and Long-Term Results. J Bone Joint Surg Am 2015; 97(15): 1238–45.
10. *Fuhrmann RA, Zollinger-Kies H, Kundert HP.* Mid-term results of scarf osteotomy in hallux valgus. Int Orthop 2010; 34(7): 981–9.
11. *Crevoisier X, Mouhsine E, Ortolano V, Udin B, Dutoit M.* The scarf osteotomy for the treatment of hallux valgus deformity: a review of 84 cases. Foot Ankle Int 2001; 22(12): 970–6.
12. *Coetzee JC.* Scarf osteotomy for hallux valgus repair: the dark side. Foot Ankle Int 2003; 24(1): 29–33.
13. *Davies MB, Blundell CM, Marquis CP, McCarthy AD.* Interpretation of the scarf osteotomy by 10 surgeons. Foot Ankle Surg 2011; 17(3): 108–12.
14. *Jeuken RM, Schotanus MG, Kort NP, Deenik A, Jong B, Hendrickx RP.* Long-term follow-up of a randomized controlled trial comparing scarf to Chevron osteotomy in hallux valgus correction. Foot Ankle Int 2016; 37(7): 687–95.
15. *Deenik A, Verburg A, Louwerens JW, de Waal Malefijt M, de Bie R.* Evidence of treatment algorithms for hallux valgus. JSM Foot Ankle 2016; 1(1): 1003.
16. *Hatch DJ, Santrock RD, Smith B, Dayton P, Weil L Jr.* Triplane hallux abducto valgus classification. J Foot Ankle Surg 2018; 57(5): 972–81.
17. *Okuda R, Kinoshita M, Yasuda T, Jotoku T, Kitano N, Shima H.* The shape of the lateral edge of the first metatarsal head as a risk factor for recurrence of hallux valgus. J Bone Joint Surg Am 2007; 89(10): 2163–72.
18. *Okuda R, Kinoshita M, Yasuda T, Jotoku T, Kitano N, Shima H.* Postoperative incomplete reduction of the sesamoids as a risk

factor for recurrence of hallux valgus. J Bone Joint Surg Am 2009; 91(7): 1637–45.

19. *Kaufmann G, Sinz S, Giesinger JM, Braito M, Biedermann R, Dammerer D.* Loss of Correction After Chevron Osteotomy for Hallux Valgus as a Function of Preoperative Deformity. Foot Ankle Int 2019; 40(3): 287–96.
20. *Park CH, Lee W.* Recurrence of Hallux Valgus Can Be Predicted from Immediate Postoperative Non-Weight-Bearing Radiographs. J Bone Joint Surg 2017; 99(14): 1190–7.
21. *Lai MC, Rikhraj IS, Woo YL, Yeo W, Ng YCS, Koo K.* Clinical and Radiological Outcomes Comparing Percutaneous Chevron-Akin Osteotomies vs Open Scarf-Akin Osteotomies for Hallux Valgus. Foot Ankle Int 2018; 39(3): 311–7.
22. *Lee M, Walsh J, Smith MM, Ling J, Wines A, Lam P.* Hallux Valgus Correction Comparing Percutaneous Chevron/Akin (PECA) and Open Scarf/Akin Osteotomies. Foot Ankle Int 2017; 38(8): 838–46.
23. *Samaras D, Gougoulias N, Varitimidis S, Hantes M, Karachalios T, Malizos K,* et al. Midterm experience of Scarf osteotomy as a new technique in a General Orthopaedic Department. Foot (Edinb) 2019; 40: 68–75.

Received on December 26, 2022
Revised on March 5, 2023
Accepted on March 9, 2023
Online First March 2023

ORIGINAL ARTICLE

UDC: 615.463::616.314]:616.314-089.843
DOI: https://doi.org/10.2298/VSP221110016D

The effect of different cementation techniques on the amount of remaining excess cement depending on the crown-abutment margin level

Uticaj različitih tehnika cementiranja na količinu rezidualnog cementa u zavisnosti od lokalizacije margine krunica-nosač

Aleksandar Djordjević, Jelena Todić, Sanja Simić, Dragoslav Lazić, Zoran Vlahović, Ljiljana Šubarić

University of Priština/Kosovska Mitrovica, Faculty of Medical Sciences, Department of Dentistry, Kosovska Mitrovica, Serbia

Abstract

Background/Aim. One of the disadvantages of the cement-retained fixed implant-supported restorations is the residual cement, which is found on the superstructure after the cementation procedure and has been identified as a risk factor for the occurrence of peri-implantitis. The aim of the study was to examine the influence of cementation techniques on the amount of residual cement at different levels of demarcation of the abutment in relation to the gingiva in the process of cementing restorations on implants. **Methods.** The research was conducted in *in vitro* conditions on casts obtained after implant placement. The abutments are milled at the level of the gingiva, 1.5 mm subgingivally and 3 mm subgingivally**.** Zirconium dioxide ceramic restorations were cemented using a standard cementation technique, a cementation technique using Teflon tape, and a precementation method using a silicone replica of the abutment and a 3D printed replica. The amount of residual cement was measured by photograph analysis. Adobe Photoshop was used for software analysis of photographs and determination of cement surface. Statistical data processing was performed in the SPSS program, and the Kruskal-Wallis test was used for data analysis. **Results.** A comparative analysis of the effectiveness of cementation techniques at the gingival margin level revealed a statistically significant difference in the amount of residual cement in relation to the cementation technique ($p < 0.001$). Analyzing the cementation technique effectiveness at the level of the finish line, 1.5 mm subgingivally, it was established that there was a statistically significant difference in the amount of residual cement compared to the cementation technique ($p = 0.001$). Comparing the effectiveness of cementation techniques at the 3 mm subgingival finish line level, it was established that there was a statistically significant difference in the amount of residual cement compared to the cementation technique ($p < 0.001$). **Conclusion.** Subgingival localization significantly affects the amount of residual cement in fixed prosthetic restorations on implants. Applying precementation techniques significantly reduces the amount of residual cement.

Key words:
dental cements; dental implantation; denture, partial, fixed; in vitro techniques; methods.

Apstrakt

Uvod/Cilj. Jedan od nedostataka cementom fiksiranih nadoknada na implantatima predstavlja rezidualni cement, koji se nalazi na suprastrukturi nakon postupka cementiranja i označen je kao faktor rizika od pojave periimplantitisa. Cilj rada bio je da se ispita uticaj tehnika cementiranja na količinu rezidualnog cementa na različitim nivoima demarkacije nosača (*abutment*) u odnosu na gingivu u postupku cementiranja nadoknada na implantatima. **Metode.** Istraživanje je sprovedeno u *in vitro* uslovima na radnim modelima dobijenim nakon ugradnje implantata. Nosači su frezovani u nivou gingive, subgingivalno 1.5 mm i subgingivalno 3 mm. Nadoknade od cirkonijum dioksid keramike cementirane su standardnom tehnikom cementiranja, tehnikom cementiranja upotrebom teflonske trake i metodom precementiranja, upotrebom silikonske replike nosača i 3D štampane replike. Merenje količine rezidualnog cementa vršeno je analizom fotografije. Za potrebe softverske analize fotografije i određivanja površine cementa korišćen je program *Adobe Photoshop*. Statistička obrada podataka rađena je u SPSS programu, a za analizu podataka korišćen je Kruskal-Wallis test. **Rezultati.** Uporednom analizom efikasnosti tehnika cementiranja na nivou gingivalne margine ustanovljeno je da je postojala statistički značajna razlika u količini zaostalog cementa u odnosu na tehniku cementiranja ($p < 0,001$). Analizom efikasnosti tehnika cementiranja na nivou demarkacije 1.5

Correspondence to: Aleksandar Djordjević, University of Priština/Kosovska Mitrovica, Faculty of Medical Sciences, Department of Dentistry, Anri Dinana bb, 38 220 Kosovska Mitrovica, Serbia. E-mail: sasa-91@live.com

mm, ustanovljeno je da je postojala statistički značajna razlika u količini zaostalog cementa u odnosu na tehniku cementiranja ($p = 0{,}001$). Upoređivanjem efikasnosti tehnika cementiranja na nivou demarkacije 3 mm, ustanovljeno je da je postojala statistički značajna razlika u količini zaostalog cementa u odnosu na tehniku cementiranja ($p < 0{,}001$). **Zaključak.** Subgingivalna lokalizacija značajno utiče na količinu rezidualnog cementa kod fiksnih protetskih nadoknada na implantatima. Primenom tehnika precementiranja značajno se smanjuje količina rezidualnog cementa.

Ključne reči:
stomatološki cementi; stomatološka implantacija; zubna proteza, parcijalna, fiksna; in vitro; metodi.

Introduction

Fixed implant-supported prosthetic restorations can be screw-retained or cement retained. Both have their advantages and limitations [1]. The main advantage of screw-retained restorations is retrievability, while fracturing of the screw and achieving passive fit in the construction of a larger span are more complex and represent the most common challenges [2]. As an alternative, restorations fixed by the cementing process have been presented. These restorations are similar to conventional ones; they are technically simple to make, less sensitive to errors, and allow better passive fitting of the compensation in long-span constructions [3]. Various studies have shown that the biggest disadvantage of cement restorations on implants is residual cement (excess cement) [4, 5].

The presence of residual cement can lead to biological complications in the form of peri-implant mucositis and peri-implantitis [6]. Peri-implantitis, a pathological condition affecting the peri-implant tissues, is characterized by gingival inflammation and progressive bone loss around the implant [7]. Residual cement was found in a large number of patients with clinical or radiological signs of peri-implantitis [8].

Biological variations in the attachment epithelium, collagen fibers, and the relationship of the peri-implant tissues with the implant compared to the natural tooth result in a higher degree of permeability. Differences in peri-implant soft tissue structures allow the flow of cement deep below the gingival level leading to difficulty removing it in clinical conditions [9].

Various factors affect the cement flow in the cementing process, as well as the appearance of residual cement. Some of them are the amount of cement used, the cementation technique, the design of the abutment, and the gingival emergence profile; the location of the crown-abutment margin is mentioned as an important means [10].

The localization of the crown-abutment margin can be above the gingiva, at the gingival level, or below the gingival level [11]. In order to achieve better aesthetic results in clinical conditions, most therapists opt for subgingival localization of the crown-abutment margin. Belser et al. [12] proposed subgingival localization of the crown-abutment margin at the level of 1–2 mm, while Andersson et al. [13] proposed subgingival localization of the margin in order to achieve a better emergency profile defined by the superstructure, which is still the starting point of many clinicians. In order to control the amount of residual cement, various cementation techniques have been presented. The most commonly used cementation techniques are the standard technique [14], the technique using polytetrafluoroethylene (PTFE) tape, i.e., the Teflon tape [15], and precementation techniques with an abutment replica made in different ways [16]. However, there is not enough data in the literature about which cementation technique gives the best results depending on the localization of the margin finish line. The aim of this study was to examine the effectiveness of different cementation techniques on the amount of remaining excess cement depending on the crown-abutment margin location level.

Methods

The research was conducted *in vitro* on 3D-printed casts with artificial gingiva obtained after the implants were placed in clinical conditions. Specimens were divided into three groups in relation to the margin location (equigingival, subgingival 1.5 mm, and subgingival 3 mm). In each group, five measurements were made for each tested cementation technique.

The process of placing dental implants was achieved according to a two-phase protocol (MIS Implants Technologies Ltd, Israel) (Figure 1). The procedure of taking an impression was carried out according to a digital protocol. A scan body was placed on the implant, and an intraoral scanner 3Shape (3Shape, Copenhagen K, Denmark) was used for the scanning procedure (Figure 2). Digital master casts with artificial gingival masks were printed with a 3D printer (Asiga, MaxUV, Alexandria, Australia). Abutments were placed in the working models and milled (AF350, Amann Girrbach, Austria) using a titanium burr with shoulder finish line design (Edenta®, Austria).

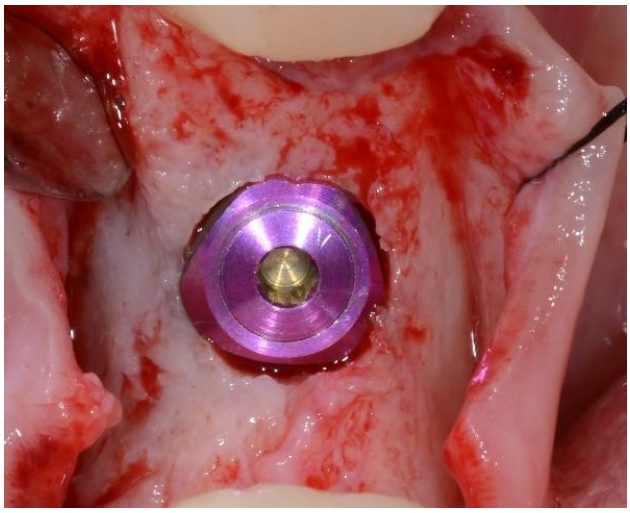

Fig. 1 – Implant placement in clinical conditions.

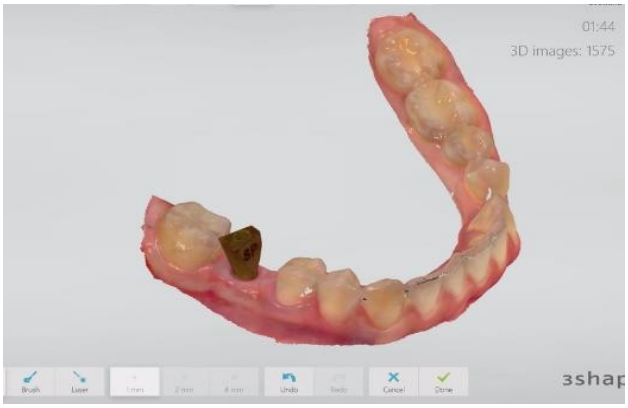

Fig. 2 – Intraoral digital scanning protocol.

The crowns were made with CAD/CAM technology from zirconium dioxide ceramics (SHOFU Disk ZR Lucent Supra, Shofu Dental Corporation, USA). The superstructures were designed in TRIOS Design Studio (3Shape, Copenhagen K Denmark). In the design of the superstructures, a space for cement of 50 μm was provided between the abutment and the crown. Furthermore, in the crown design process, an opening was created for access to the abutment screw, which enabled the removal of the abutment-crown sculpt from the replica after cementing for the photographing procedure. The opening was closed with a composite (GC Gradia Direct Posterior, GC Corporation, Alsip, USA) before the cementation procedure to prevent any effect on the cement flow. The restorations were finished with polishing and glazing. The standard cementation technique (ST) involved the preparation of cement according to the manufacturer's instructions. The same amount of cement (0.06 mL) was defined and applied to the crown using a 1 mL syringe. Following cement placement, the crown was settled on the abutment with moderate digital compression and controlled pressure. After setting, excess cement was removed with a probe, curette, and interdental floss (Super floss, OralB) using magnification under an operating microscope Zumax (Zumax Medical Co., Ltd UK) at ×16 magnification.

The second cementation technique, the PTFE technique, involved placing and adapting a Teflon tape under the margin of the abutment and crown junction (Figure 3). Cementation protocol and excess cement was removed according to the standard protocol (Figure 4).

Fig. 3 – Teflon tape placed to prevent cement flow.

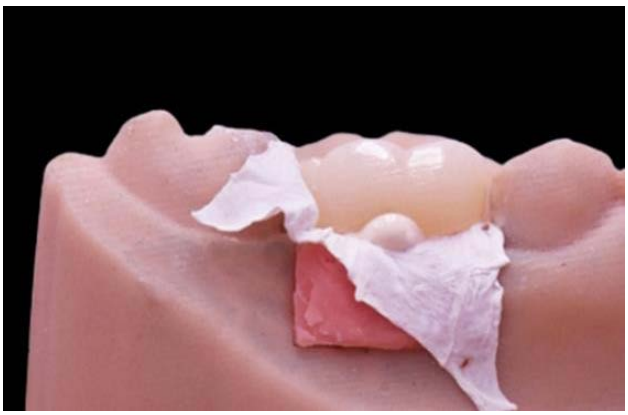

Fig. 4 – Crown placed on abutment during cementation procedure.

The third and fourth tested techniques are precementation procedures. In the third tested cementation technique, the silicone replica technique, abutment replicas were made of silicone (polyvinyl siloxane) and used for the precementation procedure. Teflon tape is placed into the superstructures, which aims to provide space for luting material. Consequently, silicone (PD Presigum light body, Allershausen, Germany) was inserted into the crown space (Figure 5). The silicone key replica was used to extrude the cement in the precementation procedure (Figure 6).

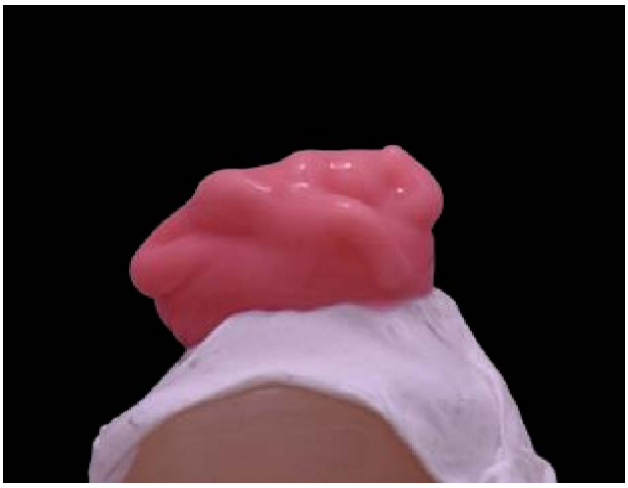

Fig. 5 – Making a silicone replica key.

Fig. 6 – Silicone replica used for precementation procedure.

The fourth cementation technique, the digital replica technique, was also tested, where instead of silicone, an abutment replica was printed with a 3D printer (Asiga, MaxUV, Alexandria, Australia). Since the abutments were scanned for suprastructure design, the same file was used for replica printing. Printed 3D resin replicas were used for the precementation procedure (Figures 7 and 8). Zinc oxide non-eugenol cement (Temp-Bond™, Kerr Corporation, USA) was used in the cementation procedure.

The amount of residual cement was measured by photograph analysis. A Digital Single Lens Reflex (DSLR) camera (Nikon, D7200) with a macro lens (Nikon 105 mm) and softbox flashes was used for photography. On the camera, a holder designed to accept the abutment-superstructure unit was fixed. The holder was used to ensure the same distance between the camera lens and the object being photographed. After the cementation procedure, the abutment-crown assembly was removed from the model and placed on the holder for the photography procedure. Photography was performed from four directions – mesial, distal, vestibular, and oral. Adobe Photoshop (Adobe©, San Jose, California, USA) was used for software analysis of photographs and measurement of residual cement surface area (Figure 9). The resulting numerical values are summed for each photo and displayed as a unique area in pixels.

Depending on the type of variables and normal distribution, data description is description is presented with numbers, arithmetic mean ± standard deviation, median, and range (minimum–maximum). The Kruskal-Wallis test was used as a method for testing statistical hypotheses. Statistical hypotheses were tested at the level of statistical significance (alpha level) of 0.05. All data were processed in the IBM SPSS Statistics 22 (SPSS Inc., Chicago, IL, USA) software package.

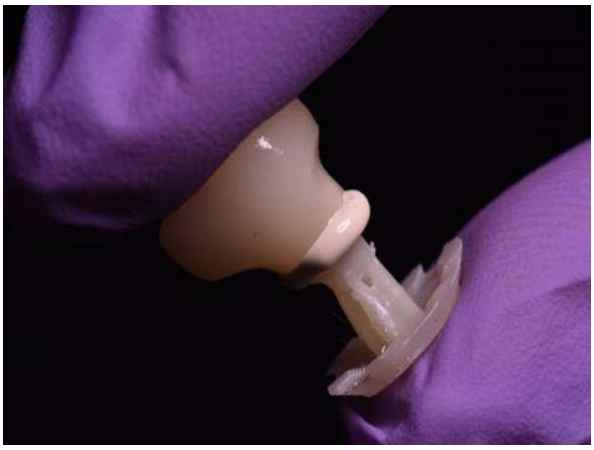

Fig. 7 – 3D-printed abutment replica used for precementation procedure.

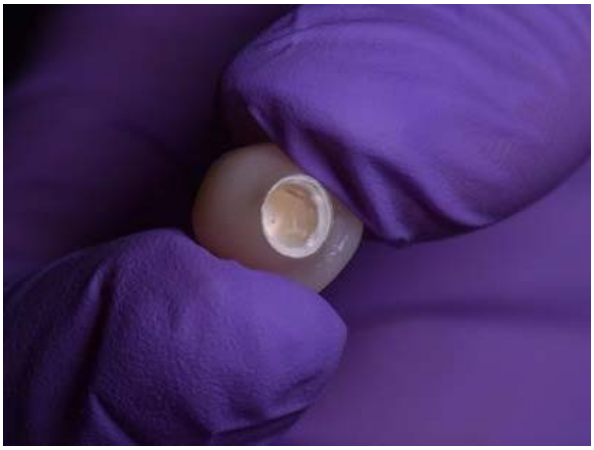

Fig. 8 – Remaining cement in the crown after the precementation procedure.

Fig. 9 – Measurement of residual cement area in software after photographing.

Results

A comparative analysis of the effectiveness of the cementation techniques at the equigingival level found that there was a statistically significant difference in the amount of residual cement compared to the cementation technique (Kruskal-Wallis = 17.857; $p < 0.001$) (Table 1).

Analyzing the effectiveness of the cementation techniques at the 1.5 mm subgingival margin position, it was established that there was a statistically significant difference in the amount of residual cement in relation to the cementation technique (Kruskal-Wallis = 17.583; $p = 0.001$) (Table 2).

A comparative analysis of the effectiveness of the cementation techniques at the 3 mm subgingival margin position revealed that there was a statistically significant difference in the amount of residual cement compared to the cementation technique (Kruskal-Wallis = 17.857; $p < 0.001$) (Table 3).

Depending on the cement margin location, there was a statistically significant difference in the amount of residual cement in all tested techniques (Kruskal-Wallis = 12,5; $p = 0.002$) (Figure 10).

Table 1

Values shown in pixels of different cementation techniques with margin at the gingival level

Cementation technique	n	mean ± SD	median	min–max
Standard	5	30787,2 ± 533,3	30456	30326–31423
Silicone replica	5	14014,0 ± 432,7	13872	13592–14597
PTFE	5	29854,4 ± 193,7	29785	29628–30129
Digital replica	5	11396,8 ± 395,6	11489	10784–11744

SD – standard deviation; min – minimum; max – maximum; PTFE – polytetrafluoroethylene i.e. Teflon tape.

Table 2

Values shown in pixels of different cementation techniques with 1.5 mm subgingival margin level

Cementation technique	n	mean ± SD	median	min–max
Standard	5	127120,8 ± 1586,7	126937	125260–129370
Silicone replica	5	15991,6 ± 98,6	16005	15836–16078
PTFE	5	123849,6 ± 1252,1	124352	122279–125321
Digital replica	5	11602,8 ± 408,0	11753	11000–11944

For abbreviations, see Table 1.

Table 3

Values in pixels of different cementation techniques with 3 mm subgingival margin level

Cementation technique	n	mean ± SD	median	min–max
Standard	5	152093,6 ± 1805,0	151670	150369–154214
Silicone replica	5	16651,8 ± 325,8	16606	16167–17012
PTFE	5	149146,2 ± 1043,1	149047	148018–150350
Digital replica	5	12200,2 ± 280,0	12123	11896–12612

For abbreviations, see Table 1.

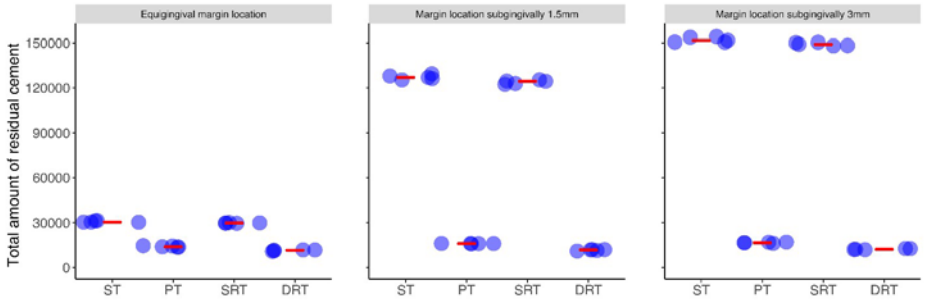

Fig. 10 – The values of residual cement amount in pixels of each individual measurement in relation to cementing technique and localization of margin location (represented by blue circles). The red line indicates the median. ST – standard technique; PT – polytetrafluoroethylene technique; SRT – silicone replica technique; DRT – digital replica technique.

Discussion

In our study, the largest amount of cement was found at the localization of a margin 3 mm below the gingival level using the ST. The results of our research are in correlation with the study of Linkevicius et al. [17], who indicate that deeper subgingival localization of the abutment-crown margin is a risk factor for remaining excess cement occurrence. The inability to remove cement from visually inaccessible places and places with more difficult access are major risk factors that can lead to residual cement occurrence [18]. The results that subgingival localization of the margin location leads to more difficult cement removal have been also confirmed in the study by Agar et al. [19]. This research also states that insisting on cement removal can lead to mechanical damage to the abutment and superstructure, which represents a point for the accumulation of dental plaque with consequent inflammation of the peri-implant soft tissues. In our research, when the localization of the abutment-crown margin was 1.5 mm subgingivally, there was a difference in relation to the position of 3 mm, but this difference was not statistically significant. Research indicates that any subgingival localization represents a potential risk of residual cement [6, 11]. In a clinical study by Wilson [8], it is stated that clinicians overestimate their ability to remove excess cement. In this study, up to 80% of the restorations had residual cement, even though the subjects were sure the excess cement had been completely removed. In our study, a statistically significantly smaller difference in the amount of cement was confirmed when the localization was at the level of the gingiva. The appearance of residual cement was present in the proximal regions due to the more difficult access because of the adjacent teeth; however, the total amount of cement differs significantly compared to other locations.

In addition to the difference in the amount of cement, it was observed, in our study, that the depth of margin location also affects the direction of cement flow. In the case of the margin positioned at 3 mm, part of the residual cement was located deep below the abutment-restoration margin, in some parts even at the junction of the abutment and the implant replica. In contrast, with a margin location at 1.5 mm below the gingival level, excess cement was retained in the space of the artificially formed sulcus in the region of the junction of the restoration, with the abutment higher in the occlusal direction.

The results of our study also show that the cementation technique plays an important role in the amount of residual cement. The highest amount of residual cement was observed with the ST. Studies by Wadhwani et al. [20] indicate that with the ST, the most important thing is the method of cement application and the amount of cement used. This research found that the majority of clinicians use significantly more cement than is really necessary, which leads to the appearance of residual cement due to the impossibility of its removal in deeply positioned margin positions.

Our research showed that the use of Teflon tape in deeply localized margins has no effect on the amount of residual cement. It was noted, however, that the placement of Teflon tape affects the direction of cement movement, preventing the flow of the cement in the direction of the implants. Furthermore, during the experiment, it was noted that using Teflon tape is more difficult to manipulate; it is time-consuming and can lead to splitting and entrapment between the crown and abutment, especially at the subgingival margin location. Similar observations were confirmed by Andrijauskas et al. [21], who compared the retraction cord and dental dam technique.

Our study showed that the amount of residual cement could be significantly reduced using a cementation technique with precementation procedures with the help of a replica abutment. Regardless of superstructure-abutment junction depth, a minimal amount of residual cement was identified. The results of our research are correlated with the study of Jagathpal et al. [16], who state in their research that the precementation procedures reduce the risk of residual cement, especially when a 3D-printed abutment replica model was used as an analog. However, there is not enough data in the literature on whether this amount of cement is sufficient for the long-term retention of the restoration and the utility value of the techniques in multi-member constructions, and further research in this direction is necessary.

Conclusion

With all limitations of *in vitro* study, it can be concluded that subgingival localization significantly affects the amount of residual cement in fixed prosthetic restorations on implants by cementing with a ST. By applying precementation techniques, the amount of residual cement can be reduced even in subgingival localizations of abutment-crown margins.

REFERENCES

1. *Wittneben JG, Joda T, Weber HP, Brägger U.* Screw retained vs. cement retained implant-supported fixed dental prosthesis. Periodontol 2000 2017; 73(1): 141–51.
2. *Lee A, Okayasu K, Wang HL.* Screw- versus cement-retained implant restorations: Current concepts. Implant Dent 2010; 19(1): 8–15.
3. *Ma S, Fenton A.* Screw- versus cement-retained implant prostheses: a systematic review of prosthodontic maintenance and complications. Int J Prosthodont 2015; 28(2): 127–45.
4. *Pesce P, Canullo L, Grusovin MG, de Bruyn H, Cosyn J, Pera P.* Systematic review of some prosthetic risk factors for periimplantitis. J Prosthet Dent 2015; 114(3): 346–50.
5. *Korsch M, Obst U, Walther W.* Cement-associated periimplantitis: a retrospective clinical observational study of fixed implant-supported restorations using a methacrylate cement. Clin Oral Implants Res 2014; 25(7): 797–802.
6. *Quaranta A, Lim ZW, Tang J, Perrotti V, Leichter J.* The Impact of Residual Subgingival Cement on Biological Complications

Around Dental Implants: A Systematic Review. Implant Dent 2017; 26(3): 465–74.
7. *Staubli N, Walter C, Schmidt JC, Weiger R, Zitzmann NU*. Excess cement and the risk of peri-implant disease - a systematic review. Clin Oral Implants Res 2017; 28(10): 1278–90.
8. *Wilson TG Jr*. The positive relationship between excess cement and peri-implant disease: a prospective clinical endoscopic study. J Periodontol 2009; 80(9): 1388–92.
9. *Korsch M, Walther W, Bartols A*. Cement-associated peri-implant mucositis. A 1-year follow-up after excess cement removal on the peri-implant tissue of dental implants. Clin Implant Dent Relat Res 2017; 19(3): 523–9.
10. *Linkevicius T*. How Abutment Margin Design Influences Cement Flow: Abutment Selection and Cement Margin Site. In: *Wadhwani C,* editor. Cementation in Dental Implantology: An Evidence-Based Guide. 2015th ed. Berlin: Springer; 2015. p. 101–12.
11. *Gehrke P, Bleuel K, Fischer C, Sader R*. Influence of margin location and luting material on the amount of undetected cement excess on CAD/CAM implant abutments and cement-retained zirconia crowns: an in-vitro study. BMC Oral Health 2019; 19(1): 111.
12. *Belser UC, Mericske-Stern R, Bernard JP, Taylor TD*. Prosthetic management of the partially dentate patient with fixed implant restorations. Clin Oral Implants Res 2000; 11(Suppl 1): 126–45.
13. *Andersson B, Odman P, Lindvall AM, Brånemark PI*. Cemented single crowns on osseointegrated implants after 5 years: results from a prospective study on CeraOne. Int J Prosthodont 1998; 11(3): 212–8.
14. *Canullo L, Cocchetto R, Marinotti F, Oltra DP, Diago MP, Loi I*. Clinical evaluation of an improved cementation technique for implant-supported restorations: a randomized controlled trial. Clin Oral Implants Res 2016; 27(12): 1492–9.
15. *Hess TA*. A technique to eliminate subgingival cement adhesion to implant abutments by using polytetrafluoroethylene tape. J Prosthet Dent 2014; 112(2): 365–8.
16. *Jagathpal AJ, Vally ZI, Sykes LM, du Toit J*. Comparison of excess cement around implant crown margins by using 3 extraoral cementation techniques. J Prosthet Dent 2021; 126(1): 95–101.
17. *Linkevicius T, Vindasiute E, Puisys A, Peciuliene V*. The influence of margin location on the amount of undetected cement excess after delivery of cement-retained implant restorations. Clin Oral Implants Res 2011; 22(12): 1379–84.
18. *Sancho-Puchades M, Crameri D, Özcan M, Sailer I, Jung RE, Hämmerle CHF,* et al. The influence of the emergence profile on the amount of undetected cement excess after delivery of cement-retained implant reconstructions. Clin Oral Implants Res 2017; 28(12): 1515–22.
19. *Agar JR, Cameron SM, Hughbanks JC, Parker MH*. Cement removal from restorations luted to titanium abutments with simulated subgingival margins. J Prosthet Dent 1997; 78(1): 43–7.
20. *Wadhwani C, Hess T, Piñeyro A, Opler R, Chung KH*. Cement application techniques in luting implant-supported crowns: a quantitative and qualitative survey. Int J Oral Maxillofac Implants 2012; 27(4): 859–64.
21. *Andrijauskas P, Zukauskas S, Alkimavicius J, Peciuliene V, Linkevicius T*. Comparing effectiveness of rubber dam and gingival displacement cord with copy abutment in reducing residual cement in cement-retained implant crowns: A crossover RCT. Clin Oral Implants Res 2021; 32(5): 549–58.

Received on November 10, 2022
Revised on February 22, 2023
Accepted on February 24, 2023
Online First March 2023

ORIGINAL ARTICLE

UDC: 616.24-006-08-036-037
DOI: https://doi.org/10.2298/VSP220627019N

Prognostic value of tumor-infiltrating T-lymphocytes density in the therapeutic response to initial platinum-based chemotherapy in patients with non-small cell lung cancer

Prognostička vrednost „gustine“ tumor-infiltrišućih T-limfocita u terapijskom odgovoru na inicijalnu hemioterapiju zasnovanu na platini kod bolesnika sa nesitnoćelijskim karcinomom pluća

Lora Novaković Lacković*†, Ljilja Latinović Tadić*‡, Mirko Stanetić*†, Marko Lacković§

***University of Banja Luka, Faculty of Medicine, Banja Luka, Republic of Srpska, Bosnia and Herzegovina; University Clinical Center of the Republic of Srpska, †Clinic for Pulmonary Diseases, ‡Department of Pathology, §Internal Clinic, Banja Luka, Republic of Srpska, Bosnia and Herzegovina**

Abstract

Background/Aim. The fact that lung carcinomas, like other solid tumors, can be immunogenic may have a substantial prognostic value in non-small cell lung cancer (NSCLC). Specific cytotoxic T-lymphocytes (CTL) can be demonstrated in most patients with primary tumors of different histological types. Two main groups of T-lymphocytes participate in the coupled recognition of tumor-specific antigens – CTL ($CD8^+$) and helper T-lymphocytes ($CD4^+$). The aim of the study was to assess the relationship between the tumor infiltration of T-lymphocytes and the therapeutic response to initial chemotherapy. **Methods.** Data were obtained from patients with NSCLC whose therapeutic response after four cycles of initial platinum-based chemotherapy was observed in relation to the density of tumor-infiltrating T-lymphocytes ($CD4^+$ and $CD8^+$) in small tumor biopsy samples. The therapeutic response was assessed in line with Response Evaluation Criteria in Solid Tumors (RECIST) 1.1 therapeutic response evaluation system. Based on the expected therapeutic response, the patients were divided into three groups: favorable therapeutic response patients (complete and partial regression), stable disease patients, and disease progression patients. To assess the density of $CD4^+$ and $CD8^+$ T-lymphocytes, the number of lymphocytes was determined at ×200 magnification (1.1 mm^2). Three visual fields with the densest lymphocyte infiltrate were selected for counting, and the values of all individual fields were added up. Based on the mean value, the samples were classified into the following groups: score 0, score 1, score 2, and score 3. During statistical data processing, low infiltration density combined score 0 and score 1 groups, and high infiltration density combined score 2 and score 3 groups. Based on the collected data, a database was created in SPSS 22.0 software and used for further statistical analysis. Statistical analysis of the data included descriptive and analytical statistics methods. **Results.** There was no significant difference in the distribution of $CD4^+$ T-lymphocytes and $CD8^+$ T-lymphocytes in the epithelial component of the tumor between patients with a different therapeutic response ($\chi^2 = 2.977$; $p = 0.226$ and $\chi^2 = 1.329$; $p = 0.515$, respectively). There was no significant influence of the infiltration density of $CD4^+$ T-lymphocytes and $CD8^+$ T-lymphocytes in the stromal component of the tumor on the therapeutic response ($\chi^2 = 0.606$; $p = 0.739$ and $\chi^2 = 5.167$; $p = 0.076$, respectively). **Conclusion.** The research did not prove that patients with a high level of tumor-infiltrating $CD4^+$ and $CD8^+$ T-lymphocytes in the epithelial and stromal component of the NSCLC had a better therapeutic response to standard initial chemotherapy.

Key words:
carcinoma, non-small cell lung; cd4-positive t-lymphocytes; prognosis, t-lymphocytes; t-lymphocytes, cytotoxic; treatment outcome.

Apstrakt

Uvod/Cilj. Činjenica da karcinomi pluća, kao i drugi solidni tumori, mogu biti imunogeni, može imati značajnu prognostičku vrednost kod nesitnoćelijskog karcinoma pluća (NSĆKP). Specifične citotoksične T-limfocite (CTL) moguće je dokazati kod većine bolesnika sa primarnim tumorima različitih histoloških tipova. Dve glavne grupe T-limfocita učestvuju u prepoznavanju tumor-specifičnih antigena: CTL ($CD8^+$) i pomoćnički

Correspondence to: Lora Novaković Lacković, University Clinical Center of the Republic of Srpska, Clinic for Pulmonary Diseases, 12 beba bb, 78 000 Banja Luka, Republic of Srpska, Bosnia and Herzegovina. E-mail: lora.novakovic@kc-bl.com

(*helper*) T limfociti (CD4+). Cilj rada bio je da se proceni veza između infiltracije T-limfocita u tumor i terapijskog odgovora na inicijalnu hemioterapiju. **Metode.** U istraživanju su korišćeni podaci bolesnika sa NSĆKP, čiji je terapijski odgovor nakon inicijalna četiri ciklusa hemioterapije platinom posmatran u odnosu na „gustinu" tumor-infiltrišućih T-limfocita (CD4+ i CD8+) u malim uzorcima biopsije tumora. Terapijski odgovor procenjivan je u skladu sa *Response Evaluation Criteria in Solid Tumor* (RECIST) 1.1 sistemom procene terapijskog odgovora. Na osnovu očekivanog terapijskog odgovora, bolesnici su bili podeljeni u tri grupe: bolesnici sa povoljnim terapijskim odgovorom (kompletna i delimična regresija), bolesnici u stabilnoj fazi bolesti i bolesnici sa progresijom bolesti. Broj limfocita za procenu gustine CD4+ i CD8+ T-limfocita određen je uz uvećanje x200 (1,1 mm^2). Za brojanje su odabrana tri vidna polja sa „najgušćim" infiltratom limfocita, zatim su vrednosti svih pojedinačnih polja sabrane. Na osnovu srednje vrednosti, uzorci su klasifikovani u sledeće grupe: skor 0, skor 1, skor 2, skor 3. Prilikom statističke obrade podataka, niska gustina infiltracije objedinila je grupe skora 0 i 1, a visoka gustina infiltracije objedinila je grupe skora 2 i 3. Na osnovu prikupljenih podataka kreirana je baza u softveru SPSS 22.0 koja je korišćena za dalju statističku analizu. Statistička analiza podataka obuhvatila je deskriptivne i analitičke statističke metode. **Rezultati.** Nije bilo značajne razlike u distribuciji CD4+ T-limfocita i CD8+ T-limfocita u epitelnoj komponenti tumora između bolesnika sa različitim terapijskim odgovorom (χ^2 = 2,977; p = 0,226 i χ^2 = 1,329; p = 0,515, redom). Nije bilo značajnog uticaja gustine infiltracije CD4+ T-limfocita i CD8+ T-limfocita u stromalnoj komponenti tumora na terapijski odgovor (χ^2 = 0,606; p = 0,739 i χ^2 = 5,167; p = 0,076, redom). **Zaključak.** Istraživanjem nije dokazano da bolesnici sa visokim nivoom tumor infiltririšućih CD4+ i CD8+ T-limfocita u epitelnoj i stromalnoj komponenti NSĆKP imaju bolji terapijski odgovor na standardnu inicijalnu hemioterapiju.

Ključne reči:
pluća, nesitnoćelijski karcinom; limfociti t, cd4; limfociti t; prognoza, limfociti t, citotoksični; lečenje, ishod.

Introduction

The number of patients with lung cancer has been increasing since the late 1960s, and the increase is more pronounced in women [1]. The introduction and application of chemotherapy protocols based on platinum achieved a significant improvement in patient survival. However, a median survival 'plateau', which is still less than one year, has also been reached [2, 3]. Despite the observed progress in treating patients with lung cancer, their survival is still poor. The five-year survival rate of patients with non-small cell lung cancer (NSCLC) is about 60% in those with localized disease, 33% in patients with regionally advanced disease, and only 6% in patients with distant metastases [4, 5]. The high mortality rate from lung cancer is a consequence of its ability to spread locally and/or metastasize very early after its formation. As many as 30–55% of operated stage IB to IIIA patients have recurrence after surgery and die from metastases [6].

The modern therapeutic approach recommends tumor genotyping and identification of mutations in specific oncogenes. Patients with metastatic NSCLC with a targetable oncogenic molecular driver variant and a PD-L1 expression level of 1% or more should receive first-line targeted therapies that yield higher response rates than immune checkpoint inhibitors (lower response rates) [7]. Nevertheless, platinum-based chemotherapy is still seen as the "gold standard" treatment for most patients with NSCLC.

Ideas about a certain connection between immunity and tumors date back to the beginning of the 19th century. Under ideal conditions, the anti-tumor immune response protects the body from developing cancer. This self-perpetuating cyclical process begins with the release of antigen from the tumor cell and ends with the killing of the tumor cell [7]. The key step of this cycle is when T-lymphocytes recognize tumor cells as dangerous. The recognition triggers the effector mechanisms of cellular immunity, i.e., the activation and multiplication of T-lymphocytes entering the bloodstream and reaching the tumor. Based on tumor-presenting antigens, T-lymphocytes attack and destroy cancer cells, thus releasing new antigens that start a new immune cycle [8].

In most patients with primary tumors of different histological types, it is possible to demonstrate specific cytotoxic T-lymphocytes (CTLs). CTLs (CD8+) and helper T-lymphocytes (CD4+) participate in the coupled recognition of tumor-specific antigens. Research shows that abundant infiltration of CTLs indicates a better prognosis and clinical course of the disease [9, 10].

The fact that different types of infiltrating immune cells in lung carcinomas have various effects on tumor progression may have a substantial prognostic value. The literature data support the notion of immune recognition and elimination of malignant cells [11]. The aim of the study was to assess the relationship between the infiltration density of tumor-infiltrating lymphocytes (TIL) and therapeutic response to initial chemotherapy.

Methods

A retrospective/prospective study conducted at the Clinic for Pulmonary Diseases and the Institute of Pathology of the University Clinical Center (UCC) in the Republic of Srpska (RS), Bosnia and Herzegovina, included patients from January 1, 2012, to June 30, 2014. The prospective part of the research lasted until the deadline for the follow-up of the respondents and was completed on June 30, 2017. The study was approved by the Ethics Committee of the UCC, RS (No 01-9-368.2/16 from June 06, 2016).

Patients

The research included 93 patients with NSCLC histologically verified by the Institute of Pathology of the RS UCC. The patients were treated at the Clinic for Pulmonary Diseases of the RS UCC.

Study design

To include patients in the research, the following was required: a histological diagnosis of NSCLC; the absence of previously diagnosed cancer of the lungs or other organs; the patients had to be radio-/chemonaive; locally advanced or metastatic disease [the tumor-T, node-N, and metastasis-M (TNM) – IIIA, IIIB, IIIC or IVA and IVB stage] confirmed clinically; the absence of epidermal growth factor receptor mutations.

Based on the expected therapeutic response, the patients were divided into three groups: favorable response patients (complete and partial regression), stable disease patients, and disease progression patients. The therapeutic response was assessed after the initial four cycles of platinum chemotherapy, in line with Response Evaluation Criteria in Solid Tumors (RECIST) 1.1 therapeutic response evaluation system: Stable Disease; Partial Response – 30% size reduction of the target lesion taking the initial dimension of the target lesion as a reference; Complete Response – complete disappearance of extranodal lesions with reduction of nodal lesions to < 10 mm in shorter diameter and disease progression; Progressive Disease – minimum 20% lesion size increase.

Evaluation of $CD4^+$ and $CD8^+$ T-lymphocytes density was accomplished with samples obtained by tumor biopsy before initial chemotherapy. For histological and immunohistochemical (IHC) analysis, the formalin-fixed and paraffin-embedded tissues were cut into 4–5 μm thick semiserial sections on a rotary microtome (microTec Cut 4055 SLEE MAINZ). After staining, according to the standard protocol for the routine hematoxylin-eosin method, the tissues are mounted in dibutylphthalate polystyrene xylene medium and analyzed with an Olympus BX41 light microscope (Olympus, Tokyo, Japan). For correct histological differentiation of lung tumors, IHC staining was used with antibodies for CK7, p63, TTF1, CK5/6, napsin A, synaptophysin, and chromogranin A. The prepared tumor tissues were IHC analyzed according to the selected antibodies range on an automated platform for IHC staining (Ventana BenchMark GX). All used monoclonal antibodies (SP35, SP57, SP141, SP52, D5/16B4, 4A4, SP11, LK2H10, MRQ-60) for immunophenotyping of tumor cells and detection of $CD4^+$ and $CD8^+$ T-lymphocytes were optimally diluted (ready-to-use format) and compatible with the detection system for visualization (ultraView Universal DAB detection kit) and other Ventana Medical Systems, Inc. reagents prepared for automatic staining. The software-designed protocol for antigen visualization included tissue deparaffinization, antigen unmasking, visualization of immune deposits in the tissue, and contrasting the surrounding tissue. Verified positive and negative control tissue was added to each tumor tissue sample to control the quality of IHC staining. The number of $CD4^+$ and $CD8^+$ T lymphocytes with positive staining were counted in epithelial and stromal components of the tumor (Figures 1 and 2). To assess the density of $CD4^+$ and $CD8^+$ T-lymphocytes, the number of lymphocytes was determined at ×200 magnification (1.1 mm^2). Three visual fields with the densest infiltrate were selected for counting, and the values of all individual fields were added up. The preparations were read by a pathologist using a four-tiered scale based on the mean value: score 0 (no lymphocytes or without inflammatory infiltration), score 1 (1–19 lymphocytes or rare infiltration densi-

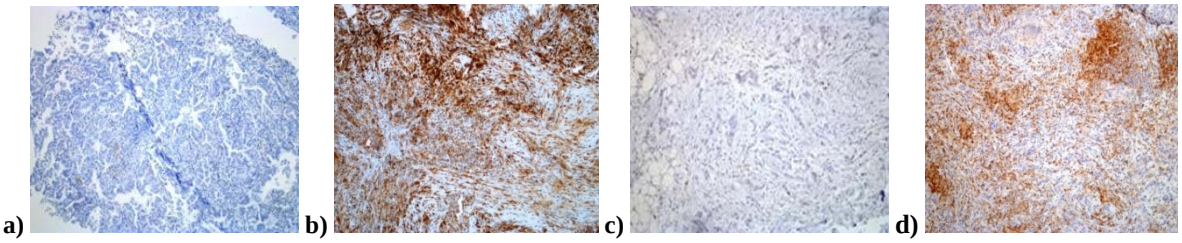

Fig. 1 – Immunohistochemical staining of tumor tissue with anti-CD4 antibody: a) Low density of $CD4^+$ T-lymphocytes in the epithelial component; b) High density of $CD4^+$ T-lymphocytes in the epithelial component; c) Low density of $CD4^+$ T-lymphocytes in the stromal component; d) High density of $CD4^+$ T-lymphocytes in the stromal component (×200 magnification, 1.1 mm^2).

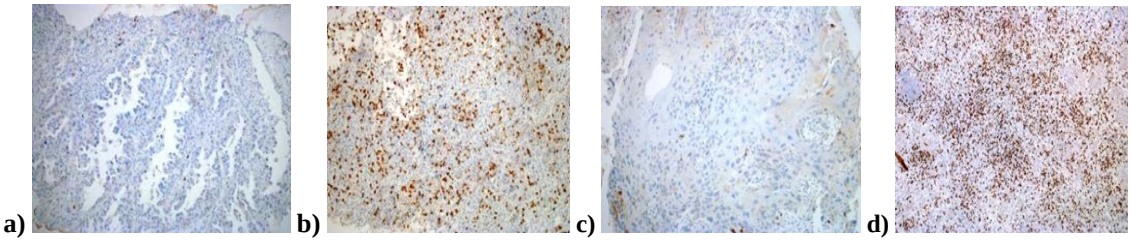

Fig. 2 – Immunohistochemical staining of tumor tissue with anti-CD8 antibody: a) Low density of $CD8^+$ T-lymphocytes in the epithelial component; b) High density of $CD8^+$ T-lymphocytes in the epithelial component; c) Low density of $CD8^+$ T-lymphocytes in the stromal component; d) High density of $CD8^+$ T-lymphocytes in the stromal component (×200 magnification, 1.1 mm^2).

ty), score 2 (20–49 lymphocytes or moderately infiltration density), and score 3 (more than 50 lymphocytes or high infiltration density) [12, 13]. During statistical processing of the data, due to the small number of samples in the group scores 2 and 3, case patients with TIL categories 0 to 1 were put in the low-TIL group, and those with scores 2 and 3 were grouped as high-TIL tumor patients.

Statistical analysis

Statistical analysis was performed using SPSS for Windows (Version 22; SPSS, Chicago, IL, USA). Descriptive data for all groups and variables will be presented as numbers and percentages and compared with the χ^2 test. The independent variable used in the research is a therapeutic response. A statistically significant difference was defined at the $p < 0.05$ level and a difference of very high statistical significance at the $p < 0.01$ level.

Results

The obtained data showed no patient with a complete therapeutic response.

We did not prove any differences in the distribution of $CD4^+$ T-lymphocytes in the epithelial component of the tumor between patients with a different therapeutic response ($\chi^2 = 2.977$; $p = 0.226$). Moreover, we did not prove any significant differences in the distribution of $CD8^+$ T-lymphocytes in the epithelial component of the tumor between patients with a different therapeutic response ($\chi^2 = 1.329$; $p = 0.515$) (Table 1, Figure 3).

There was no statistically significant influence of the infiltration density of $CD4^+$ T-lymphocytes in the stromal component of the tumor on the therapeutic response ($\chi^2 = 0.606$; $p = 0.739$). Also, there was no statistically significant influence of the infiltration density of $CD8^+$ T-lymphocytes in the stromal component of the tumor on the therapeutic response ($\chi^2 = 5.167$; $p = 0.076$) (Table 2, Figure 4).

Table 1

Distribution of patients in relation to the density of infiltration $CD4^+$ and $CD8^+$ T-lymphocytes in the epithelial component of the tumor

Response to therapy	Low density		High density	
	$CD4^+$	$CD8^+$	$CD4^+$	$CD8^+$
Partial response	27 (38.0)	24 (36.9)	4 (18.2)	7 (25)
Stable disease	22 (31.0)	21 (32.3)	9 (40.9)	10 (35.7)
Progressive disease	22 (31.0)	20 (30.8)	9 (40.9)	11 (39.3)
Total	71 (100.0)	65 (100.0)	22 (100.0)	28 (100.0)

All values are expressed as numbers (percentages).

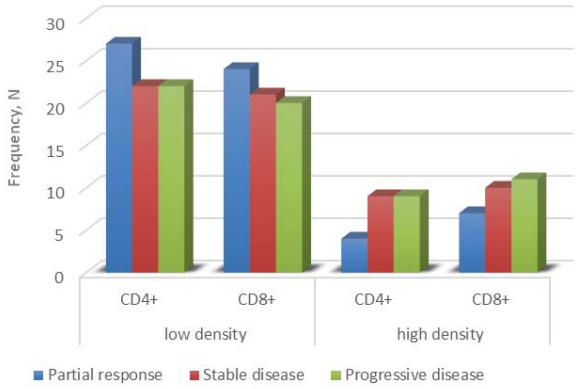

Fig. 3 – Distribution of patients in relation to the density of infiltration of $CD4^+$ and $CD8^+$ T-lymphocytes in the epithelial component of the tumor.
N – number.

Table 2

Distribution of patients in relation to the density of infiltration CD4+ and CD8+ T-lymphocites in the stromal component

Response to therapy	Low density		High density	
	$CD4^+$	$CD8^+$	$CD4^+$	$CD8^+$
Partial response	14 (32.6)	14 (38.9)	17 (34.0)	17 (29.8)
Stable disease	13 (30.2)	7 (19.4)	18 (36.0)	24 (42.1)
Progressive disease	16 (37.2)	15 (41.7)	15 (30.0)	16 (28.1)
Total	43 (100.0)	36 (100.0)	50 (100.0)	57 (100.0)

All values are expressed as number (percentages).

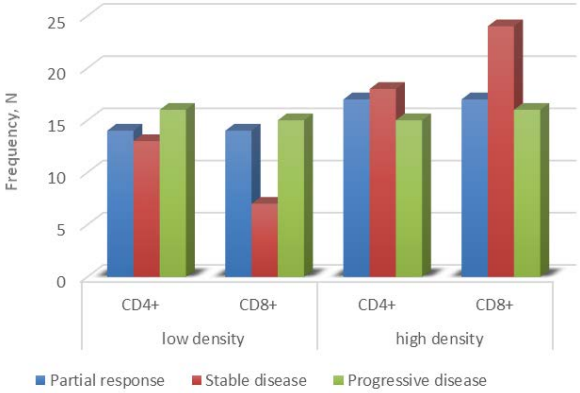

Fig. 4 – Distribution of patients in relation to the density of infiltration of CD4⁺ and CD8⁺ T-lymphocytes in the stromal component of the tumor.
N – number.

We did not prove that the density (low/high) of the inflammatory CD4⁺ T-lymphocyte infiltrate in the epithelial component of the tumor [χ^2 (1) = 2.977; p = 0.084] and the stromal component of the tumor [χ^2 (1) = 0.022; p = 0.883] were relevant for partial response to initial chemotherapy.

The results of the Pearson's χ^2 test [χ^2 (1) = 5.099; p = 0.024] demonstrate a significant difference in the distribution of patients in terms of response to therapy (stable disease) based on CD8⁺ T-lymphocytes density in the stromal component of the tumor (Table 2, Figure 4).

Discussion

Despite evident progress and the discovery of new molecules (target therapy and immunotherapy), conventional platinum-based chemotherapy remains the "gold standard" for most patients suffering from NSCLC. Initial treatment involves four cycles of chemotherapy. In addition to platinum, the most frequently added are etoposide, gemcitabine, paclitaxel, docetaxel, or vinorelbine because combined therapies provide a better therapeutic response and overall survival (OS) rate compared to those without platinum. Chemotherapy with cisplatin results in a small but statistically significant improvement in survival compared with good supportive care [14, 15]. The median OS in patients with advanced NSCLC not treated with chemotherapy is 4.5 months. The use of chemotherapy improves the one-year OS rate from 10–20% to 30–50% [16].

The clear superiority of one platinum-containing combination over another was demonstrated in controlled trials [17]. The most frequently applied protocols in our research were cisplatin-etoposide, 44 (47.3%), and cisplatin-gemcitabine, 28 (30.1%). Other platinum-based protocols used included paclitaxel, docetaxel, and vinorelbine.

There are two components of tumor tissue – parenchyma (made up of tumor cells) and tumor stroma. These two components are closely related. Parenchyma is the part of the tumor that determines its biological properties. Tumor stroma consists of an extracellular matrix, blood vessels, and cellular elements that define tumor growth and evolution. Inflammatory cells also belong to the cellular components of the tumor stroma. T-lymphocytes are a significant factor for local (*in situ*) tumor immunity. Conducted studies on the prognostic role of immune cells in NSCLC gave contradictory results [18–20]. In searching for an answer to the connection between a high density of lymphocyte infiltration and therapeutic response, it is necessary to distinguish subtypes of TIL [21].

Regarding the research results, we concluded that the density (low/high) of inflammatory CD4⁺ T-lymphocyte infiltrate in the epithelial and stromal components was irrelevant for optimal response to the initial chemotherapy.

A systematic review and meta-analysis of studies that gave a correlation between the infiltration density of CD4⁺ T-lymphocytes and OS and progression-free survival showed that CD4⁺ T-lymphocytes were associated with slightly improved OS (hazard ratio: 0.82; 95% confidence interval: 0.69–0.98) [22]. A positive relationship between tumor-infiltrating CD4⁺ T-lymphocytes density and the response to chemotherapy in an examination of the density of TIL (high and low) and the response to chemotherapy was not observed by pooling patients with complete and partial responses [23]. CD4⁺ T-lymphocytes are thought to have the ability to suppress or regulate cellular immunity. However, their presence can potentially promote tumor growth. That indicates their inability to provide an effective immune response and leads to the conclusion that tumor-infiltrating T-lymphocytes are functionally impaired and incompletely activated and that they include regulatory subtypes that vary depending on the type of cancer [24].

Research performed to clarify the relationship between the number of tumor-infiltrating T-lymphocytes and clinical and pathological characteristics and clinical outcomes in patients with NSCLC showed that individual high density of CD4⁺ or CD8⁺ T-lymphocytes had no prognostic significance for therapeutic response to conventional chemotherapy. Although the level of infiltration by CD8⁺ T cells alone had no prognostic significance, the survival rate was signifi-

cantly higher for patients with both 'high' $CD8^+$ and 'high' $CD4^+$ T-cell infiltration than for the other two groups according to whether their tumors exhibited a 'high' or 'low' level of $CD4^+$ or $CD8^+$ T-lymphocyte infiltration (log-rank test, $p = 0.006$) [25].

Follow-up of the OS rate did not identify an interaction between TIL and chemotherapy treatment, as the OS rate in patients who received and those who did not receive chemotherapy was 0.88 and 0.90, respectively [26].

The research did not find any significant differences in the frequency distribution of $CD8^+$ T-lymphocytes in the epithelial and stromal components in patients with a favorable therapeutic response. The level of inflammatory $CD8^+$ T-lymphocyte infiltrate in the stromal component of the tumor had positive prognostic significance in patients with stable disease.

Literature data concluded that a high $CD8^+$ T-lymphocyte infiltration level in NSCLC is a favorable prognostic factor [23, 27]. Assessing $CD8^+$ T-lymphocyte infiltration in the stromal component of the tumor is more significant for prognostic value than assessing $CD8^+$ T-lymphocyte infiltration in the epithelial component of the tumor [28]. Although estimating the numbers of macrophages and $CD8^+$ T-cells in cancer nests and stroma are valuable biomarkers for predicting the prognosis of stage IV NSCLC patients treated with chemotherapy, we still cannot forecast the response to chemotherapy by counting them [29].

Meanwhile, numerous available research results did not prove any prognostic significance for total intraepithelial T cells and their subtypes ($CD8^+$ and $CD4^+$ T-lymphocytes) in patients with NSCLC [30].

The ability of tumor cells to produce immunosuppressive factors in the microenvironment, thereby impairing the ability of $CD8^+$ T-lymphocytes-mediated tumor cell lysis, might be a possible explanation for the results of this research [31, 32]. Most tumor antigens recognized by $CD8^+$ T-lymphocytes are mainly endogenously synthesized cytoplasmic or nuclear proteins displayed in complex with major histocompatibility complex (MHC) class I molecules. Low cytotoxicity of $CD8^+$ T-lymphocytes is caused by poor expression of the MHC class I complex performed by tumor cells [33]. $CD8^+$ T-lymphocytes can only recognize antigens within MHC class I molecules. That is also because the proliferation and differentiation of $CD8^+$ T cells in CTL require co-stimulation and/or the help of $CD4^+$ T-lymphocytes, which recognize peptides in complex with MHC class II molecules. TIL density assessed in small biopsy samples is valid. However, it cannot reliably represent their density in the entire tumor because of the heterogeneity of $CD8^+$ T-lymphocytes in NSCLC. That is why additional studies are recommended before valid clinical conclusions can be drawn. These studies would directly measure the prognostic or predictive value of $CD8^+$ T-lymphocyte count in small biopsy specimens [34].

Limitations of the study

The shortcomings of the conducted research are the sample size. We should assume that the observed occurrences regarding the sample size would also gain statistical significance. Other shortcomings of the conducted research are the small bioptic samples.

Conclusion

The prognostic significance of TIL is controversial. Different tumor sampling strategies can give inconsistent results on the density of TIL and change the identification of tumors with a high density of TIL, which requires the standardization of IHC staining, scoring system, and localization. The spatial distribution of tumor-infiltrating cells in the tumor microenvironment is heterogeneous, so counting T-lymphocytes in small biopsy samples cannot reliably represent their density in the entire tumor. Future research should focus on the functional analysis of $CD4^+$ and $CD8^+$ T-lymphocytes and assess the inflammatory infiltrate density as a prognostic factor in immunotherapy.

Conflict of interest

The authors declare no conflict of interest.

REFERENCES

1. *International Agency for Research on Cancer – World Health Organization*. Cancer Over Time – Age-standardized rate (World) per 100 000, incidence, males and females [Internet]. Lyon, FR: International Agency for Research on Cancer; 2016 [accessed 2023 May 22]. Available from: https://gco.iarc.fr/overtime/en/dataviz/trends?populations=75200&multiple_populations=1&sexes=1_2
2. *Bunn PA Jr, Kelly K*. New combinations in the treatment of lung cancer: a time for optimism. Chest 2000; 117(4 Suppl 1): 138S–143S.
3. *Bunn PA Jr*. Chemotherapy for advanced non-small-cell lung cancer: who, what, when, why? J Clin Oncol 2002; 20(18 Suppl): 23S–33S.
4. *American Cancer Society*. Lung Cancer – Early Detection, Diagnosis, and Staging [Internet]. Atlanta, GA: American Cancer Society; 2019 [updated 2023 March 1; accessed 2023 May 18]. Available from: https://www.cancer.org/content/dam/CRC/PDF/Public/8705.00.pdf
5. *Bray F, Ferlay J, Soerjomataram I, Siegel RL, Torre LA, Jemal A*. Global cancer statistics 2018: GLOBOCAN estimates of incidence and mortality worldwide for 36 cancers in 185 countries. CA Cancer J Clin 2018; 68(6): 394–424.
6. *Uramoto H, Tanaka F*. Recurrence after surgery in patients with NSCLC. Transl Lung Cancer Res 2014; 3(4): 242–9.
7. *Mazieres J, Drilon A, Lusque A, Mhanna L, Cortot AB, Mezquita L*, et al. Immune checkpoint inhibitors for patients with advanced lung cancer and oncogenic driver alterations: results from the IMMUNOTARGET registry. Ann Oncol 2019; 30(8): 1321–8.
8. *Chen DS, Mellman I*. Oncology Meets Immunology: The Cancer-Immunity Cycle. Immunity 2013; 39(1): 1–10.
9. *Ganesan AP, Johansson M, Ruffell B, Yagui-Beltrán A, Lau J, Jablons DM*, et al. Tumor-infiltrating regulatory T cells inhibit

endogenous cytotoxic T cell responses to lung adenocarcinoma. J Immunol 2013; 191(4): 2009–17.
10. *Ishibashi Y, Tanaka S, Tajima K, Yoshida T, Kuwano H*. Expression of Foxp3 in non-small cell lung cancer patients is significantly higher in tumor tissues than in normal tissues, especially in tumors smaller than 30 mm. Oncol Rep 2006; 15(5): 1315–9.
11. *Fridman WH, Pagès F, Sautès-Fridman C, Galon J*. The immune contexture in human tumours: impact on clinical outcome. Nat Rev Cancer 2012; 12(4): 298–306.
12. *Galon J, Pagès F, Marincola FM, Angell HK, Thurin M, Lugli A*, et al. Cancer classification using the Immunoscore: a worldwide task force. J Transl Med 2012; 10: 205.
13. *Donnem T, Kilvaer TK, Andersen S, Richardsen E, Paulsen EE, Hald SM*, et al. Strategies for clinical implementation of TNM-Immunoscore in resected nonsmall-cell lung cancer. Ann Oncol 2016; 27(2): 225–32.
14. *Hanna N, Johnson D, Termin S, Baker S Jr, Brahmer J, Ellis PM*, et al. Systemic therapy for stage IV non-small-cell lung cancer: American Society of Clinical Oncology clinical practice guideline update. J Clin Oncol 2017; 35(30): 3484–515.
15. *Pirker R, Filipits M*. Adjuvant Therapy in Patients With Completely Resected Non-small-cell Lung Cancer: Current Status and Perspectives. Clin Lung Cancer 2019; 20(1): 1–6.
16. *Schiller JH, Harrington D, Belani CP, Langer C, Sandler A, Krook J*, et al. Comparison of four chemotherapy regimens for advanced non-small-cell lung cancer. N Engl J Med 2002; 346(2): 92–8.
17. *Baggstrom MQ, Stinchcombe TE, Fried DB, Poole C, Hensing TA, Socinski MA*. Third-generation chemotherapy agents in the treatment of advanced non-small cell lung cancer: a meta-analysis. J Thorac Oncol 2007; 2(9): 845–53.
18. *Bindea G, Mlecnik B, Tosolini M, Kirilovsky A, Waldner M, Obenauf AC*, et al. Spatiotemporal dynamics of intratumoral immune cells reveal the immune landscape in human cancer. Immunity 2013; 39(4): 782–95.
19. *Dunn GP, Old LJ, Schreiber RD*. The immunobiology of cancer immunosurveillance and immunoediting. Immunity 2004; 21(2): 137–48.
20. *Dieu-Nosjean MC, Antoine M, Danel C, Heudes D, Wislez M, Poulot V*, et al. Long-term survival for patients with non-small-cell lung cancer with intratumoral lymphoid structures. J Clin Oncol 2008; 26(27): 4410–7.
21. *Brambilla E, Le Teuff G, Marguet S, Lantuejoul S, Dunant A, Graziano S*, et al. Prognostic Effect of Tumor Lymphocytic Infiltration in Resectable Non-Small-Cell Lung Cancer. J Clin Oncol 2016; 34(11): 1223–30.
22. *Gooden MJ, de Bock GH, Leffers N, Daemen T, Nijman HW*. The prognostic influence of tumour-infiltrating lymphocytes in cancer: a systematic review with meta-analysis. Br J Cancer 2011; 105(1): 93–103.
23. *Liu H, Zhang T, Ye J, Li H, Huang J, Li X*, et al. Tumor-infiltrating lymphocytes predict response to chemotherapy in patients with advance non-small cell lung cancer. Cancer Immunol Immunother 2012; 61(10): 1849–56.
24. *Nakamura H, Saji H, Ogata A, Hosaka M, Hagiwara M, Kawasaki N*, et al. Immunologic parameters as significant prognostic factors in lung cancer. Lung Cancer 2002; 37(2): 161–9.
25. *Hiraoka K, Miyamoto M, Cho Y, Suzuoki M, Oshikiri T, Nakakubo Y*, et al. Concurrent infiltration by CD8+ T cells and CD4+ T cells is a favourable prognostic factor in non-small-cell lung carcinoma. Br J Cancer 2006; 94(2): 275–80.
26. *Jackute J, Zemaitis M, Pranys D, Sitkauskiene B, Miliauskas S, Bajoriunas V*, et al. The prognostic influence of tumor infiltrating Foxp3(+)CD4(+), CD4(+) and CD8(+) T cells in resected non-small cell lung cancer. J Inflamm (Lond) 2015; 12: 63.
27. *Schalper KA, Brown J, Carvajal-Hausdorf D, McLaughlin J, Velcheti V, Syrigos KN*, et al. Objective measurement and clinical significance of TILs in non-small cell lung cancer. J Natl Cancer Inst 2015; 107(3): dju435.
28. *Dobrzanski MJ, Reome JB, Hylind JC, Rewers-Felkins KA*. CD8-mediated type 1 antitumor responses selectively modulate endogenous differentiated and nondifferentiated T cell localization, activation, and function in progressive breast cancer. J Immunol 2006; 177(11): 8191–201.
29. *Kawai O, Ishii G, Kubota K, Murata Y, Naito Y, Mizuno T*, et al. Predominant Infiltration of Macrophages and CD8+T Cells in Cancer Nests Is a Significant Predictor of Survival in Stage IV Nonsmall Cell Lung Cancer. Cancer 2008; 113(6): 1387–95.
30. *Kirshberg S, Izhar U, Amir G, Demma J, Vernea F, Beider K*, et al. Involvement of CCR6/CCL20/IL-17 axis in NSCLC disease progression. PLoS One 2011; 6: e24856.
31. *Salih HR, Rammensee HG, Steinle A*. Cutting edge: down-regulation of MICA on human tumors by proteolytic shedding. J Immunol 2002; 169(8): 4098–102.
32. *Wald O, Shapira OM, Izhar U*. CXCR4/CXCL12 axis in non small cell lung cancer (NSCLC) pathologic roles and therapeutic potential. Theranostics 2013; 3(1): 26–33.
33. *Kataki A, Scheid P, Piet M, Marie B, Martinet N, Martinet Y*, et al. Tumor infiltrating lymphocytes and macrophages have a potential dual role in lung cancer by supporting both host-defense and tumor progression. J Lab Clin Med 2002; 140(5): 320–8.
34. *Obeid JM, Wages NA, Hu Y, Deacon DH, Slingluff CL Jr*. Heterogeneity of $CD8^+$ tumor-infiltrating lymphocytes in non-small-cell lung cancer: impact on patient prognostic assessments and comparison of quantification by different sampling strategies. Cancer Immunol Immunother 2017; 66(1): 33–43.

Received on June 27, 2022
Revised on February 3, 2023
Accepted on March 21, 2023
Online First April 2023

ORIGINAL ARTICLE

UDC: 616.314
DOI: https://doi.org/10.2298/VSP220329010P

Evaluation of the impacted maxillary canines position, determination of the possible indicators of the impaction difficulty, and the risk factors for adjacent teeth root resorption

Procena položaja impaktiranih gornjih očnjaka, određivanje mogućih pokazatelja težine impakcije i faktora rizika od resorpcije korenova susednih zuba

Tina Pajević, Dina Vasović, Jovana Juloski, Ljiljana Vučić, Branislav Glišić

University of Belgrade, Faculty of Dental Medicine, Department of Orthodontics, Belgrade, Serbia

Abstract

Background/Aim. An impacted tooth is a tooth that could not erupt and take its place in the dental row. Impacted maxillary canines are a very frequent problem in orthodontic practices. They are the second most impacted teeth, right after the third molars. The aim of this cross-sectional study was to evaluate the two-dimensional and three-dimensional position of the impacted maxillary canines and make a descriptive study analysis of possible indicators of the impaction difficulty and risk factors for adjacent tooth root resorption. **Methods.** In this study, 94 subjects with 116 diagnosed maxillary canine impaction were included. The two-dimensional position of the impacted canines (IC) was evaluated on the panoramic projection of the cone beam computed tomography (CBCT) images. Canine position (CP) to the X, Y, and Z-axis was measured and scored using the novel classification system that incorporates three-dimensional information of CBCT imaging – the KPG index. Based on the KPG index value, impaction was defined as easy, moderate, difficult, and extremely difficult. In order to determine indicators of impaction difficulty and risk factors of root resorption of adjacent teeth, qualitative variables (gender, side of impaction, etc.) and quantitative variables [age, canine distance to the occlusal plane (OccP), etc.] were tested with multiple logistic regression. **Results.** The mean age of the subjects was 19.8 ± 5.2 years. The impactions were twice as prevalent in females compared to males. Most (71.4%) impactions were unilateral in palatal position of the canines. Adjacent root resorption was present in 27.3% of cases of impaction, and the central incisor was mostly affected. More than half of the impactions were of moderate level. In univariable analysis, canine distance to sagittal medial line (SML), angle between canine and SML, OccP, and first premolar, respectively, were significant in impaction difficulty prediction. Multivariable analysis showed that angle between canine and the first premolar could be a risk factor for adjacent root resorption. **Conclusion.** Most impacted maxillary canines were in the palatal position, with a KPG index value of moderate difficulty. Besides the position to the OccP and SML, angle between canine and the first premolar should be estimated, as a part of diagnostic procedures, to evaluate the risk of adjacent root resorption, prevent resorption, and decide on the treatment plan.

Key words:
cone-beam computed tomography; risk factors; tooth impacted; tooth resorption.

Apstrakt

Uvod/Cilj. Impaktirani zub je zub koji nije mogao da izbije i zauzme odgovarajuće mesto u zubnom nizu. Impaktirani maksilarni očnjaci su veoma čest problem u ortodontskoj praksi. Po učestalosti slučajeva impakcije, maksilarni očnjaci su na drugom mestu, iza umnjaka. Cilj studije preseka bio je da se proceni dvodimenzionalni i trodimenzionalni položaj impaktiranih maksilarnih očnjaka, kao i da se deskriptivnom studijom analiziraju mogući pokazatelji težine impakcije i faktori rizika od resorpcije korenova susednih zuba. **Metode.** Studijom je obuhvaćeno 94 ispitanika sa 116 impaktiranih očnjaka. Položaj očnjaka u dvodimenzionalnom sistemu ispitan je na panoramskoj projekciji snimka dobijenog metodom kompjuterizovane tomografije konusnog zraka (KTKZ). Položaj očnjaka duž X, Y i Z ose ispitan je i procenjen primenom novog sistema klasifikacije, koji uključuje trodimenzionalne informacije iz snimka KTKZ – KPG indeksa. Na osnovu vrednosti KPG indeksa, impakcija je bila ocenjena kao laka, umerena, teška i

Correspondence to: Tina Pajević, University of Belgrade, Faculty of Dental Medicine, Department of Orthodontics, Gastona Gravijea 2, 11 000 Belgrade, Serbia. E-mail: tina.pajevic@stomf.bg.ac.rs

veoma teška. Da bi se utvrdili pokazatelji težine impakcije i faktori rizika od resorpcije korenova susednih zuba, primenom multivariacione regresije ispitivane su kvalitativne varijable (pol, strana impakcije, itd.), kao i kvantitativne varijable [životno doba, položaj očnjaka prema okluzalnoj ravni (OkR), itd.]. **Rezultati.** Prosečna starost ispitanika bila je 19,8 ± 5,2 godina. Učestalost impakcija kod žena bila je dva puta veća nego kod muškaraca. Većina (71,4%) impakcija bile su unilateralne, sa palatinalnim položajem očnjaka. Resorpcija korenova susednih zuba uočena je kod 27,3% slučajeva, a impakcijom je najčešće bio zahvaćen centralni sekutić. U više od polovine impaktiranih očnjaka težina impakcije je bila umerena. U univarijabilnoj analizi, rastojanje očnjaka od sagitalne medijalne linije (SML), nagib očnjaka prema SML i OkR, kao i nagib očnjaka prema prvom premolaru pokazali su statističku značajnost za procenu težine impakcije**.** Multivarijabilnom analizom ustanovljeno je da nagib očnjaka prema prvom premolaru može biti pokazatelj rizika od resorpcije korenova susednih zuba. **Zaključak.** Većina impaktiranih očnjaka bila je palatinalno postavljena, sa vrednostima KPG indeksa koji je ukazivao na umerenu težinu impakcije. Pored položaja očnjaka prema OkR i SML, u okviru dijagnostičkih procedura trebalo bi izmeriti i nagib očnjaka prema prvom premolaru, kako bi se procenio rizik od resoprcije korenova susednih zuba, sprečila resorpcija i odredio plan terapije.

Ključne reči:
tomografija, kompjuterizovana, konusna; faktori rizika; zub, impakcija; zub, koren, resorpcija.

Introduction

Impacted maxillary canines are very frequent in orthodontic practices. Maxillary canines are diagnosed as impacted if the eruption is delayed above the age of 14 years. They are the second most impacted teeth, right after the third molars [1, 2], due to the longest path to travel and the longest time to reach the occlusal plane compared to other permanent teeth during their development [3]. Dewel [3] has described a number of different positions in which upper canines pass in the most crowded part of the maxilla in order to reach their position in the occlusion. Since the development of the canines takes a long time, those teeth are at significant risk of negative environmental factors that can influence their eruption and cause impaction.

A recently published study reported the prevalence of the impacted maxillary canines from 1.7% to 4.7% [4]. Sexual dimorphism is also observed in the maxillary canine impaction; it affects females two to three times more frequently than males [5]. Maxillary canines could be unilaterally or bilaterally impacted; unilateral impaction appears more frequently than bilateral [4, 6, 7]. Considering the spatial position, palatally displaced canines appear more frequently compared to the buccal position [8–10]. Impacted canines (ICs) are often associated with an increased risk for adjacent tooth root resorption. The most frequently affected teeth are incisors, although, in some cases, premolars could also be affected. The prevalence of root resorption of the lateral incisors, according to the literature, ranges from 18.5% to 70% [11–13].

The position of the IC crown and root tips varies not only in the vestibulo-oral direction but also in mesio-distal and occluso-gingival directions. A precise description of the canine position (CP) in the bone in relation to local anatomical structures and distance to referent planes is essential in creating an appropriate treatment plan and treatment outcome prediction. To summarize CP in all three planes, the KPG index was proposed in 2009 [14]. The canine crown and root tip in X, Y, and Z-axis are graded based on the distance to referent planes where the crown and root tips should be properly placed. The index is the sum of these grades, and its value is used for the 3D classification of the impaction difficulty. A good level of index agreement with the clinician's evaluation of impactions was reported, so it was proposed that the KPG index could be used in orthodontic practice [15].

The use of the KPG index is particularly helpful in epidemiological investigations of the ICs. The results of these studies could help create national healthcare protocols for the early diagnosis and early management of the ICs with the appropriate scheme of preventive and interceptive measurements. The aims of this study were to evaluate the two-dimensional and three-dimensional position of the impacted maxillary canines and determine the gender distribution of the impaction, possible predictors of the impaction difficulty, and potential risk factors for adjacent tooth root resorption.

Methods

The study included 94 patients with 116 ICs treated at the Department of Orthodontics, Faculty of Dental Medicine, University of Belgrade, Serbia, referred from the primary health care centers for further diagnostics and treatment. This investigation was approved by the Ethics Committee of the Faculty of Dental Medicine, University of Belgrade, on February 22, 2017 (No. 36/4).

The inclusion criteria were patients with at least one diagnosed unerupted maxillary canine on the panoramic radiographs. The standard diagnostic procedure included clinical evaluation (intraorally, canines were not palpable labially, palatal bulge was present), study cast analysis, and radiographic analysis. On the panoramic radiograph, maxillary canines were considered impacted if more than two-thirds of tooth roots were developed, but the tooth was still totally or partially in the bone. Exclusion criteria were patients with clefts and syndromes and patients in active orthodontic treatment of impaction before and during this study. Besides panoramic radiographs, all patients that were referred to take cone beam computed tomography (CBCT) scans of the maxilla at the Radiological Center of the Faculty of Dental Medicine, University of Belgrade, were included in this study. CBCT scans were taken on the same scanner,

Cranex® 3D (Soredex, PaloDEx Group Oy Finland), in the standard resolution with a 61 x 78 cm field of view and voxel size of 0.30 mm. The scan/exposure time was 20.1/4.7 s, and the imaging value was 60kV/6.3–12.5mA. Visualization and evaluation of Digital Imaging and Communication in Medicine (DICOM) files for each patient were done in the software OnDemand3D (Cybermed Inc., South Korea). The time interval between clinical and CBCT evaluations was four to six weeks apart.

For each patient, the following parameters were collected: general data regarding the gender and age of the patient; bilateral or unilateral canine impaction; the side of the impaction in cases of unilateral impaction; the presence of the deciduous canine; space between the lateral incisor and first premolar.

The IC localization was evaluated both two-dimensionally and three-dimensionally.

The two-dimensional evaluation was done on the panoramic view of the CBCT scan, and the following measurements were included: the distance of the canine crown tip to the sagittal medial line (SML); the distance of the canine crown tip from the occlusal plane (OccP); the distance of the apex to SML; the angle between canine and SML (Figure 1); the angle between canine and OccP (Figure 1); the angle between canine and lateral incisor (Figure 2); the angle between canine and first premolar (Figure 2).

The three-dimensional evaluation was conducted in the sagittal, coronal, and axial view of the CBCT scans and included: canine mesio-distal diameter; contact with lateral incisor classified as present or absent contact; localization in the vestibulo-oral direction, which was classified as vestibular, palatal, or in the middle of the alveolar ridge; resorption of the adjacent teeth, classified as absent resorption, resorption of the lateral incisor, resorption of the central incisor, resorption of the first premolar; localization of the tooth root and crown tips along X, Y, and Z-axis according to KPG index.

Both the canine crown and root tips were evaluated by the KPG index. All measurements were performed by one examiner. One month after the first measurement, the same investigator repeated the measurements for 39 randomly selected canines. The evaluation was conducted in the X, Y, and Z spatial planes. A panoramic view of the CBCT scan was used to measure the crown and root tip position in X and Y planes (Figures 3, 4, and 5). The crown and root tip

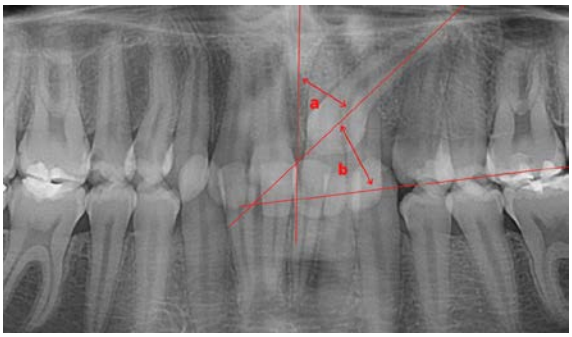

Fig. 1 – Measurements of the two-dimensional parameters on the panoramic view of the cone beam computed tomography. Red arrows annotate: a) Angle between canine and sagittal medial line; b) Angle between canine and occlusal plane.

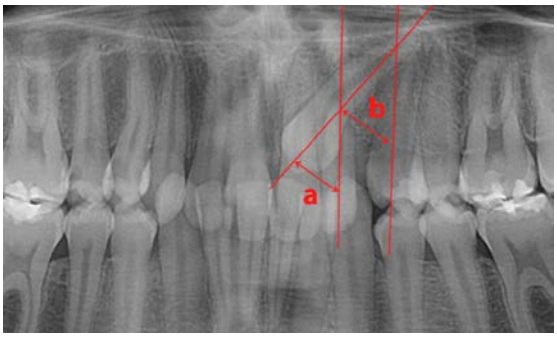

Fig. 2 – Measurements of the two-dimensional parameters on the panoramic view of the cone beam computed tomography. Red arrows annotate: a) Angle between canine and lateral incisor; b) Angle between canine and first premolar.

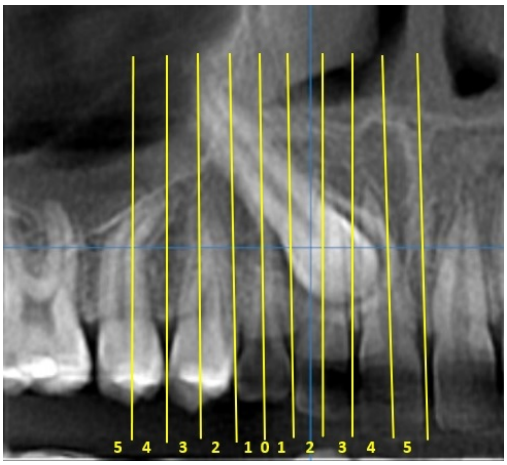

Fig. 3 – Three-dimensional evaluation of the impacted canines crown and root tip along the X-axis according to KPG index measurements. In this case, the canine crown tip was given a score of 4 and the root tip score of 2.

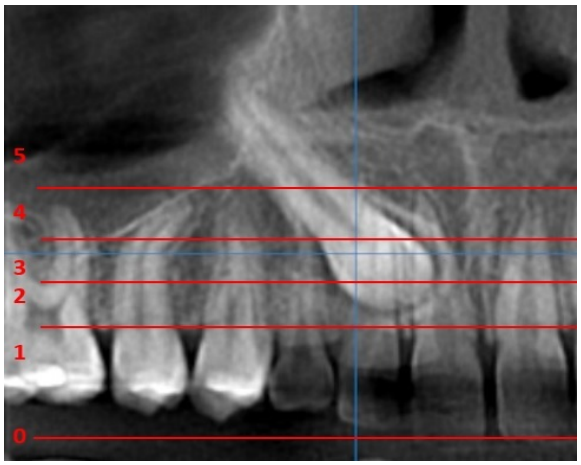

Fig. 4 – Canine crown tip evaluation along the Y-axis on the panoramic view of the cone beam computed tomography scan. In this patient, the canine crown tip along the Y-axis was given a score of 2.

position along the Z axis were analyzed on the axial view (Figures 6 and 7 a–d). Due to difficulties in estimating the crown and root tip position along the Z axis using the authors' [15] original scheme, in Figure 7, both the coronal and sagittal views of the crown and root position were evaluated in order to give the appropriate score. For each tooth cusp and root tip position in every coordinate plane, a score from 0–5 was given, according to deviation from their normal position. The more deviated root and crown tip position had a higher score. For every plane, there were two scores, one for the crown and one for the root tip. The sum of six scores gives a cumulative score that was used to evaluate the difficulty of the impaction. Based on the authors' definition, impaction was easy for the cumulative KPG index score 0–9, moderate for 10–14, difficult for 15–19, and extremely difficult for values 20 and above [14, 16].

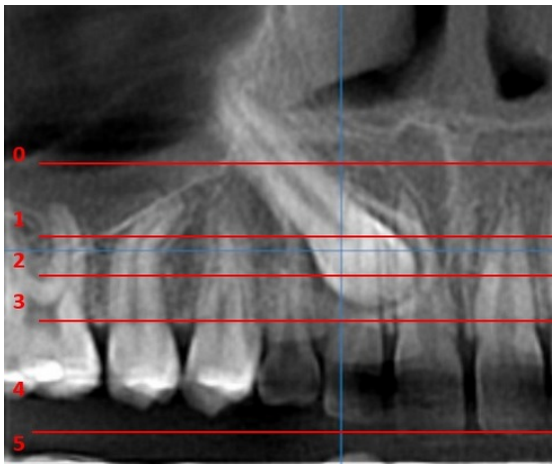

Fig. 5 – Canine root tip position along the Y-axis is graded reversed in comparison to the scores for the crown tip. For this canine root tip, the grade was 0.

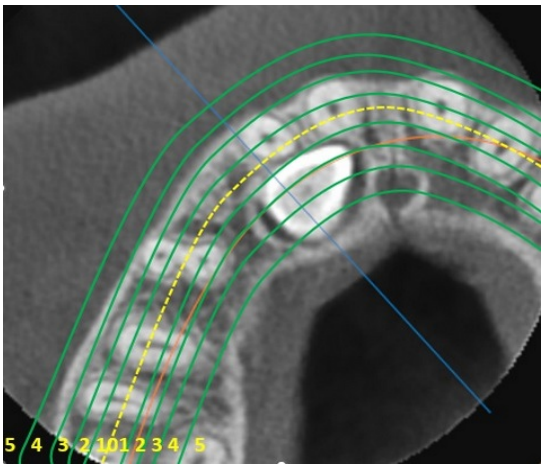

Fig. 6 – Canine crown evaluation along the Z-axis. This canine crown tip was graded a score of 2.

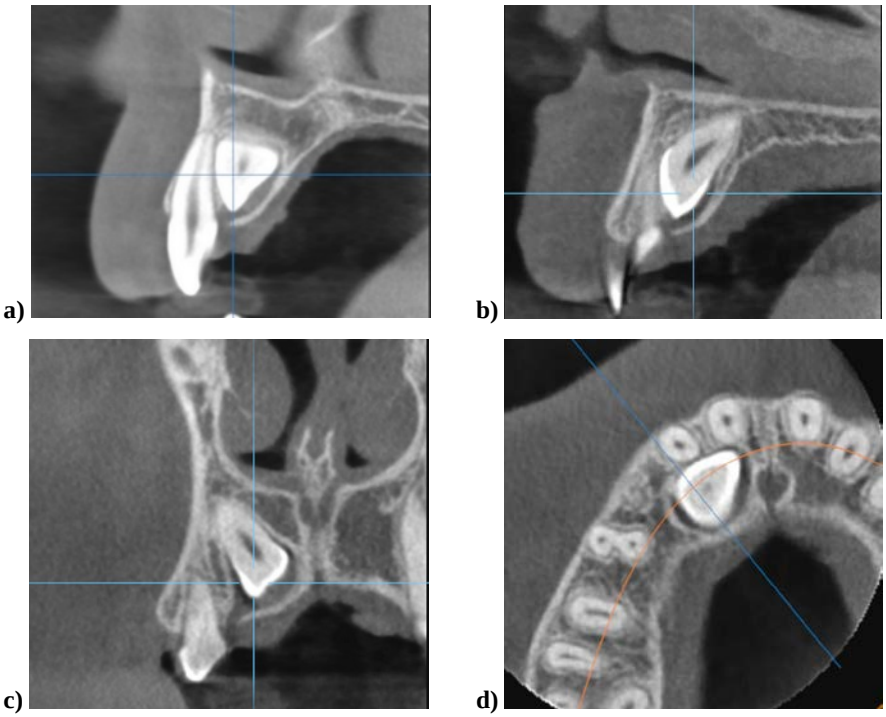

Fig. 7 – a) Sagittal position of the canine crown tip; b) Sagittal position of the canine root tip; c) Coronal view of the impacted canine; d) Axial view. Because of the difficulty to estimate the crown and root tip position along the Z-axis based on the authors' original scheme [15], besides the axial, both the coronal and sagittal view of the crown and root position were evaluated in order to give the appropriate score. For this canine crown tip, the score along the Z-axis was 2, and for the root tip, the score was 4.

Statistical analysis

Statistical analysis was performed using SPSS Version 19.0. (IBM Corp. Released 2010. IBM SPSS Statistics for Windows, Version 19.0. Armonk, NY: IBM Corp, USA). All canines were numbered and measured separately by one examiner. Distribution of the ICs by gender, age, side of the jaw, presence of deciduous canine, three-dimensional position, localization, difficulty, and contact with lateral incisor was evaluated by frequency. Descriptive statistics, such as mean and standard deviation (SD), were used for the two-dimensional quantitative variables (distance of the canine crown tip from SML, the angle between canine and SML, etc.). A total of 39 canines were randomly selected, and their KPG index was measured once again one month after the first measurement. The intra-observer reliability was evaluated with an intraclass correlation coefficient for the numerical variables, while Cohen's kappa was calculated for the categorical variables. The connection between probability for adjacent teeth resorption and investigated factors (gender, age, bilateral or unilateral impaction, size of the canine, presence of the deciduous canine, space between the lateral incisor and first premolar, two-dimensional and three-dimensional parameters) was analyzed with multiple logistic regression. Likewise, the logistic regression was conducted to test the connection between investigated factors and impaction difficulty. The results were calculated as an odds ratio with a 95% confidence interval. For all tests, the level of significance was $p < 0.05$.

Results

Intra-observer reliability for the KPG index value indicated a high agreement between first and repeated measurements. The intraclass correlation coefficient was 0.93, whereas Cohen's kappa value for the individual crown and root tips varies from 0.29 to 0.77 (Table 1). Out of 94 patients, most of the individuals were females, presented by two-thirds of the total number of subjects (Table 2). The mean patient age was 19.8 ± 5.2, so most patients were late adolescents or young adults, with canine apex closed in more than half (60.3%) of the sample. From 116 ICs, most were unilateral impactions with almost equal distribution of the left and right-side affected, and only 21 patients had bilateral impaction. Deciduous canines were extracted in 61 (58.7%) patients, which was expected based on the patient's age. The bilateral presence of deciduous canines was rare [only 12 (11.5%) patients]. The average diameter of the ICs was 7.2 mm ± 0.8 mm, with an average space for the tooth in the arch of only 3.9 mm ± 2.2 mm.

Two-dimensional parameters of the CP showed that the average canines crown tip position was 7.4 mm ± 3.3 mm and 7.3 mm ± 4.4 mm from OccP and SML, respectively (Table 3). Distance from the OccP signifies that CP in the vertical plane was not too high compared to its final position in the occlusion. The angles between canine and SML, OccP, lateral incisor, and first premolar, respectively, although with large SD, were all sharp, with the smallest value for the angle between canine and first premolar.

Three-dimensional parameters showed that most [80 (71.4%)] ICs were in the palatal position (Table 4). Most [73 (68.2%)] ICs had no contact with the lateral incisor. Furthermore, in most [72 (72.7%)] cases, resorption of the adjacent teeth was absent. In the cases where resorption of the adjacent teeth was detected, the tooth that was most affected was the central incisor, 17 (17.2%). The impaction was moderate in 62 (55.9%) cases, while 28 (25.2%) cases were difficult, 19 (17.1%) were easy, and only 2 (1.8%) were

Table 1

Results for the intra-observer reliability for the KPG index measurements

Intra-observer reliability	Crown tip X-axis	Root tip X-axis	Crown tip Y-axis	Root tip Y-axis	Crown tip Z-axis	Root tip Z-axis	KPG index value
Cohen's kappa	0.77	0.49	0.57	0.29	0.34	0.66	
Intraclass correlation coefficient							0.93

Table 2

Frequency and mean values for the first five parameters

Parameter	Values
Gender	
male	31 (33)
female	63 (67)
Age, years	19.83 ± 5.18
Side of canine impaction	
bilateral	21 (22.3)
right side	36 (38.3)
left side	37 (39.4)
Presence of the deciduous canines	
extracted	61 (58.7)
unilateral presence of deciduous canine	31 (29.8)
bilateral presence of deciduous canines	12 (11.5)
Space between lateral incisor and first premolar, mm	3.99 ± 2.17

All values are expressed as numbers (percentages) or mean ± standard deviation.

Table 3

Frequency and means for the two-dimensional parameters

Parameter	Values
Distance of the canine crown tip to SML, mm	7.32 ± 4.39
Distance of the canine crown tip from OccP, mm	7.43 ± 3.26
Distance of the apex to SML, °	20.69 ± 3.37
Angle between canine and SML, °	37.92 ±15.78
Angle between canine and OccP, °	52.24 ±19.39
Angle between canine and lateral incisor, °	43.5 ± 17.89
Angle between canine and first premolar, °	34.52 ± 6.37

All values are expressed as mean ± standard deviation.
SML – sagittal medial line; OccP – occlusal plane.

Table 4

Descriptive values for the three-dimensional parameters

Parameter	Values
Canine mesio-distal diameter, mm	7.25 ± 0.75
Contact with lateral incisor	
absent	73 (68.2)
present	34 (31.8)
Localization in the vestibulo-oral direction	
vestibular	25 (22.3)
palatal	80 (71.4)
in the middle of the alveolar ridge	7 (6.3)
Resorption of the adjacent teeth	
absent	72 (72.7)
resorption of the lateral incisor	4 (4)
resorption of the central incisor	17 (17.2)
resorption of the first premolar	6 (6.1)
Impaction difficulty	
easy	19 (17.1)
moderate	62 (55.9)
difficult	28 (25.2)
extremely difficult	2 (1.8)
KPG index average	12.55 ± 3.29

All values are expressed as numbers (percentages) except for canine mesio-distal diameter and average KPG index, which are shown as mean ± standard deviation.

extremely difficult. Each of the investigated parameters was tested separately with univariable logistic regression analysis for possible connection with probability for the adjacent tooth root resorption. Only parameters that showed $p < 0.25$ were included in the further analysis. In Table 5, there is a list of variables that were significant after simple logistic regression and were, therefore, included in the multiple logistic regression. After forward and backward logistic regression methods analysis, almost all parameters became statistically insignificant. The only parameter included in the preliminary model was the angle between the canine and the first premolar. The goodness-of-fit was analyzed with the Hosmer-Lemeshow test and confirmed that the preliminary model was the final model. Although the area under the curve (AUC) was 0.64, the 95% confidence interval was 0.50–0.78, so it had no high predictive value. According to this model, for every increase of the angle between the canine and first premolar for 1°, the odds for adjacent tooth root resorption increased by 1.04 times (Table 5).

Another multiple logistic regression was performed to test the connection between all investigated parameters and impaction difficulty. For that purpose, the first categorical scale for the impaction difficulty with four values (1 – easy, 2 – moderate, 3 – difficult, 4 – extremely difficult) was transformed into a binary scale with two outcomes (0 – easy and moderate, 1 – difficult and extremely difficult). Again, simple logistic regression was used for every single parameter to test its individual significance. Table 6 presents parameters that showed significance after simple logistic regression. Two-dimensional parameters, such as the distance of the canine crown tip to SML, the angle between canine and SML, OccP, and first premolar, respectively, were highly significant ($p < 0.01$) after univariable analysis. When these parameters were included in the multivariable analysis, forward and backward logistic regression methods did not keep the same independent variables; therefore, further multiple logistic regression could not be performed. Although the final model was not established, the individual

Table 5

Parameters included in the multivariable logistic regression to investigate possible association to adjacent tooth root resorption

Parameter	*p*	OR	95% CI for OR	
Presence of the deciduous canines				
extracted	Ref.			
unilateral presence of deciduous canine	0.05	0.28	0.08	1.02
bilateral presence of deciduous canines	0.08	0.27	0.06	1.16
Distance of the canine crown tip to SML	0.06	0.9	0.81	1.00
Distance of the canine crown tip from OccP	0.04*	1.17	1.01	1.35
Mesio-distal diameter of the lateral incisor	0.23	1.63	0.73	3.63
Angle between canine and SML	0.07	1.03	1.00	1.06
Angle between canine and first premolar	0.02*, **	1.04	1.01	1.07
KPG index	0.01*	1.24	1.05	1.45
Impaction difficulty				
easy	Ref.			
moderate	0.22	0.14	0.01	3.31
difficult	0.41	0.30	0.02	5.16
extremely difficult	0.84	0.75	0.04	13.24
Contact with lateral incisor				
absent	Ref.			
present	0.20	1.84	0.73	4.68

OR – odds ratios; CI – confidence interval; Ref. – reference category.
***p* < 0.05; ***p* – the only parameter that was included in the final model to predict adjacent tooth root resorption.**
For abbreviations, see Table 3.

Table 6

Parameters tested for the possible prediction of the impaction difficulty (outcomes of the dependent variable were 0 – easy and moderate impaction, 1 – difficult and extremely difficult impaction)

Parameter	*p*	OR	95% CI for OR	
Side of the impaction				
right	Ref.			
left	0.07	3.71	0.91	15.13
bilateral	0.23	2.40	0.58	9.98
Bilateral or unilateral canine impaction				
unilateral	Ref.			
bilateral	0.10	3.00	0.80	11.24
Distance of the canine crown tip to SML	0.00*	0.70	0.60	0.82
Distance of the canine crown tip from OccP	0.07	1.14	0.99	1.31
Space between lateral incisor and first premolar	0.05	0.81	0.66	1.00
Angle between canine and SML	0.00*	1.07	1.03	1.11
Angle between canine and lateral incisor	0.24	1.02	0.99	1.04
Angle between canine and OccP	0.00*	0.93	0.90	0.97
Angle between canine and first premolar	0.00*	1.06	1.03	1.10
Localization in the vestibulo-oral direction				
vestibular	Ref.			
palatal	0.35	0.25	0.01	4.60
in the middle of the alveolar ridge	0.28	3.29	0.38	28.75
Resorption of the adjacent teeth				
absent	Ref.			
resorption of the lateral incisor	0.69	1.57	0.17	14.42
resorption of the central incisor	0.75	1.67	0.74	37.73
resorption of the first premolar	0.07	9.17	0.86	97.69

***p* < 0.01. For abbreviations, see Table 3.**

impact of distance of the canine crown tip to SML, angle between canine and SML, OccP, and first premolar separately, was significant; hence, each of them could be interpreted as a factor with high probability prediction of the impaction difficulty.

Discussion

In this study, the canine two-dimensional and three-dimensional position was evaluated along with the gender distribution of the impaction. CP along X, Y, and Z-axis

was measured and used to determine impaction difficulty. Investigated parameters (gender, age, side of the impaction, two-dimensional and three-dimensional parameters) were tested to find potential predictors of the impaction difficulty and define the probability for adjacent tooth root resorption.

Considering the two-dimensional parameters of the impacted CP, the mean distance of the canine crown tip from the OccP was 7.4 mm ± 3.3 mm. That signifies that in the vertical plane, the IC crown tip was in line with the cervical third of the incisor root or was occlusal to the cemento-enamel junction of the incisors. Similar studies reported a higher position of the ICs, where teeth were at the middle or apical third of the incisor root [6, 17, 18]. The angle between canine and SML in the present study was 37.9° ± 15.8°. This angle corresponds to the alpha angle (inclination of the canine to the midline) in the study by Rafflenbeul et al. [17], while Naoumova and Kjellberg [19] have reported smaller values of alpha angle for unilateral and bilateral impactions.

Impaction was mostly unilateral, with almost equal affection of the right and left sides of the maxilla. Bilateral impaction was present in 22.3% of the investigated impactions. These results are consistent with recent literature findings where bilateral impactions were found in 20–25% of cases [4, 6, 20].

Subjects in this study were late adolescents or young adults. Even though the normal path of the shift in the eruption of the permanent canines was disturbed, 58.7% of the deciduous canines were absent. That could be explained by the patient's age and morphological and physiological characteristics of deciduous teeth that are not assumed to last a lifetime. Furthermore, it is possible that some of the deciduous canines were extracted as an interceptive treatment for permanent canine impaction. Still, based on the patient's age and canine root development (more than two-thirds of the root developed), even if the deciduous canines were extracted before, this could not be a confounding factor in the study since extraction has not led to a spontaneous eruption of the permanent successor.

Space for the IC was reduced in the dental arch, which was expected considering the patient's age and extraction of the deciduous canines. Although the malocclusion was not investigated in this study, the intra-arch forces direction contributing to mesial migration of the posterior teeth could be one of the reasons for this space reduction for canine placement in the upper dental arch. Migration of the teeth into extraction space was one of the side effects of the early interceptive extraction of the primary canines [19].

Findings regarding gender indicate sexual dimorphism of canine impaction since females were twice more often affected compared to males, and these results agree with findings from the literature [5, 6, 20]. Sacerdoti and Baccetti [7] have found that female-to-male prevalence of palatally displaced ICs was in a ratio of 3:1. On the contrary, some investigations reported similar prevalence among males and females [17, 18]. In the interpretation of these findings, the possibility of women seeking orthodontic treatment more often should be considered. Women appeared to be more critical in evaluating the aesthetics of the smile [21]. Likewise, younger persons are more critical in judging smiles compared to older people [22]. In our study, it could be possible that young females were more motivated to conduct orthodontic treatment; hence, it could impact the gender distribution of the sample.

The values of the KPG index for most of the teeth showed moderate impaction. When the impaction difficulty was tested in relation to the investigated parameter, the simple logistic regression showed that the distance of the canine crown tip to SML and the angle between the canine and SML, OccP, and first premolar, respectively, were highly significant. That could be interpreted in a manner that the value of each of these parameters could predict impaction difficulty. Investigating the impact of initial CP on the final treatment outcome, a systematic review has found with a low level of certainty that canine alpha angle, vertical position, and sector position influence the treatment duration and success [23].

In this study, resorption of the incisors or first premolar was detected in 27 (27.3%) cases of the investigated impactions. Most of the resorptions were diagnosed on the central incisors of the same side of the maxilla. These findings disagree with other studies, where lateral incisors were the most affected teeth [6, 8, 13, 17]. A possible explanation for our findings could be the vestibulo-oral position of the ICs. Most of the ICs were palatally displaced in the present investigation. Palatally ICs caused a reduction of the intercanine width of the upper arch. The reduced intercanine width, along with proximity to the midline and angulation of the palatally ICs, could contribute to a higher prevalence of central incisors root resorption. Multiple logistic regression analysis was used to find the model which would explain the relationship between investigated factors and the resorption of the adjacent teeth. All two and three-dimensional parameters were tested to define the factors that will best predict root resorption. The analysis has shown that the angle between the canine and the first premolar was the only predictor of probability for adjacent tooth root resorption. The test value signifies that for each angle increase of 1°, the probability for adjacent tooth root resorption increases by 1.04 times. According to Sosars et al. [24], the only parameter on the panoramic radiographs that could predict severe resorption of the incisors was the canine angle to the midline. That was with moderate predictive value based on the area under the receiver operating curve. Another study described gender, canine apex, its vertical position, and magnification as predictors of root resorption [25]. Rafflenbeul et al. [17] have described the contact between canine and adjacent teeth roots as the only possible risk factor for root resorption. The angle between the axis of the lateral incisor and the ICs is found to be in a positive relationship to lateral incisor root resorption [12]. Investigation of the incisors root resorption in the cases of palatally displaced ICs presented canine contact with lateral incisor, the presence of peg-shaped lateral incisors, and the size of the canine dental follicle as predictors of incisor root resorption [26]. Similar, severe incisor root resorption was described to be significantly associated with gender, size of the

dental follicle of the ICs, and anomalies of the lateral incisors [27]. Ericson and Kurol [28] proposed the position of the canine crown, degree of canine development, and inclination of the eruption path as factors that increased the risk for adjacent tooth root resorption. According to a systematic review, when the resorption of the incisors is detected, the most frequent is the slight resorption of the apical third of the incisor root [29].

Differences in the proposed risk factors for adjacent tooth root resorption found in the literature could be a consequence of different factors taken into consideration, particularly parameters of tooth position. Furthermore, there are differences in the statistical tests for factors evaluation and creation of the model or equation to predict possible adjacent tooth root resorption. Uribe et al. [30] used comprehensive multivariate analysis to thoroughly test multiple clinical parameters and radiographic parameters on the panoramic radiographs and cephalograms and their impact on the canine impaction prediction. The authors have not found significant predictors of canine impaction. In our study, multiple logistic regression was used to test the influence of both numerical and categorical variables to create a model that could predict tooth root resorption and impaction difficulty. The final model included the angle between the canine and the first premolar, presenting this variable as statistically significant to predict root resorption of the adjacent tooth. Considering the period when the impaction of the upper canines occurs, that is, the period of the jaw growth and completion of the permanent dentition, with the tooth eruption sequence in the maxilla, this parameter is also clinically significant. Prospective follow-up studies could help us strengthen the presented model and describe the potential model in order to define the impaction difficulty since the model for impaction difficulty could not be established in the present study.

Two-dimensional parameters were evaluated on the reconstructed panoramic image on the CBCT scans since the panoramic radiographs were not obtained from the same equipment. Even though the image is reconstructed from the specific software, it is proposed to be a more reliable tool in dental angulation analysis compared to the panoramic radiographs in the region of the canines and premolars [31]. There could be differences in the data interpretation due to the different software used for tooth position analysis [32]. Still, using this projection along with other views on the CBCT images is suggested as more reliable in precise CP analysis and adjacent root resorption compared to the panoramic radiographs [32, 33].

In the present study, the KPG index was used to evaluate the impacted CP in all three planes of space. As a 3D index, it is proposed to be helpful in the precise evaluation of the canine crown position on the CBCT scans, with a good inter-rater agreement in perceiving impaction difficulty [15, 34]. Nevertheless, it was reported that the index reliability could be influenced by using different software for visualizing the CBCT images [35]. Its clinical efficacy in treatment time and evaluation of impaction difficulty could not be confirmed based on the previous investigation [15]. Future prospective clinical trials could help in the investigation of the KPG index as a 3D index to confirm its diagnostic reliability and clinical efficacy in the evaluation of the impaction difficulty and, therefore, create a treatment plan and strategy.

Conclusion

Results of the present investigation suggest that during a comprehensive diagnostic procedure of the impacted maxillary canines, two-dimensional and three-dimensional parameters should be evaluated. In this study, most of the impactions of the maxillary canines were unilateral, palatal, and with moderate difficulty. Besides canine distance to SML and angle to SML and OccP to estimate impaction difficulty, the angle between canines and the first premolar should be given special attention since this angle could be a possible predictor of the adjacent tooth root resorption. This parameter should also be considered during patient follow-up.

Conflict of interest

The authors report no conflict of interest.

REFERENCES

1. *Al-Zoubi H, Alharbi AA, Ferguson DJ, Zafar MS*. Frequency of impacted teeth and categorization of impacted canines: A retrospective radiographic study using orthopantomograms. Eur J Dent 2017; 11(1): 117–21.
2. *Proffit WR, Fields Jr HW, Sarver DM*. Contemporary Orthodontics. 4th ed. St. Louis: Mosby; 2007.
3. *Dewel BF*. The upper cuspid: Its development and impaction. Angle Orthod 1949; 19(2): 79–90.
4. *Lövgren ML, Dahl O, Uribe P, Ransjö M, Westerlund A*. Prevalence of impacted maxillary canines-an epidemiological study in a region with systematically implemented interceptive treatment. Eur J Orthod 2019; 41(5): 454–9.
5. *Becker A, Smith P, Behar R*. The incidence of anomalous maxillary lateral incisors in relation to palatally-displaced cuspids. Angle Orthod 1981; 51(1): 24–9.
6. *Grisar K, Piccart F, Al-Rimawi AS, Basso I, Politis C, Jacobs R*. Three-dimensional position of impacted maxillary canines: Prevalence, associated pathology and introduction to a new classification system. Clin Exp Dent Res 2019; 5(1): 19–25.
7. *Sacerdoti R, Baccetti T*. Dentoskeletal features associated with unilateral or bilateral palatal displacement of maxillary canines. Angle Orthod 2004; 74(6): 725–32.
8. *Lai CS, Bornstein MM, Mock L, Heuberger BM, Dietrich T, Katsaros C*. Impacted maxillary canines and root resorptions of neighbouring teeth: a radiographic analysis using cone-beam computed tomography. Eur J Orthod 2013; 35(4): 529–38.
9. *Liu DG, Zhang WL, Zhang ZY, Wu YT, Ma XC*. Localization of impacted maxillary canines and observation of adjacent incisor resorption with cone-beam computed tomography. Oral Surg Oral Med Oral Pathol Oral Radiol Endod 2008; 105(1): 91–8.

10. *Walker L, Enciso R, Mah J.* Three-dimensional localization of maxillary canines with cone-beam computed tomography. Am J Orthod Dentofacial Orthop 2005; 128(4): 418–23.
11. *Mitsea A, Palikaraki G, Karamesinis K, Vastardis H, Gizani S, Sifakakis I.* Evaluation of Lateral Incisor Resorption Caused by Impacted Maxillary Canines Based on CBCT: A Systematic Review and Meta-Analysis. Children (Basel) 2022; 9(7): 1006.
12. *Kalavritinos M, Benetou V, Bitsanis E, Sanoudos M, Alexiou K, Tsiklakis K,* et al. Incidence of incisor root resorption associated with the position of the impacted maxillary canines: A cone-beam computed tomographic study. Am J Orthod Dentofacial Orthop 2020; 157(1): 73–9.
13. *Simić S, Nikolić P, Stanišić Zindović J, Jovanović R, Stošović Kalezić I, Djordjević A,* et al. Root Resorptions on Adjacent Teeth Associated with Impacted Maxillary Canines. Diagnostics (Basel) 2022; 12(2): 380.
14. *Kau CH, Pan P, Gallerano RL, English JD.* A novel 3D classification system for canine impactions--the KPG index. Int J Med Robot 2009; 5(3): 291–6.
15. *Kau CH, Lee JJ, Souccar NM.* The validation of a novel index assessing canine impactions. Eur J Dent 2013; 7(4): 399–404.
16. *San Martín DE, English JD, Kau CH, Gallerano RL, McGrory KR, Salas AM,* et al. The KPG index--a novel 3D classification system for maxillary canine impactions. Tex Dent J 2012; 129(3): 265–74.
17. *Rafflenbeul F, Gros CI, Lefebvre F, Bahi-Gross S, Maizeray R, Bolender Y.* Prevalence and risk factors of root resorption of adjacent teeth in maxillary canine impaction, among untreated children and adolescents. Eur J Orthod 2019; 41(5): 447–53.
18. *Jain S, Debbarma S.* Patterns and prevalence of canine anomalies in orthodontic patients. Med Pharm Rep 2019; 92(1): 72–8.
19. *Naoumova J, Kjellberg H.* The use of panoramic radiographs to decide when interceptive extraction is beneficial in children with palatally displaced canines based on a randomized clinical trial. Eur J Orthod 2018; 40(6): 565–74.
20. *Simić S, Pavlović J, Nikolić PV, Vujačić A, Vukićević V, Jovanović R.* The prevalence of peg-shaped and missing lateral incisors with maxillary impacted canines. Vojnosanit Pregl 2019; 76(1): 61–66.
21. *Bolas-Colvee B, Tarazona B, Paredes-Gallardo V, Arias-De Luxan S.* Relationship between perception of smile esthetics and orthodontic treatment in Spanish patients. PLoS One 2018; 13(8): e0201102.
22. *Pithon MM, Bastos GW, Miranda NS, Sampaio T, Ribeiro TP, Nascimento LE,* et al. Esthetic perception of black spaces between maxillary central incisors by different age groups. Am J Orthod Dentofacial Orthop 2013; 143(3): 371–5.
23. *Grisar K, Luyten J, Preda F, Martin C, Hoppenreijs T, Politis C,* et al. Interventions for impacted maxillary canines: A systematic review of the relationship between initial canine position and treatment outcome. Orthod Craniofac Res 2021; 24(2): 180–93.
24. *Sosars P, Jakobsone G, Neimane L, Mukans M.* Comparative analysis of panoramic radiography and cone-beam computed tomography in treatment planning of palatally displaced canines. Am J Orthod Dentofacial Orthop 2020; 157(5): 719–27.
25. *Alqerban A, Jacobs R, Fieuws S, Willems G.* Predictors of root resorption associated with maxillary canine impaction in panoramic images. Eur J Orthod 2016; 38(3): 292–9.
26. *Alemam AA, Abu Alhaija ES, Mortaja K, AlTawachi A.* Incisor root resorption associated with palatally displaced maxillary canines: Analysis and prediction using discriminant function analysis. Am J Orthod Dentofacial Orthop 2020; 157(1): 80–90.
27. *Chaushu S, Kaczor-Urbanowicz K, Zadurska M, Becker A.* Predisposing factors for severe incisor root resorption associated with impacted maxillary canines. Am J Orthod Dentofacial Orthop 2015; 147(1): 52–60.
28. *Ericson S, Kurol J.* Resorption of maxillary lateral incisors caused by ectopic eruption of the canines. A clinical and radiographic analysis of predisposing factors. Am J Orthod Dentofacial Orthop 1988; 94(6): 503–13.
29. *Schroder AGD, Guariza-Filho O, de Araujo CM, Ruellas AC, Tanaka OM, Porporatti A.* To what extent are impacted canines associated with root resorption of the adjacent tooth?: A systematic review with meta-analysis. J Am Dent Assoc 2018; 149(9): 765–77. e8.
30. *Uribe P, Ransjö M, Westerlund A.* Clinical predictors of maxillary canine impaction: a novel approach using multivariate analysis. Eur J Orthod 2017; 39(2): 153–60.
31. *Peck JL, Sameshima GT, Miller A, Worth P, Hatcher DC.* Mesiodistal root angulation using panoramic and cone beam CT. Angle Orthod 2007; 77(2): 206–13.
32. *Alqerban A, Jacobs R, Fieuws S, Willems G.* Comparison of two cone beam computed tomographic systems versus panoramic imaging for localization of impacted maxillary canines and detection of root resorption. Eur J Orthod 2011; 33(1): 93–102.
33. *Jung YH, Liang H, Benson BW, Flint DJ, Cho BH.* The assessment of impacted maxillary canine position with panoramic radiography and cone beam CT. Dentomaxillofac Radiol 2012; 41(5): 356–60.
34. *Dalessandri D, Migliorati M, Visconti L, Contardo L, Kau CH, Martin C.* KPG index versus OPG measurements: a comparison between 3D and 2D methods in predicting treatment duration and difficulty level for patients with impacted maxillary canines. Biomed Res Int 2014; 2014: 537620.
35. *Dalessandri D, Migliorati M, Rubiano R, Visconti L, Contardo L, Di Lenarda R,* et al. Reliability of a novel CBCT-based 3D classification system for maxillary canine impactions in orthodontics: the KPG index. Sci World J 2013; 2013: 921234.

Received on March 29, 2022
Revised on January 3, 2023
Accepted on February 3, 2023
Online First February 2023

ORIGINAL ARTICLE

UDC: 615.276::615.035.7
DOI: https://doi.org/10.2298/VSP221229021S

Prescription patterns of diclofenac in patients with cardiovascular diseases or at high risk for cardiovascular diseases at primary health care level in Montenegro: retrospective, national, drug utilization study

Propisivanje diklofenaka bolesnicima sa kardiovaskularnim bolestima ili visokim rizikom od razvoja kardiovaskularnih bolesti na nivou primarne zdravstvene zaštite u Crnoj Gori: retrospektivna, nacionalna, studija upotrebe leka

Maja Stanković*, Nemanja Turković*†, Silva Dobrić‡, Nemanja Rančić‡§

***Institute for Medicines and Medical Devices of Montenegro, Podgorica, Montenegro; †University of Montenegro, Faculty of Medicine, Podgorica, Montenegro; ‡University of Defence, Faculty of Medicine of the Military Medical Academy, Belgrade, Serbia; §Military Medical Academy, Center for Clinical Pharmacology, Belgrade, Serbia**

Abstract

Background/Aim. Diclofenac, a non-selective inhibitor of cyclooxygenase with analgesic, anti-inflammatory, and antipyretic effects, is one of the most prescribed nonsteroidal anti-inflammatory drugs (NSAIDs). The aim of this study was to analyze the prescription patterns of diclofenac systemic formulations at primary health care (PHC) level in Montenegro, in patients with cardiovascular (CV) diseases (CVD) and patients with risk factors for CVD, from 2016 to 2020. **Methods.** A retrospective national drug utilization study was conducted and it included patients with CVD, to whom prescribing diclofenac was contraindicated, and patients with risk factors for CVD, to whom diclofenac could be prescribed but with increased precaution. PHC information system has been used as a source of medical data for these patients. **Results.** Within the observed period, prescribing diclofenac systemic formulations, dominantly oral formulations in 75 mg dose, increased by 36.9% [from 4.6 of defined daily doses (DDD) /1,000 inhabitants/day in 2016 to 6.3 DDD/1,000 inhabitants/day in 2020]. A rising trend in prescribing diclofenac was also recorded in patients with CVD or those with risk factors for CVD, to whom diclofenac prescribing is contraindicated. Out of the overall number of patients who were prescribed diclofenac in 2016, 2017, 2018, 2019, and 2020, 16%, 18%, 24%, 15%, and 20% of them, respectively, already had a CVD or some risk factor for CVD. Most CV patients (39.7%), for whom the use of diclofenac was contraindicated, had ischemic heart disease and were prescribed 40.7% of the total amount of diclofenac prescribed for this group of patients (expressed in DDD/1,000 inhabitants/day for the given medicine). The majority (77.4%) of CV patients to whom the drug could be prescribed, but with increased precautions, had hypertension, and they were prescribed 77.2% of the total amount of diclofenac prescribed for this group of patients (expressed in DDD/1,000 inhabitants/day for the given medicine). **Conclusion.** Despite the undertaken regulatory measures aimed at a safer prescription of diclofenac to patients with CVD or at high risk of developing CVD, this medicine is still widely prescribed at the level of PHC in Montenegro, even in cases that represent a contraindication for its use.

Key words:
cardiovascular diseases; delivery of health care; diclofenac; drug utilization; montenegro.

Apstrakt

Uvod/Cilj. Diklofenak, neselektivni inhibitor ciklooksigenaze sa analgetskim, protivupalnim i antipiretičkim dejstvima, jedan je od nesteroidnih protivupalnih lekova (NSPUL) koji se najčešće propisuje. Cilj rada bio je da se istraže propisivanje i potrošnja sistemskih formulacija diklofenaka na nivou primarne zdravstvene zaštite (PZZ) u Crnoj Gori (CG), kod bolesnika sa kardiovaskularnim (KV) bolestima (KVB) i bolesnika sa faktorima rizika od KVB, u periodu od 2016. do 2020. godine. **Metode.** Sprovedena je retrospektivna, nacionalna studija upotrebe leka, koja je uključivala bolesnike sa KVB kojima je bilo kontraindikovano propisivanje diklofenaka,

Correspondence to: Maja Stanković, Institute for Medicines and Medical Devices of Montenegro, Boulevard Ivana Crnojevića 64a, 81 000 Podgorica, Montenegro. E-mail: maja.stankovic@cinmed.me

kao i bolesnike sa faktorima rizika od KVB, kojima se diklofenak mogao propisati uz pojačane mere opreza. Kao izvor podataka o bolesnicima korišćeni su podaci iz informacionog sistema PZZ. **Rezultati.** U posmatranom periodu, propisivanje sistemskih formulacija diklofenaka, dominatno oralnih, u jačini od 75 mg, povećana je za 36,9% [sa 4,6 definisanih dnevnih doza (DDD)/1 000 stanovnika/dan u 2016., na 6,3 DDD/1 000 stanovnika/dan u 2020. godini]. Zabeležen je trend rasta propisivanja diklofenaka bolesnicima sa KVB, ili onim sa faktorima rizika od KVB, kojima je propisivanje diklofenaka kontraindikovano. Od ukupnog broja bolesnika kojima je tokom 2016, 2017, 2018, 2019. i 2020. godine bio propisan diklofenak, njih 16%, 18%, 24%, 15% i 20%, redom, već je imalo KVB ili neki faktor rizika od KVB. Najviše (39,7%) KV bolesnika, kojima je bila kontraindikovana primena diklofenaka, imalo je ishemijsku bolest srca i njima je bilo propisano 40,7% od ukupno propisane količine diklofenaka za grupu KV bolesnika (izraženo u DDD/1 000 stanovnika/dan za dati lek). Najviše (77,4%) KV bolesnika kojima se lek mogao propisati, ali uz pojačane mere opreza, imalo je hipertenziju i njima je bilo propisano 77,2% ukupno propisane količine diklofenaka za grupu KV bolesnika (izraženo u DDD/1 000 stanovnika/dan za dati lek). **Zaključak.** Uprkos preduzetim regulatornim merama, čiji je cilj bezbednija primena sistemskih formulacija diklofenaka, bolesnicima sa KVB ili visokim rizikom od razvoja KVB se i dalje široko propisuje ovaj lek na nivou PZZ u CG, čak i u slučajevima koji predstavljaju kontraindikaciju za njegovu primenu.

Ključne reči:
kardiovaskularne bolesti; primarno zdravstveno zbrinjavanje; diklofenak; lekovi, korišćenje; crna gora.

Introduction

Diclofenac, a non-selective inhibitor of cyclooxygenase with analgesic, anti-inflammatory, and antipyretic effects, is one of the most prescribed nonsteroidal anti-inflammatory drugs (NSAIDs) in treating numerous acute and chronic painful and/or inflammatory conditions [1]. It is estimated that 14 million Americans aged 45 and above take one of the NSAIDs daily, among which diclofenac is one of the leading drugs. Since the global population is growing older, it is estimated that the rising trend in consumption of these medicines will continue, taking into account the expected growth of the prevalence of inflammatory diseases with accompanying pain (osteoarthritis and other inflammatory conditions) [2]. Diclofenac was also the most used NSAID according to the results of a study that included 15 participant countries worldwide [3]. Namely, the consumption of diclofenac and etoricoxib, both of them being NSAIDs, with recognized cardiovascular (CV) risk constitutes one-third of the consumption of all NSAIDs analyzed in the study.

Reports on the consumption of drugs in Montenegro (MNE) indicate very high consumption of diclofenac [more than 40 daily defined doses (DDD)/1,000 inhabitants/day] [4]. In comparison, in Croatia (an EU member country), consumption is significantly lower, and in 2020, it amounted to 11.63 DDD/1,000 inhabitants/day [5], while in Norway, one of the leading countries in terms of rational drug use, consumption is only 5.62 DDD/1,000 inhabitants/day [6].

Considering the safety of diclofenac systemic formulations, a topic that has attracted the attention of the professional public for years, refers to the CV safety of diclofenac, which resulted in the adoption of new recommendations issued by the European Medicines Agency (EMA) regarding the systemic use of diclofenac in patients with CV diseases (CVD) or with risk factors for CVD [7]. These recommendations have been introduced into appropriate sections of the Summary of Product Characteristics (SmPC) of diclofenac. They were also adopted in MNE by the Institute for Medicines and Medical Devices of Montenegro (CInMED) [8–10]. Additionally, in 2015, CInMED implemented the additional measure of minimizing (reducing) risks of unsafe diclofenac prescribing in a way that it had notified healthcare professionals *via* letter – Direct Healthcare Professional Communication of introduced restrictions in diclofenac prescribing in patients with CVD or with risk factors for CVD [11, 12].

Systemic formulations of diclofenac are available to patients in MNE and, for years back, they have been on the list of medicines funded by mandatory health insurance in MNE, which is also one of the reasons that contribute to the wide diclofenac prescribing at the primary health care level, i.e., outpatient care settings (OCS) [13].

Pursuant to the knowledge of the safety profile of this drug concerning CV adverse reactions, high exposure of patients to diclofenac may pose a serious public health concern.

The aim of this study was to analyze prescribing diclofenac systemic formulations in patients with CVD to whom diclofenac prescribing is contraindicated and patients with risk factors for CVD to whom diclofenac may be prescribed with special warnings and precautions at the OCS in MNE from 2016 to 2020. The aim was also to assess if the primary care physicians when prescribing diclofenac take into account the latest, evidence-based information on its safety, indicated in the SmPC, revised in MNE in 2015.

Methods

Data sources

An observational, retrospective, national drug utilization study was conducted [14]. Analysis of prescribing diclofenac systemic formulations was performed in a five-year time period (January 1, 2016, to December 31, 2020) on primary health care information system (PHCIS) prescribing data. This information system is implemented in all 18 healthcare centers in MNE. Generating the diclofenac prescribing database was enabled due to the developed Data Warehouse (DW) system at the level of the entire OCS in

MNE. DW system is a central repository of integrated diclofenac prescribing data collected in real-time as well as historical data of diclofenac prescribing captured from the electronic medical records of patients. This research included the entire system of the OCS in MNE, which is why this research belongs to a group of national-based studies.

The following data were extracted and analyzed from the PHCIS: the overall number of patients who were prescribed the systemic formulations of diclofenac; the overall number of patients who were prescribed systemic formulations of diclofenac, with CVD contraindicated for diclofenac prescribing [congestive heart failure, ischemic heart disease (IHD), peripheral arterial disease, cerebrovascular disease], as well as with diseases that represent risk factors for CVD, for which there are special warnings and precautions in prescribing diclofenac (hypertension, hyperlipidemia, diabetes mellitus – DM); on all drugs on the market in MNE, that contain diclofenac as an active substance, but in different pharmaceutical form, strength (dose), and different method of use, except for diclofenac intended for local (topical) use.

Patients

The study included patients of both genders older than 18 years. Based on the data from their electronic medical records, the patients were prescribed diclofenac in the five-year time period. In the observed time period, as seen from their medical records, these patients had CVD or at least one of the risk factors for CVD, which represents a contraindication or requires special warnings and precautions for prescribing the systemic formulation of diclofenac.

As seen from their electronic medical records, these patients underwent screening of all diagnoses in order to determine whether CVD was characterized as a contraindication or whether some of the diseases with known CV risk factors were among patients' diagnoses, which required special warnings or precautions before prescribing systemic formulation of diclofenac. In PHCIS, medical diagnoses are classified according to the International Classification of Diseases (ICD) [15]. The selected diagnoses are shown in the supplement of this article.

According to SmPC [10], the use of diclofenac is contraindicated in patients with established congestive heart failure (New York Heart Association – NYHA, class II–IV), IHD, peripheral arterial disease, or cerebrovascular disease. At the same time, patients with significant risk factors for CVD (e.g., hypertension, hyperlipidemia, DM, smoking) should only be treated with diclofenac after careful consideration.

Consumption of systemic formulations of diclofenac was analyzed using the standard methodology of the World Health Organization based on DDD/1,000 inhabitants/day and Anatomic Therapeutic Chemical classification of medicines [16].

Results

Although the total number of patients who were prescribed systemic formulations of diclofenac decreased from 2016 to 2020 (from 94,269 to 79,168 patients), that trend was not noticed in the case of patients with risk factors for CVD, where, except for 2019, the trend of increase in number of patients with prescribed diclofenac was present. Concerning the total number of patients who in 2016, 2017, 2018, 2019, and 2020 were prescribed the systemic formulations of diclofenac, 16%, 18%, 24%, 15%, and 20% of them, respectively, had risk factors for CVD for diclofenac prescribing (Table 1).

Within the observed five-year time period, prescribing diclofenac systemic formulations to the target population, expressed in the number of prescribed diclofenac packaging, marked the growth trend in the first three years (2016–2018), with a decline in prescribing in 2019 and 2020 compared to 2018 (Figure 1).

The highest (39.7%) number of CV patients, who had contraindications for diclofenac prescribing, had IHD, while the highest (77.4%) number of patients to whom diclofenac could be prescribed but with increased precautions had hypertension (Table 2).

When it comes to the consumption of diclofenac systemic formulations, expressed in the number of DDD/1,000 inhabitants/day, in patients with CVD, its continuous growth was observed. Within the observed period, the consumption increased by 36.9% (from 4.6 to 6.3 DDD/1,000 inhabitants/day) (Figure 2).

Consumption of diclofenac systemic formulations in patients with CVD, who had contraindications for diclofenac prescribing, accompanied the trend of its increased prescribing. Namely, there was a noticeable increase in

Table 1

Total number of patients and number of patients with cardiovascular disease (CVD) or risk for CVD (contraindications and special warnings and precautions for use) who have been prescribed systemic formulations of diclofenac during the five-year period (2016–2020) in Montenegro

Year	Patients on diclofenac therapy, n	Patients with CVD on diclofenac therapy, n (%)
2016	94,269	15,602 (16)
2017	95,112	17,060 (18)
2018	93,598	22,923 (24)
2019	93,435	14,530 (15)
2020	79,168	15,702 (20)

n – number.

diclofenac consumption in this group of patients, while in 2019 and 2020, a mild decline in consumption was observed.

Consumption of diclofenac systemic formulations in patients with risk factors for CVD, to whom diclofenac has to be prescribed, with particular precaution, recorded a continuous increase − from 4.1 in 2016 to 5.8 DDD/1,000 inhabitants/day in 2020, which is an increase of 41.5% (Figure 2).

Analysis of diclofenac systemic formulations consumption concerning CVD, or diseases designated as CV risk factors, also showed that diclofenac, although contraindicated, was mostly prescribed to the patients suffering from IHD (with 40.7% of those patients), while among the diseases requiring special precautions for diclofenac prescribing, hypertension dominated (with 77.2% of those patients) (Table 3).

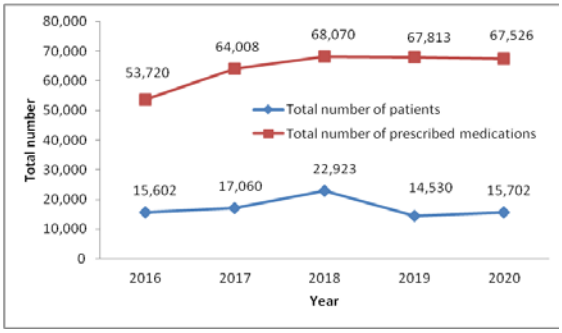

Fig. 1 – Total number of prescribed systemic formulations of diclofenac and number of patients with cardiovascular disease (CVD) or risk factors for CVD (contraindications and special warnings and precautions for use) who have been prescribed the drug during the five-year period (2016–2020) in Montenegro.

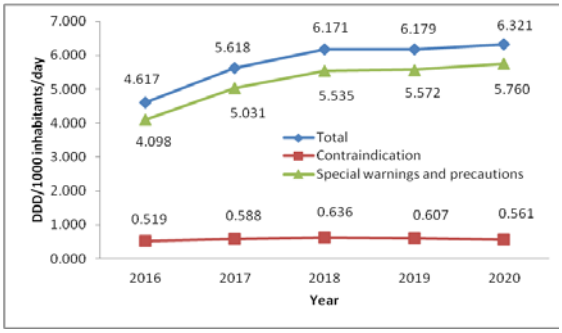

Fig. 2 – Total consumption of systemic formulations of diclofenac in patients with cardiovascular disease (CVD) or risk factors for CVD (contraindications and special warnings and precautions for use) expressed as the number of daily defined dose (DDD)/1,000 inhabitants/day during the five-year period (2016–2020).

Table 2

Number of patients with cardiovascular disease (CVD) or risk for CVD who have been prescribed systemic formulations of diclofenac during the five-year period (2016–2020) in Montenegro (according to the primary diagnosis)

Parameter	2016	2017	2018	2019	2020	Total
CVD						
congestive heart failure	95	87	102	63	40	387
ischemic heart disease	753	785	1,004	619	569	3,730
other heart diseases	507	488	597	369	330	2,291
diseases of arteries, small arteries, and capillaries	151	156	221	154	141	823
cerebrovascular disease	371	390	529	374	364	2,028
diseases of the heart of pulmonary origin and diseases of the blood vessels of the lungs	14	20	46	26	28	134
Disease as a risk factor for CVD						
hypertension	10,561	11,713	15,836	10,025	11,013	59,148
hyperlipidemia	330	350	403	263	289	1,635
diabetes mellitus	2,820	3,071	4,185	2,637	2,928	15,641
Total	15,602	17,060	22,923	14,530	15,702	85,817

Table 3

Consumption of systemic formulations of diclofenac expressed as the number of daily defined dose (DDD)/1,000 inhabitants/day during the five-year period (2016–2020) in patients with cardiovascular disease (CVD) or risk for CVD in Montenegro

Disease	2016	2017	2018	2019	2020	Total
CVD						
congestive heart failure	0.0313	0.0300	0.0283	0.0210	0.0181	0.1286
ischemic heart disease	0.2077	0.2457	0.2615	0.2466	0.2252	1.1867
other heart diseases	0.1384	0.1487	0.1519	0.1336	0.1241	0.6966
diseases of arteries, small arteries, and capillaries	0.0384	0.0420	0.0471	0.0460	0.0487	0.2222
cerebrovascular disease	0.1010	0.1175	0.1381	0.1485	0.1355	0.6407
diseases of the heart of pulmonary origin and diseases of the blood vessels of the lungs	0.0026	0.0050	0.0112	0.0122	0.0115	0.0426
Disease as a risk factor for CVD						
hypertension	3.1617	3.8670	4.2565	4.3121	4.4586	20.0613
hyperlipidemia	0.0873	0.0987	0.0966	0.0951	0.1004	0.4781
diabetes mellitus	0.8434	1.0638	1.1797	1.1636	1.1994	5.4499

If the consumption of systemic formulations of diclofenac in patients with CVD was analyzed regarding the type of systemic formulations (oral, parenteral, rectal), the continuous growth in consumption of oral formulations, the decline in consumption of parenteral formulations since 2017, and continuous decline in consumption of rectal formulations of diclofenac were observed. Oral formulations of diclofenac made up 98% of total diclofenac systemic formulations consumption (Table 4).

Analysis of the consumption of diclofenac systemic formulations, represented as the number of prescribed packaging of diclofenac to a targeted population, indicates the highest consumption of diclofenac in patients with IHD (40.3%) and other CV (25.8%) and cerebrovascular diseases (19.2%) of all CVD contraindications for prescribing diclofenac (Table 5), and patients with hypertension (76.6%) and DM (21.5%) of all cases of diseases as risk factors for CVD that require special warnings and precautions for using diclofenac (Table 6).

Table 4

Consumption of systemic formulations of diclofenac expressed as the number of daily defined dose (DDD)/1,000 inhabitants/day during the five-year period (2016–2020) in Montenegro in relation to the route of administration of systemic formulations of the drug

Route of administration	2016	2017	2018	2019	2020
Oral	4.523	5.520	6.079	6.091	6.262
Parenteral	0.090	0.095	0.091	0.086	0.060
Rectal	0.004	0.003	0.002	0.001	0.000

Table 5

Number of prescribed packages of diclofenac to patients with cardiovascular disease contraindications in different strengths (doses) and pharmaceutical forms during the five-year period (2016–2020)

Parameter	Route of administration (dose)					Total
	oral (mg)			parenteral (mg/mL)	rectal (mg)	
Congestive heart failure	50	75	100	75/3	50	
2016	4	188	138	20	-	350
2017	6	204	100	44	-	354
2018	5	219	59	71	-	354
2019	-	174	32	57	-	263
2020	-	153	32	5	-	190
[1]Ischemic heart disease						
2016	58	1,298	820	275	8	2,459
2017	76	1,710	763	339	10	2,898
2018	36	2,189	420	329	9	2,983
2019	2	2,026	445	297	1	2,771
2020	1	1,978	295	98	-	2,372
Other heart diseases						
2016	92	861	496	338	1	1,788
2017	50	1,078	382	373	-	1,883
2018	28	1,269	211	381	-	1,889
2019	9	1,120	195	262	1	1,587
2020	2	1,078	152	224	-	1,456
Diseases of arteries, small arteries, and capillaries						
2016	6	289	64	241	1	601
2017	15	322	68	172	1	578
2018	3	370	56	227	-	656
2019	-	325	99	199	-	623
2020	1	369	68	176	2	616
[2]Cerebrovascular diseases						
2016	24	525	272	338	6	1,165
2017	22	673	264	297	-	1,256
2018	10	848	126	323	-	1,307
2019	1	896	216	346	1	1,460
2020	1	828	173	233	-	1,235
Diseases of the heart of pulmonary origin and diseases of the blood vessels of the lungs						
2016	-	23	1	4	-	28
2017	-	37	6	9	-	52
2018	-	95	1	3	-	99
2019	-	105	10	-	-	115
2020	-	99	-	-	-	99

Note: Rectal administration of diclofenac included doses other than 50 mg only for [1] ischemic heart disease (25 mg; 50 mg) and [2] cerebrovascular diseases (12.5 mg; 25 mg; 50 mg).

Table 6

Number of prescribed packages of diclofenac to patients with risk factors for cardiovascular disease (special warnings and precautions) in different strengths (doses) and pharmaceutical forms during the five-year period (2016–2020)

Parameter	Route of administration (dose)					Total
		oral (mg)		parenteral (ng/mL)	rectal (mg)	
[1]Hypertension						
2016	971	20,816	11,563	2,719	137	36,206
2017	1,042	28,230	11,097	3,016	104	43,489
2018	529	35,487	7,635	2,748	65	46,464
2019	183	34,918	9,096	2,531	57	46,785
2020	142	38,028	7,414	1,735	16	47,335
Hyperlipidemia						
2016	27	556	342	70	3	998
2017	36	710	282	124	-	1,152
2018	10	840	120	86	-	1,056
2019	2	789	169	117	-	1,077
2020	-	864	149	90	-	1,103
[2]Diabetes mellitus						
2016	250	5,469	3,052	1,328	26	10,125
2017	294	7,816	2,901	1,326	9	12,346
2018	151	9,662	2,224	1,220	5	13,262
2019	21	9,274	2,520	1,314	3	13,132
2020	54	10,077	2,083	902	4	13,120

Note: Rectal administration of diclofenac included doses other than 50 mg for [1] hypertension and [2] diabetes mellitus (12.5 mg; 25 mg; 50 mg).

Diclofenac was most frequently prescribed to the target population in formulations for oral use, in a dose of 75 mg (63.7% compared to other systemic formulations and doses of diclofenac). However, diclofenac was also prescribed in a dose of 100 mg where, in case the patients took it twice a day, the total daily dose exceeded the maximum permitted one of 150 mg. The contribution of diclofenac 100 mg oral formulations compared to other diclofenac doses and formulations amounted to 18.8% (Table 5).

Similarly, prescribing diclofenac 75 mg and 100 mg oral formulations in patients with risk factors for CVD amounted to 70.7% and 21.1%, respectively, compared to other systemic formulations and doses of diclofenac (Table 6).

Discussion

In a comprehensive multi-annual analysis of CV safety of diclofenac, the EMA concluded that the data on prescribing diclofenac systemic formulations are mainly unavailable and restricted and do not represent actual patients' exposure to diclofenac. That is why the EMA recommended that, in countries in which diclofenac is on the market, research is conducted according to the design of drug utilization study, aiming at gathering information on prescribing diclofenac, with special attention to the population taking this drug (age, gender, contraindications, given doses, length of use). Based on the results, the goal was to recommend efficient measures of reducing risks from diclofenac serious CV adverse reactions [14].

Taking into account the EMA recommendation, we wanted to analyze the prescription patterns of diclofenac systemic formulations by physicians at the OCS in MNE, to patients with CVD or with risk factors for CVD, in the five-year period (2016–2020). This time period followed the update of the SmPC of diclofenac with information on new contraindications and special warnings and precautions in 2015, approved by CInMED and based on the EMA recommendation. Additional motive and reason for conducting this study in MNE was the information on growing consumption of diclofenac and significantly higher values of DDD/1,000 inhabitants/day in MNE compared to the European Union (EU) countries and countries with high standards of healthcare, like the Scandinavian countries, which were used for comparison [4].

The largest study conducted so far in Europe, in which the prescription patterns of diclofenac to patients with CVD were investigated, was the study conducted by Morales et al. [17]. This study researched the impact of the EMA recommendations on CV contraindications (IHD, congestive heart failure, peripheral arterial disease, cerebrovascular diseases) and special warnings and precautions (hypertension, hyperlipidemia, DM) introduced in EU SmPC for diclofenac on prescribing this drug to patients with CVD or with risk factors for CVD. The study was conducted in four European countries: Denmark, the Netherlands, England, and Scotland. In all these countries, the implementation of SmPC with new CV safety information resulted in a decrease in diclofenac prescribing. In the first three months after introducing the EMA recommendation, the results showed a significant immediate absolute decrease in prescribing diclofenac to the following patients: those with IHD, peripheral arterial disease, and hyperlipidemia in all countries; patients with hypertension and diabetes in the Netherlands, England, and Scotland; patients with congestive heart failure and cerebrovascular disease in England and Scotland. Within the time period after three months

following the adoption of the EMA recommendation (post-intervention), a significant decrease has been noted in prescribing diclofenac to patients with IHD, peripheral arterial disease, hypertension, hyperlipidemia, and diabetes in the Netherlands and to patients with congestive heart insufficiency, IHD, peripheral arterial disease, and hypertension in Scotland. In England, the rates of prescribing diclofenac gradually decreased, while in Denmark, the changes in prescribing diclofenac had been more prominent after the earlier analysis of the EMA on CV safety risks of the systemic use of diclofenac in 2012. Although there has been a significant decrease in prescribing diclofenac, the authors indicate that some patients with CVD, which is a contraindication for the drug, continued having it prescribed, the extent of which varied by country and CVD.

A study was also conducted in Germany to investigate the impact of the EMA-recommended restrictions on the prescription of systemic formulations of diclofenac, with an emphasis on patients who have CV contraindications for diclofenac prescription or to whom diclofenac can be prescribed but with precaution. It was concluded that the overall decline in diclofenac initiation between 2011 and 2014 was largely independent of the presence or absence of new CV contraindications. The proportion of diclofenac initiators with a new contraindication remained at a high level (more than one in ten patients), indicating the need for research at the prescriber level (e.g., interventional studies) and additional measures to improve patient safety [18].

Contrary to the countries that were the subject of the above-mentioned study, in Lithuania, in the same period, diclofenac was the most frequently prescribed NSAID. In 2016, the contribution of diclofenac to the overall consumption of NSAIDs amounted to 30.0% [16]. Lithuania is an EU country also bound by the EMA recommendation and decisions of the European Commission. In the eleven years of the time period (2005–2016), the consumption of drugs that belong to pharmacotherapeutic groups N02B (other pain killers and antipyretics) and M01A (anti-inflammatory medicines and anti-rheumatics, non-steroidal) was increased in Lithuania by 22.8%, and from 58.4 in 2005 to 71.68 DDD/1,000 inhabitants/day in 2016, respectively. It can be indicated that despite the restrictions in prescribing diclofenac recommended by the EMA, consumption of diclofenac, as well as COX-2 inhibitors and piroxicam, was still high and growing within the observed period, while consumption of safer therapeutic alternatives (paracetamol, naproxen) was relatively low compared to the Scandinavian countries which have a prominent significant trend of decline in consumption of diclofenac and increase in consumption of paracetamol and naproxen [19].

In general, prescription databases provide an excellent infrastructure base for research in pharmacoepidemiology and pharmacovigilance. They contain information about patients, their medical and other characteristics, and all prescribed drugs, which gives the possibility of researching potential interactions between drugs, with a focus on clinically significant interactions. However, the continuous improvement of these databases, especially in implementing standardized coding systems and medical dictionaries, will provide a better understanding of the effectiveness and safety of drugs in routine clinical practice [20–25].

In Denmark, a study was conducted to examine the potential of prescription registries to capture individual-level use of aspirin and other nonsteroidal anti-inflammatory drugs, including diclofenac. It was concluded that the possibility of identifying NSAID use from prescription registries in Denmark is high. Low-dose aspirin and nonaspirin NSAID use varied substantially between 1999 and 2012. Notably, the use of cyclooxygenase-2 inhibitors nearly ceased, the use of diclofenac decreased markedly, and naproxen use remained unaltered [26].

Analysis of the data on prescribing systemic formulations of diclofenac in MNE from 2016 through 2020 shows that, despite new contraindications and precautions when prescribing diclofenac to patients with CVD as risk factors for CVD, this drug was widely prescribed to these patients. Namely, out of the overall number of patients who were prescribed diclofenac in that period, on average, almost every fifth patient had one of the CVD posing a contraindication or requiring special precaution in diclofenac prescribing. In the observed time period, diclofenac consumption was increased by 36.9% in patients with CVD or with risk factors for CVD. The highest (39.7%) number of CV patients to whom diclofenac was contraindicated but prescribed had IHD, while the highest (77.4%) number of patients to whom diclofenac can be prescribed but with increased precaution had hypertension. IHDs (*angina pectoris, infarctus myocardii, morbus cordis ischaemicus, cardiomyopathia ischaemica*) constitute serious clinically significant conditions which in the patients taking diclofenac may lead to an increase in their morbidity and mortality and increase the costs of healthcare due to the necessary treatment of these patients [27].

Our research showed that oral formulations of diclofenac in the dose of 75 mg were the most commonly prescribed diclofenac formulations at the OCS in MNE (63.7%) compared to other systemic formulations of diclofenac and doses. However, oral 100 mg formulations of diclofenac also made a significant contribution, which is potentially a risk factor for the progression of CVD when taking into account that the maximum daily dose of diclofenac is 150 mg. The diclofenac SmPC indicates that the risk of its serious adverse effects may be reduced using the lowest effective dose in the shortest possible period of time necessary for controlling the symptoms [10]. Bearing in mind the high consumption of diclofenac in MNE, as well as its safety risk in patients with CVD, as a routine measure to minimize (reduce) the risks, CInMED approved all systemic formulations of diclofenac to be dispensed only on prescription, with the aim of getting necessary physician's supervision over the use of diclofenac [28]. Despite that, however, it is obvious that diclofenac is irrationally prescribed at the OCS in MNE, even in patients contraindicated for diclofenac prescribing, which may result in serious health consequences for individual patients and the entire population. Therefore, it is necessary to take additional

measures (regulatory and educational) in order to raise the awareness of healthcare workers about the need to comply with the EMA and CInMED recommendations when prescribing diclofenac to patients with CVD. That refers not only to diclofenac but also to other medicines with recognized safety risks.

The main advantage of this study is that it included the entire system of primary health care in MNE, providing comprehensive insight into the prescribing practice of diclofenac – a drug with established CV risk at the level of healthcare that is mostly prescribed.

Nevertheless, the study has some limitations, such as the fact that it did not include the period before the adoption of regulatory measures by CInMED. That restricted the use of systemic formulations of diclofenac in patients with CVD. Therefore, it is unknown whether the obtained data on prescribing/consuming the drug in the observed five-year time period after the adoption of those measures indicate a decrease or increase compared to the previous period. PHCIS, which enabled the generation of data necessary for this study, was implemented in all healthcare centers in MNE after 2015. Because of that, obtaining data from the previous years was impossible. However, diclofenac consumption in MNE has been high for years, with no major oscillations. It may be assumed, therefore, that in the period before the adoption of regulatory measures regarding the increased CV risk from systemic use of diclofenac, this drug had also been prescribed to patients with CVD or with risk factors for CVD in approximately the same quantity, or probably more, than after those measures were adopted. In addition, one of the limitations of the existing PHCIS is that for some diagnoses which are risk factors for CVD, like smoking, reliable data on patients' exposure to this risk factor could not be generated from PHCIS. Healthcare professionals generally do not enter data on smoking in PHCIS as a diagnosis with the appropriate ICD code. If it is entered at all, it is done as a text field that cannot be parameterized and used for statistical analysis. For this reason, when it comes to risk factors for CVD, the focus of this article is on diagnoses (hypertension, DM, and hyperlipidemia) which are the most often precautionary measures for prescribing diclofenac.

Conclusion

The drugs containing diclofenac, intended for systemic use, are widely prescribed at the OCS in MNE, even in patients with contraindications and precautions for diclofenac prescribing, such as CV patients and patients with certain CVD risk factors. Due to high prescription and, consequently, consumption of diclofenac, designing efficient measures at the OCS is necessary in order to rationalize diclofenac prescribing. These measures would reduce CV risks from its irrational use and ultimately significantly improve public health.

R E F E R E N C E S

1. *Zhou Y, Boudreau DM, Freedman AN*. Trends in the use of aspirin and nonsteroidal anti-inflammatory drugs in the general U.S. population. Pharmacoepidemiol Drug Saf 2014; 23(1): 43–50.
2. *Davis JS, Lee HY, Kim J, Advani SM, Peng HL, Banfield E*, et al. Use of non-steroidal anti-inflammatory drugs in US adults: changes over time and by demographic. Open Heart 2017; 4(1): e000550.
3. *McGettigan P, Henry D*. Use of Non-steroidal Anti-inflammatory Drugs that Elevate Cardiovascular Risk: an Examination of Sales and Essential Medicines Lists in Low-, Middle-, and High-Income Countries. PLoS Med 2013; 10(2): e1001388.
4. *Institute for Medicines and Medical Devices*. Statistics for the annual consumption of medicines in Montenegro [Internet]. Montenegro: Institute for Medicines and Medical Devices; [accessed 2022 May 5]. Available from: https://cinmed.me/en/humane-medicines/consumption-of-medicines/ (Montenegrin)
5. *Agency for Medicinal Products and Medical Devices*. Annual Report on Drug Utilisation for 2020 [Internet]. Croatia: Agency for Medicinal Products and Medical Devices; 2020 [accessed 2022 May 5]. Available from: https://www.halmed.hr/en/Novosti-i-edukacije/Publikacije-i-izvjesca/Izvjesca-o-potrosnji-lijekova/ (Croatian)
6. *Norwegian Institute of Public Health*. Drug Consumption in Norway 2016-2020. Data from Norwegian Drug Wholesales Statistics and the Norwegian Prescription Database [Internet]. Norway: Norwegian Institute of Public Health; 2021 [accessed 2022 May 5]. Available from: https://www.fhi.no/en/publ/2021/drug-consumption-in-norway-2016-2020/
7. *European Medicines Agency (EMA)*. Assessment report for Non-Steroidal Anti-Inflammatory Drugs (NSAIDs) and cardiovascular risk. Procedure no: EMEA/H/A-5(3)/1319 [Internet]. Amsterdam, NL: European Medicines Agency; 2012 [accessed 2021 December 3]. Available from: https://www.ema.europa.eu/en/documents/referral/assessment-report-article-53-procedure-non-steroidal-anti-inflammatory-drugs-nsaids-cardiovascular_en.pdf
8. *European Medicines Agency (EMA)*. New safety advice for diclofenac – New measures aim to minimise cardiovascular risks [Internet]. Amsterdam, NL: European Medicines Agency; 2013 [accessed 2021 December 25]. Available from: https://www.ema.europa.eu/en/documents/referral/diclofenac-article-31-referral-new-safety-advice-diclofenac_en.pdf
9. *European Medicines Agency (EMA)*. New safety advice for diclofenac – CMDh endorses PRAC recommendation [Internet]. Amsterdam, NL: European Medicines Agency; 2013 [accessed 2021 December 25]. Available from: https://www.ema.europa.eu/en/news/new-safety-advice-diclofenac-cmdh-endorses-prac-recommendation#:~:text=The%20CMDh%20agreed%20with%20the,similar%20precautions%20should%20be%20applied.
10. *Institute for Medicines and Medical Devices*. Summary of product characteristics. Diclofenac, extended-release tablets, 100 mg, Galenika A.D. Serbia [Internet]. Montenegro: Institute for Medicines and Medical Devices; [accessed 2021 December 20]. Available from: https://cinmed.me/registar-humanih-lijekova/#anchor-id (Montenegrin)
11. *Institute for Medicines and Medical Devices*. Healthcare professional communication on safety of medicines containing diclofenac [Internet]. Montenegro: Institute for Medicines and Medical Devices; [accessed 2021 November 11]. Available from: https://cinmed.me/registar-humanih-lijekova/#anchor-id (Montenegrin)
12. *Institute for Medicines and Medical Devices*. Law on Medicines (Official Gazette of Montenegro 80/2020) [Internet]. Montene-

gro: Institute for Medicines and Medical Devices; 2020 [accessed 2021 November 11]. Available from: https://cinmed.me/wp-content/uploads/2023/01/Law-on-medicines-Official-Gazette-of-Montenegro-080-20-unofficial-translation.pdf

13. *Health Insurance Fund of Montenegro*. List of Medicines reimbursed by Health Insurance Fund of Montenegro [Internet]. Montenegro: Health Insurance Fund of Montenegro; [accessed 2021 November 11]. Available from: https://fzocg.me/lista-ljekova/ (Montenegrin)
14. *European Medicines Agency (EMA)*. Guideline on good pharmacovigilance practices (GVP). Module VIII – Post-authorisation safety studies (Rev 3) [Internet]. Amsterdam, NL: European Medicines Agency; 2017 [accessed 2021 December 20]. Available from: https://www.ema.europa.eu/en/documents/scientific-guideline/guideline-good-pharmacovigilance-practices-gvp-module-viii-post-authorisation-safety-studies-rev-3_en.pdf
15. *World Health Organization (WHO)*. International Classification of Diseases (ICD) 10th Revision [Internet]. Geneva, CH: World Health Organization; 2019 [accessed on 2023 May 19]. Available from: https://icd.who.int/browse10/2019/en
16. *WHO Collaborating Centre for Drug Statistics Methodology*. ATC/DDD Index 2016 [Internet]. Oslo, NO: Norwegian Institute of Public Health; 2016 [accessed on 2023 May 19]. Available from: http://www.whocc.no/atc_ddd_index/
17. *Morales DR, Morant SV, MacDonald TM, Hallas J, Ernst MT, Pottegard A*, et al. Impact of EU regulatory label changes for diclofenac in people with cardiovascular disease in four countries: Interrupted time series regression analysis. Br J Clin Pharmacol 2021; 87(3): 1129–40.
18. *Scholle O, Kollhorst B, Haug U*. Are prescribers not aware of cardiovascular contraindications for diclofenac? A claims data analysis. J Intern Med 2020; 287(2): 171–9.
19. *Kasciuškevičiūtė S, Gumbrevičius G, Vendzelytė A, Ščiupokas A, Petrikonis K, Kaduševičius E*. Impact of the World Health Organization pain treatment guidelines and the European medicines agency safety recommendations on nonsteroidal anti-inflammatory drug use in Lithuania: an observational study. Medicina (Kaunas) 2018; 54(2): 30.
20. *Schmidt M, Pedersen L, Sørensen HT*. The Danish civil registration system as a tool in epidemiology. Eur J Epidemiol 2014; 29(8): 541–9.
21. *Schmidt M, Schmidt SA, Sandegaard JL, Ehrenstein V, Pedersen L, Sørensen HT*. The Danish National Patient Registry: a review of content, data quality, and research potential. Clin Epidemiol 2015; 7: 449–90.
22. *Pottegård A, Schmidt SAJ, Wallach-Kildemoes H, Sørensen HT, Hallas J, Schmidt M*. Data resource profile: the Danish National Prescription Registry. Int J Epidemiol 2017; 46(3): 798–798f.
23. *Penning-van Beest FJ, Termorshuizen F, Goettsch WG, Klungel OH, Kastelein JJ, Herings RM*. Adherence to evidence-based statin guidelines reduces the risk of hospitalizations for acute myocardial infarction by 40%: a cohort study. Eur Heart J 2007; 28(2): 154–9.
24. *Herrett E, Gallagher AM, Bhaskaran K, Forbes H, Mathur R, van Staa T*, et al. Data resource profile: clinical practice research datalink (CPRD). Int J Epidemiol 2015; 44(3): 827–36.
25. *Alvarez-Madrazo S, McTaggart S, Nangle C, Nicholson E, Bennie M*. Data resource profile: the Scottish National Prescribing Information System (PIS). Int J Epidemiol 2016; 45(3): 714–715f.
26. *Schmidt M, Hallas J, Friis S*. Potential of prescription registries to capture individual-level use of aspirin and other nonsteroidal anti-inflammatory drugs in Denmark: trends in utilization 1999-2011. Clin Epidemiol 2014; 6: 155–68.
27. *European Medicines Agency (EMA)*. Important Medical Event List [Internet]. Amsterdam, NL: European Medicines Agency; [accessed 2022 August 10]. Available from: https://www.ema.europa.eu/en/human-regulatory/research-development/pharmacovigilance/eudravigilance/eudravigilance-system-overview
28. *Institute for Medicines and Medical Devices*. Rulebook on the form and content of a prescription, criteria for classification of medicines, as well as the manner of prescribing and dispensing medicines (Official Gazette of Montenegro 34/2015, 36/2016 and 59/2017) [Internet]. Montenegro: Institute for Medicines and Medical Devices; [accessed 2022 August 10]. Available from: https://cinmed.me/wpcontent/uploads/2023/01/Rulebookontheformandcontentofaprescriptioncriteriaforclassificationofmedicinesaswellasthemannerofprescribinganddispensingmedicines.pdf

Received on December 29, 2022
Revised on March 18, 2023
Accepted on March 21, 2023
Online First April 2023

Supplement – ICD diagnosis of relevance for research conducting

ICD-10: I20
Diagnosis: Angina pectoris
ICD-10: I21
Diagnosis: Infarctus myocardii acutus
ICD-10: I22
Diagnosis: Infarctus myocardii recidivus acutus
ICD-10: I23
Diagnosis: Complicatio acuta post infarctum cordis acutum
ICD-10: I24
Diagnosis: Morbi cordis ishaemici acuti alli
ICD-10: I25
Diagnosis: Morbus cordis ischaemicus chronicus
ICD-10: I26
Diagnosis: Embolia pulmonis
ICD-10: I27
Diagnosis: Morbi cordis pulmonales alii
ICD-10: I28
Diagnosis: Morbi vasorum pulmonis alii
ICD-10: I42
Diagnosis: Cardiomyopathia
ICD-10: I43
Diagnosis: Cardiomyopathia in morbis aliis
ICD-10: I50
Diagnosis: Insufficientia cordis
ICD-10: I60
Diagnosis: Haemorrhagia subarachnoidalis
ICD-10: I61
Diagnosis: Haemorrhagia cerebri
ICD-10: I62
Diagnosis: Haemorrhagia intracranialis non traumatica, alia
ICD-10: I63
Diagnosis: Infarctus cerebri
ICD-10: I64
Diagnosis: Apoplexia cerebri ut haemorrhagia sive infarctus non specificata
ICD-10: I65
Diagnosis: Occlusio arteriae praecerebralis et stenosis arteriae praecerebralis sine infarctus cerebri
ICD-10: I66
Diagnosis:Occlusio arteriae cerebri et stenosis arteriae cerebri sine infarctu
ICD-10: I67
Diagnosis: Morbi cerebrovasculares alli
ICD-10: I68
Diagnosis: Morbi cerebrovasculares in morbis aliis
ICD-10: I69
Diagnosis: Sequelae morbi cerebrovascularis
ICD-10: I70
Diagnosis: Atherosclerosis
ICD-10: I71
Diagnosis: Aneurysma aortae et dissectio aortae
ICD-10: I72
Diagnosis: Aneurysmata alia
ICD-10: I73
Diagnosis: Morbi vasorum periphericorum alii
ICD-10: I74
Diagnosis: Embolia ateriarum et thrombosis arteriarum
ICD-10: I77
Diagnosis: Morbi arteriales et arteriolares alli

ICD-10: I79
Diagnosis: Morbi arteriales, arteriolares et capillares in morbis aliis
ICD-10: I10
Diagnosis: Hypertensio arterialis essentialis (primaria)
ICD-10: I11
Diagnosis: Morbus cordis hypertensivus
ICD-10: I12
Diagnosis: Morbus renalis hypertensivus
ICD-10: I13
Diagnosis: Morbus cordis et morbus renis hypertensivus
ICD-10: I15
Diagnosis:Hypertensio arterialis, secundaria
ICD-10: E10
Diagnosis: Diabetes mellitus ab insulino dependens
ICD-10: E11
Diagnosis: Diabetes mellitus ad insulino independens
ICD-10: E12
Diagnosis: Diabetes mellitus malnutritionalis
ICD-10: E13
Diagnosis: Diabetes mellitus alius,specificatus
ICD-10: E14
Diagnosis: Diabetes mellitus,non specificatus
ICD-10: E78
Diagnosis: Disordines metabolismi lipoproteiniet lipidaemiae alii

CASE REPORTS

UDC: 616.438-007.46-056.7-089
DOI: https://doi.org/10.2298/VSP221205020V

Solid ectopic cervical thymus in an infant

Ektopični cervikalni timus čvrste strukture kod odojčeta

Aleksandar Vlahović*†, Milana Živković‡, Velibor Majić§, Zorka Badnjar - Ilić‖, Ninoslav Begović*¶, Ivan Dizdarević**

***University of Belgrade, Faculty of Medicine, Belgrade, Serbia; Institute for Mother and Child Health Care of Serbia "Dr. Vukan Čupić", †Department of Plastic Surgery and Burns, ¶Department of Orthopedics and Traumatology, **Department of Pediatric Cardiac Surgery, Belgrade, Serbia; ‡University Clinical Center of Serbia, Clinic for Burns, Plastic, and Reconstructive Surgery, Belgrade, Serbia; Institute for Children's Disease, §Clinic for Pediatric Surgery, ‖Clinic for Radiology, Podgorica, Montenegro**

Abstract

Introduction. Ectopic cervical thymus (ECT) occurs as a result of incomplete migration of the thymic primordia during embryogenesis. In the majority of cases, ECT is asymptomatic; however, in 10% of patients, there are different kinds of symptoms. **Case report.** A four-month-old baby boy was referred to our clinic for an evaluation of a growing large mass on the right side of the neck, present since birth. Physical examination revealed a solid, painless, soft, moderately mobile mass of irregular round shape localized on the right side of the neck, in front of the sternocleidomastoid muscle, below the parotid gland, and above the carotid lodge. The skin above the mass was unchanged. The dimensions of the mass were 40 × 32 × 15 mm. Based on the clinical and ultrasonographic findings, as well as the findings of the magnetic resonance imaging, it was suspected that the mass was an ECT. The mass was removed by surgical excision. The pathohistology report confirmed the presence of an ECT, with Hassall's corpuscles in the medulla. The postoperative course went smoothly, and the wound healed well. During the regular clinical, immunological, and ultrasound follow-ups over a period of six months, normal findings were registered. **Conclusion.** Congenital ECT is a rare congenital anomaly that must be, however, taken into account when considering the differential diagnosis of cervical tumor masses.

Key words:
congenital abnormalities; diagnosis, differential; infant; surgical procedures, operative; thymus gland.

Apstrakt

Uvod. Ektopični cervikalni timus (ECT) nastaje kao posledica nepotpune migracije primordijuma timusa tokom embriogeneze. U najvećem broju slučajeva ECT je asimptomatski, međutim kod oko 10% bolesnika postoje različite vrste simptoma. **Prikaz bolesnika.** Četvoromesečni dečak je hospitalizovan u našoj ustanovi zbog prisustva velike izrasline na desnoj strani vrata, prisutne od rođenja, sa tendencijom rasta. Fizikalnim pregledom konstatovana je čvrsta, bezbolna, meka, delimično pokretna masa nepravilnog kružnog oblika na desnoj strani vrata, ispred prednje ivice sternokleidomastoidnog mišića, iza parotidne žlezde i iznad karotidne lože. Koža iznad izrasline bila je nepromenjena. Dimenzije mase bile su 40 × 32 × 15 mm. Na osnovu kliničkog i ultrasonografskog nalaza, kao i nalaza magnetne rezonance, postavljena je sumnja da se radi o tkivu ECT. Promena je odstranjena hirurškim putem. Patohistološkim pregledom potvrđeno je prisustvo ECT, sa Hasalovim korpuskulima u meduli. Postoperativni tok protekao je uredno i rana je dobro zarasla. Na redovnim kliničkim, imunološkim i ultrazvučnim kontrolama u periodu od šest meseci registrovan je uredan nalaz. **Zaključak.** Kongenitalni ECT je retka kongenitalna anomalija koja se, međutim, mora uzeti u obzir prilikom razmatranja diferencijalne dijagnoze cervikalnih tumorskih masa.

Ključne reči:
anomalije; dijagnoza, diferencijalna; odojče; hirurgija, operativne procedure; timus.

Introduction

Ectopic cervical thymus (ECT) is an uncommon cause of neck masses [1, 2]. It results from incomplete migration of the thymic primordia during embryogenesis [3–10]. Most ECT are cystic but they can also be solid (10%) [7, 11]. Symptoms depend on the localization and size of the ectopic tissue [2, 7]. It can be asymptomatic in most (80–90%) cases; however, in a

Correspondence to: Aleksandar Vlahović, Institute for Mother and Child Health Care of Serbia "Dr. Vukan Čupić", Radoja Dakića 6–8, 11 000 Belgrade, Serbia. E-mail: aleksandarvlahovic@yahoo.com

small number of patients, there are symptoms such as pain or upper respiratory tract infection, or due to compression symptoms like stridor, dyspnea, dysphagia, and hoarseness [1, 2, 6–9, 11, 12].

The diagnosis of ECT is rarely made before the surgical treatment due to its asymptomatic nature [1, 6, 7]. It is essential to confirm the presence of the normal mediastinal thymus (if total thymectomy is performed, immunodeficiency could occur) [7–10]. Physical examination, ultrasonography (US), computed tomography, and magnetic resonance imaging (MRI) are diagnostic tools that are sufficient to establish an accurate diagnosis in the majority of cases [1, 2, 8, 9–16]. Fine needle aspiration biopsy can be an effective procedure to establish the diagnosis of ECT, and in the case of cystic ECT, this procedure can also be therapeutic [7, 10, 12, 15, 17, 18].

There are a number of neck lesions (congenital or acquired) that occur during childhood [1, 19]. The differential diagnosis includes thyroglossal duct cyst, branchial anomalies cysts, lymphadenopathy, vascular anomalies (infantile hemangioma, lymphatic malformation, venous malformation), inflammatory lesions, benign or malignant tumors, etc. [1–3, 13].

There are opponent opinions about the treatment [1–3, 8, 10]. Surgical excision is recommended based on the risk of severe clinical symptoms or malignant transformation [1, 4, 6–9, 11, 13, 16, 17]. On the other hand, some authors suggest observation with an MRI performed every six months to one year expecting involution (because of high morbidity associated with surgical excision) [10, 15, 17, 19]. Small and asymptomatic ECT requires observation (watch and wait policy); however, ECT causing compressive symptoms demands surgical management [3, 8, 10, 15].

To the best of our knowledge, 150 cases of ECT with sufficient documentation were reported in the pediatric population during the last 20 years (143 patients, seven cases with bilateral localization) [7, 18]. In ten cases, the definitive diagnosis was obtained after the autopsy, and in 106 cases, the surgical excision was performed (the final diagnosis was obtained after pathohistological analysis), while the rest were conservatively managed (observed). There were only 28 cases of surgically excised solid ECT during these 20 years, with the average age of the patients being 3.5 months [18].

Here, we present a case report of a four-month-old baby boy with ECT on the right side of his neck who underwent surgical excision.

Case report

A four-month-old baby boy was referred to the Clinic for Pediatric Surgery at the Institute for Children's Disease in Montenegro for the evaluation of a large mass on the right side of the neck. The mass has been present since birth. The mass was asymptomatic, but it was growing over time. The family history and the previous medical history were unremarkable. Physical examination revealed a painless, soft, moderately mobile, and round solid mass localized on the right side of the neck, in front of the sternocleidomastoid muscle, below the parotid gland, and above the carotid lodge. The mass was 40 × 32 × 15 mm large in diameter. No overlying skin changes or pits were apparent; the patient's neck position and mobility were not limited by the presence of the mass. US and MRI of the neck were performed (Figures 1 and 2). Following the clinical and MRI findings, the diagnosis of an ECT was highly suspected. The dimensions of a normal retrosternal thymus were 64 × 26 × 24 mm. After adequate preoperative preparation, surgical excision was done. The blunt dissection technique was performed, respecting the integrity of the pharyngeal, laryngeal, tracheal wall, and the surrounding neurovascular structures (Figure 3). The final pathohistology report confirmed the presence of an ECT tissue with Hassall's corpuscles in the medulla (Figure 4). The patient's postoperative course was unremarkable, without neurological defects or injuries. The wound healed primarily. Furthermore, clinical, immunological, and US follow-ups over a period of six months were unremarkable (Figure 5).

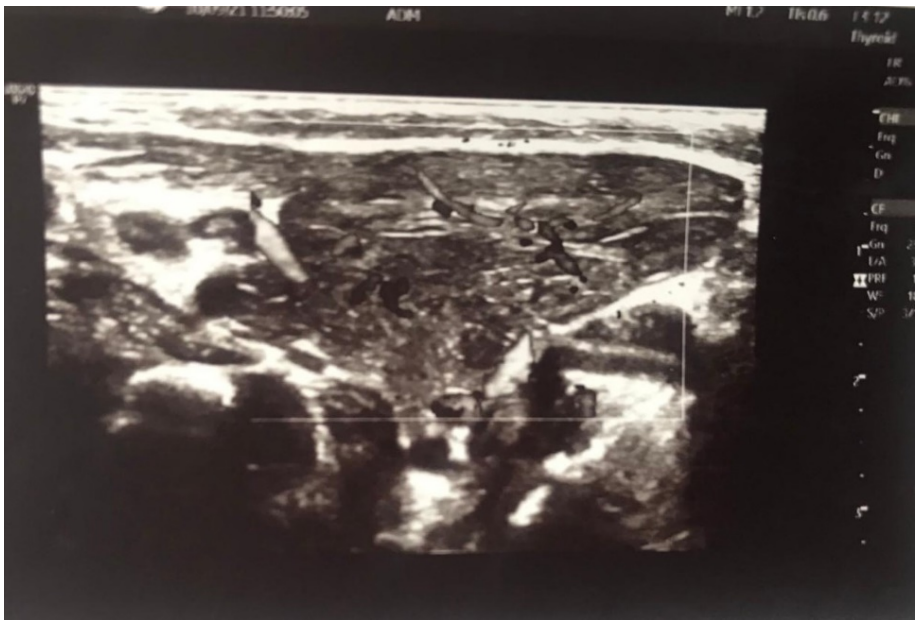

Fig. 1 – Ultrasound revealed a homogenous solid mass on the neck.

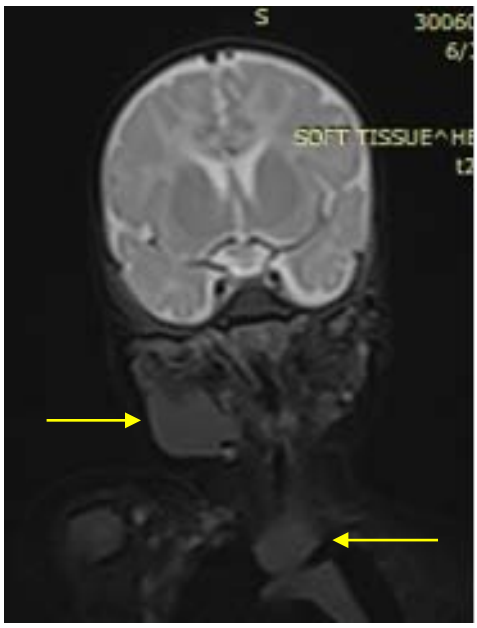

Fig. 2 – Magnetic resonance imaging of the neck. In the right parotid region of the neck (upper arrow), a homogeneous, clearly demarcated change is differentiated, which in all base sequences shows a signal that corresponds to the signal of the thymus (lower arrow).

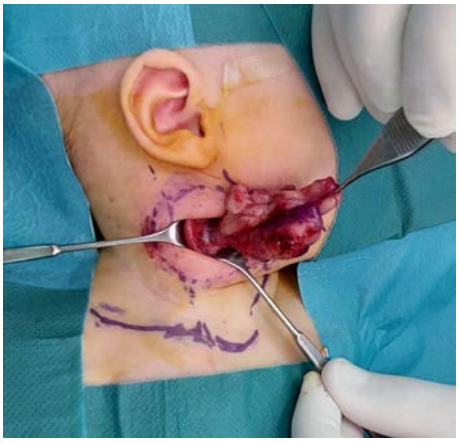

Fig. 3 – Intraoperative view of ectopic cervical thymus.

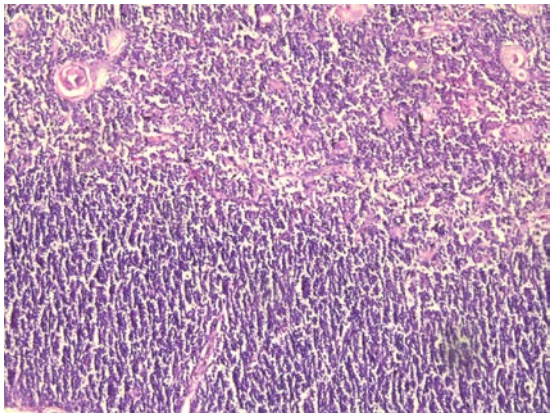

Fig. 4 – Pathohistology revealed ectopic cervical thymic tissue with Hassal's corpuscles in the medulla (hematoxylin and eosin, ×10).

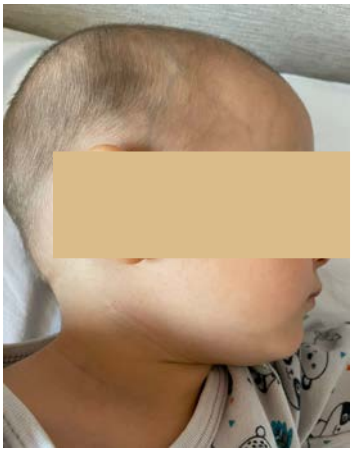

Fig. 5 – Patient six months after surgical treatment.

Discussion

The thymus is a paired organ developed from the third and occasionally fourth pharyngeal pouches during the sixth week of fetal life [2, 4, 7]. By the third month of development, the thymus matures to have a cortex and a medulla with Hassall's corpuscles [2]. Some authors suggest that ECT develops from the persistence of the thymopharyngeal duct or the degeneration of Hassall's corpuscles [1, 2, 6]. Due to its embryology, the ectopic thymus (ET) tissue can be found anywhere along the thymic pathway of descent [1, 2, 5]. For unknown reasons, according to the literature, ECT is more common on the left side (60–70% of total cases) [4, 6, 10, 13]. In our report, the ectopic tissue was on the right side of the neck, above the carotid lodge. Other authors have described ET tissue in the pharynx, subglottis, unilaterally or bilaterally in the neck [4, 5, 11].

The thymus exhibits age-related variation in weight and size. It reaches its maximum weight by puberty; after that, it slowly involutes, and the lymphoid component of the thymus is replaced by fat and connective tissue, with persistent Hassall's corpuscles [2, 7]. In our case, the normally located retrosternal thymus was 27 mm (transverse) and 24 mm (anteroposterior) in size. Çolak and Özkan [14] reported in their study that the average transverse diameter for male infants is 34.6 ± 4.9 mm, and the average anteroposterior diameter is 18.4 ± 4.0 mm.

ET exhibits hyperplasia during the first several years of life or following vaccination or infection [1, 7]. In our case, ET was 40 mm in length, while the average length, according to the literature, is 22.5 mm (ranging from 8 mm to 38 mm) [4]. Neck mass of thymic origin can be solid or, more often, cystic or both solid and cystic [2, 7, 9]. Only 10% of all ET masses have a form of the solid ET [7, 8, 11]. In our case, the presence of thymus tissue with clearly differentiated cortical and medullary zones with Hassall's corpuscles was confirmed on pathohistology.

The thymus plays an important immunological role during childhood [1, 11, 13]. Because of its immunological role, proving the presence of normal thymus tissue to avoid the occurrence of autoimmune diseases is vital. In our case, the normal thymus tissue was present, with a standard number of lymphocytes after surgery.

Cervical masses in children, whether benign or malignant, can be present with heterogeneous clinical signs [1, 4, 13]. Following the physical examination, US, and MRI findings, it can be very difficult sometimes to distinguish between benign and malignant lesions [4, 13]. A fast-growing cervical mass necessitates prompt attention with preferential screening for infectious diseases, vascular anomalies or bleeding, and malignancies due to its treatment [2, 6]. Additionally, an important consideration is the limited space in the neck to accommodate a fast-growing lesion that could have significant, sometimes fatal consequences [4, 13]. Dermoid cysts, lymph nodes, or branchial cysts should also be considered [9, 13]. In our case, an asymptomatic baby boy with normal laboratory findings was presented. According to the literature, after obtaining a complete history and physical examination, the US and the MRI have to be performed [1, 3, 4, 6, 9]. Based on the clinical and MRI findings, the lesion was highly suspected for ECT.

There are different opinions about the therapeutic approach. According to some authors, surgical excision is the treatment of choice for ECT for diagnostic and therapeutic reasons and risk of malignancy [1, 4, 6–9, 11, 13, 16, 17]. On the other hand, some authors suggest observation, especially in the case of small and asymptomatic ECT [8]. Due to the theoretical risk of infantile immunocompromising related to thymectomy, we find it reasonable to follow the mass with regular physical and imaging controls in asymptomatic children with a small mass. On the contrary, a large mass that can cause compressive symptoms has to be completely excised [1, 6, 11]. In our case, we performed surgical treatment because of the growth of the lesion, the risk of compressive symptoms, potential neoplastic degeneration, and the need for a definitive diagnosis. The blunt dissection was performed during the surgical procedure with great care to avoid injury to surrounding vital structures. There is no clear data about solid ECT recurrence (2% for cystic) [1, 2, 11]. In our case, the postoperative period was unremarkable, and there was no difference in the total number of lymphocytes or the occurrence of infection during a six-month follow-up.

Conclusion

Congenital ECT is a rare congenital anomaly that should be, however, taken into account when considering the differential diagnosis of neck masses.

REFERENCES

1. *Park JJ, Kim JW, Kim JP, Ahn SK, Jeong JH, Jeon SY.* Two cases of ectopic cervical thymus: case reports and a review of the literature. Auris Nasus Larynx 2006; 33(1): 101–5.
2. *Statham MM, Mehta D, Willging JP.* Cervical thymic remnants in children. Int J Pediatr Otorhinolaryngol 2008; 72(12): 1807–13.
3. *Purcell PL, Marquez Garcia J, Zawawi F, Propst EJ, Papsin BC, Blaser SI,* et al. Ectopic cervical thymus in children: Clinical and radiographic features. Laryngoscope 2020; 130(6): 1577–82.
4. *Chen C, Liu BB, Bian PP, Xu BC, Guo YF.* Pharyngeal ectopic thymus: a case report. Ear Nose Throat J 2021; 100(8): NP354–6.
5. *Sahhar HS, Marra S, Boyd C, Akhter J.* Ectopic subglottic thymic cyst: a rare cause of congenital stridor. Ear Nose Throat J 2003; 82(11): 873–4.
6. *Saggese D, Ceroni Compadretti G, Cartaroni C.* Cervical ectopic thymus: a case report and review of the literature. Int J Pediatr Otorhinolaryngol 2002; 66(1): 77–80.
7. *Prasad TR, Chui CH, Ong CL, Meenakshi A.* Cervical ectopic thymus in an infant. Singapore Med J 2006; 47(1): 68–70.
8. *Kotani H, Ishida T, Miyao M, Manabe S, Kawai C, Abiru H,* et al. Ectopic cervical thymus: a clinicopathological study of consecutive, unselected infant autopsies. Int J Pediatr Otorhinolaryngol 2014; 78(11): 1917–22.

9. *Clark JJ, Johnson SM*. Solid cervical ectopic thymus in an infant. J Pediatr Surg 2009; 44(7): e19–21.
10. *Tunkel DE, Erozan YS, Weir EG*. Ectopic cervical thymic tissue: diagnosis by fine needle aspiration. Arch Pathol Lab Med 2001; 125(2): 278–81.
11. *Scott KJ, Schroeder AA, Greinwald JH Jr*. Ectopic cervical thymus: an uncommon diagnosis in the evaluation of pediatric neck masses. Arch Otolaryngol Head Neck Surg 2002; 128(6): 714–7.
12. *Ishida T, Kotani H, Miyao M, Abiru H, Kawai C, Osamura T,* et al. Ectopic cervical thymus associated with infant death: 2 case reports and literature review. Int J Pediatr Otorhinolaryngol 2013; 77(9): 1609–12.
13. *Claes L, Dendooven A, van Heerden J*. Challenges in diagnosing ectopic thymus tissue in children. BMJ Case Rep 2019; 12(9): e228807.
14. *Çolak E, Özkan B*. Multidetector computed tomographic evaluation of the normal characteristics of the thymus in the pediatric population. J Belg Soc Radiol 2022; 106(1): 110.
15. *Schloegel LJ, Gottschall JA*. Ectopic cervical thymus: is empiric surgical excision necessary? Int J Pediatr Otorhinolaryngol 2009; 73(3): 475–9.
16. *Alnosair AA, Alnosair LA, Almohammed Saleh AA, Al Zaid AR, Al Albareth AS, Alkhars FS*. Solid ectopic cervical thymus: a case report. Cureus 2022; 14(5): e25142.
17. *Abakir N, Eravci FC, Emlik GD*. Symptomatic solid ectopic cervical thymus in a 2-month-old infant: case report. Turk Arch Otorhinolaryngol 2021; 59(2): 154–7.
18. *Chang A, Nataraja RM, Pudel E, Stunden R, Baré S, Pacilli M*. Diagnosis and management of ectopic cervical thymus in children: Systematic review of the literature. J Pediatr Surg 2021; 56(11): 2062–8.
19. *Rousslang L, Meldrum J, Veronica R, Poutre A, Biega T*. Ectopic cervical thymus: a common, yet rarely symptomatic pediatric neck mass. Curr Med Imaging 2021; 17(4): 544–8.

Received on December 5, 2022
Revised on March 16, 2023
Accepted on March 21, 2023
Online First April 2023

CASE REPORT

UDC: 618.4-089.5-06::616.8
DOI: https://doi.org/10.2298/VSP220901098D

Longitudinally extensive transverse myelitis after epidural anaesthesia in childbirth

Longitudinalni ekstenzivni transverzalni mijelitis posle epiduralne anestezije primenjene tokom porođaja

Dijana Damnjanović*, Milena Zamurović†, Aleksandar Vranjanac†

***Special Gynecology Hospital with Maternity Ward Jevremova Medigroup, Belgrade, Serbia; †Gynecologycal and Obstetrical Clinic "Narodni front", Belgrade, Serbia**

Abstract

Introduction. Neurological complications related to epidural anesthesia are rare, but it is necessary to recognize and diagnose them as early as possible, in order to start appropriate therapy and prevent further neurological damage. One of the rare complications of regional anesthesia described in this paper is longitudinal extensive transversal myelitis (LETM). **Case report.** A 32-year-old patient, who gave birth by Caesarean section in due term, developed LETM the very same day. Considering the neuroradiological findings that indicated to the long central lesion in the thoracic and lumbar spine, and an expected reaction to the applied immunotherapy (immunosuppressive therapy and therapeutic plasma exchange), a diagnosis of LETM was made. Even with all the therapy and regression of the lesions, the patient could not stand up without support. During the subsequent treatment, according to the instructions of the physiatrist, physical therapy was carried out, to which the patient responded slowly but favorably, with a gradual return of the function of the lower extremities. **Conclusion.** Early diagnosis and timely treatment of LETM are crucial for the prognosis of the disease and the early recovery of the patient.

Key words:
anesthesia, epidural; diagnosis; drug-related side effects and adverse reactions; delivery, obstetric; myelitis, transverse; paralysis.

Apstrakt

Uvod. Neurološke komplikacije vezane za epiduralnu anesteziju su retke, ali je neophodno što ranije ih prepoznati i dijagnostikovati, u cilju započinjanja odgovarajuće terapije i sprečavanja daljih neuroloških oštećenja. Jedna od retkih komplikacija regionalne anestezije opisane u ovom radu je longitudinalni ekstenzivni transverzalni mijelitis (LETM). **Prikaz bolesnika.** Bolesnica stara 32 godine, porođena carskim rezom u terminu, istog dana razvila je LETM. Imajući u vidu neuroradiološke nalaze koji su ukazivali na dugu centralnu leziju u torakalnom i lumbalnom delu kičme, i očekivanu reakciju na primenjenu imunoterapiju (imunosupresivna terapija i terapijska izmena plazme), postavljena je dijagnoza LETM. I pored primenjene terapije i regresije lezija, bolesnica nije mogla da ustane bez podrške. U toku kasnijeg lečenja, po instrukcijama fizijatra sprovedena je fizikalna terapija, na koju je bolesnica sporo ali povoljno reagovala, postepenim povratkom funkcije donjih ekstremiteta. **Zaključak.** Rana dijagnostika i blagovremeno lečenje LETM ključni su za prognozu bolesti i rani oporavak bolesnika.

Ključne reči:
anestezija, epiduralna; dijagnoza; lekovi, neželjeni efekti i neželjene reakcije; porođaj; mijelitis, transverzalni; paraliza.

Introduction

Neurological complications following obstetric central neural blocks rarely happen. Even though central neural blockade can cause neurological complications, it is essential to understand that neurological deficits may develop spontaneously (e.g., epidural abscess/hematoma) or as a result of the course of labor (maternal obstetric palsies) [1].

Serious, life-changing neurological complications caused by central neural blocks are rare. Immediate recognition and appropriate management are of crucial importance in reducing the risk of permanent neurological impairment [2].

We present a patient with longitudinal extensive transverse myelitis (LETM) several hours after giving birth by Caesarean section (C-section) performed under epidural anesthesia.

Correspondence to: Milena Zamurović, Gynecologycal and Obstetrical Clinic "Narodni front", Kraljice Natalije 62, 11 000 Belgrade, Serbia. E-mail: mzamurovic@gmail.com

Case report

A pregnant 32-year-old woman came to the gynecological clinic for delivery in the expected term. Contractions were irregular; however, prelabour rupture of the membranes occurred. Two years earlier, this patient gave birth by C-section, performed without complications. Medical history data indicated that the patient was healthy and pregnancy was under control; yet, during the fourth month of pregnancy, the patient was infected by COVID-19, characterized by a moderate clinical picture. Immunization against SARS-CoV-2 was not performed.

The premature rupture of the membranes, irregular uterine contractions, unfavorable obstetric findings, and the fact that previous childbirth ended with a C-section two years earlier were all indications for this delivery to be performed surgically, i.e., by C-section. After the usual preoperative preparation, a C-section was performed with epidural anaesthesia. Since the previous C-section was performed under epidural anesthesia, the decision was made to perform this one under the same anesthesia. An epidural catheter was placed in the operating room. The patient was placed in a sitting position. In sterile conditions, an 18G needle was placed in the L4/L5 space. The epidural space was identified using the saline loss of resistance technique (loss of resistance to saline – LORS). The epidural catheter was placed through the needle at a depth of 5 cm. Then the needle was taken out, and the catheter was connected to the connector and fixed at the insertion site.

After that, a 20 mL dose of 0.5% bupivacaine + fentanyl 100 μg was given, 5 mL each in frames of 5 min between doses. The patient felt pain in the lumbar region during the placement of the epidural catheter. The operative course was normal and complication-free. No anesthesiological complications were noted during the surgery. A healthy male child was delivered by C-section, weighing 3,400 g, 52 cm long, with an Apgar score of 9/10.

The same afternoon, the patient told the doctor that she did not feel well. The patient could not feel her legs nor move them. She was unable to get out of bed. The patient was examined by an anesthesiologist and internist. Laboratory blood tests were performed. All performed laboratory analyses were within physiological limits, including all inflammatory parameters and coagulation analyses. As the discomfort persisted, the patient was referred to a neurologist. The neurologist concluded that it was a case of *paraplegia flaccida*.

A lumbosacral spine computed tomography scan was indicated, followed by a magnetic resonance imaging (MRI) scan, which verified the existence of an inflammatory process of the spinal cord in the T8–T12 levels that correspond to transversal LETM accompanied by edema. Treatment was continued at a neurological clinic. The patient was examined by an internist and cardiologist; all findings were normal. Persistent weakness in the lower extremities with severe flaccid paraparesis was verified by a neurological exam together with bilaterally extinguished reflexes and hyperesthesia below knee level. Deep sensitivity was preserved, while vibration sensitivity was reduced to knee level. Muscle size, tone, mobility, and reflexes of the upper extremities were normal. Cerebellar test results were also normal. Examination of the spinal fluid obtained by lumbar punction was performed. Bacterial and viral tests in the spinal fluid were negative. Cytochemical analysis of the spinal fluid confirmed the presence of 5 lymphocytes, proteinorachia 0.52, and glycorachia 4.5 at a glycemic ratio of 6.2. All immunology and virology blood tests were negative, thus excluding the existence of autoimmune diseases [ANA (antinuclear antibody) and VDRL (venereal disease research laboratory) were negative] and viral infections [human immunodeficiency virus (HIV), herpes simplex virus (HSV), and hepatitis C virus (HCV)]. MRI examination of the endocranium confirmed normal findings. Cervical spine MRI examination showed a corrected physiological lordosis of the cervical spine, moderate symptoms of spondylosis, protrusion of C4–C5 disc, osteophyte complex with compromised root C5 right and light reduction of anterior cerebrospinal fluid spaces, with relative spinal stenosis but without any signs of myelopathy. MRI exam of the thoracic spine and thoracolumbar junction confirmed a longitudinal lesion of the spinal cord extending from the upper plate T9 distally to the T12–L1 level, easily expanding the myelin. In differential diagnostics, such findings could have corresponded to transverse myelitis, sequelae of acute disseminated encephalomyelitis, or even spinal meningitis. Bearing in mind that an MRI exam was also performed immediately after delivery, i.e., several days earlier, the results were compared, and it was noted that a partial regression of the described lesion had occurred. During the entire hospitalization, the patient was stable and afebrile. She was treated with pulse corticosteroid therapy (methylprednisolone), initially 1 g/day for five days, then with 2 g/day for another five days, followed by therapeutic plasma exchange (seven treatments in total), accompanied by physical therapy. This therapy led to improvement of the neurological condition of the patient (improved strength of the proximal leg muscles). However, even with all the therapy and regression of the lesions, the patient could not stand up without support (crutches) and could only make a few steps. For that reason, immediately after being discharged from the neurology clinic, the patient was sent to intensive physical therapy under the constant supervision of a physiatrist. During the subsequent treatment, according to the instructions of the physiatrist, physical therapy was carried out, to which the patient responded slowly but favorably, gradually regaining the function of the lower extremities.

Discussion

LETM is a neurological condition characterized by a contiguous inflammatory lesion of the spinal cord [3]. It is usually related to autoimmune disease of the central nervous system, rarely to multiple sclerosis.

The clinical course of LETM is characterized by single or multiple attacks of paraparesis or tetraparesis, sensory deficits, and bowel/bladder disturbances, and can lead to respiratory failure in severe cases [4]. The early distinction between

possible LETM etiologies is crucial in providing an accurate prognosis and guiding therapeutic strategy.

This case report presents a patient who had given birth by C-section in epidural anaesthesia and developed paraparesis the same day after delivery. During hospitalization, the vascular, inflammatory, infectious, neoplastic, and paraneoplastic nature of the disorder was analyzed. Considering the neuroradiological findings that indicated to the long central lesion in the thoracic and lumbar spine, with an expected response to the applied immunotherapy (immunosuppressive therapy and therapeutic plasma exchange), it was concluded that this was a case of LETM of incompletely clarified etiology, most likely of immunological reasons.

References cite sporadic cases of LETM, usually related to autoimmune diseases. For instance, a study by Chen et al. [5] from 2004 described seven cases of LETM accompanied by systemic lupus erythematosus; nevertheless, not many cases in which LETM clinical picture appeared immediately after delivery in epidural anesthesia have been described so far [6].

Furthermore, no available data in the literature could confirm whether or not COVID-19 infection in pregnancy could cause some unrecognized immune disorders.

Conclusion

For the recovery from LETM, early diagnostics and the introduction of adequate therapy are crucial in order to alleviate or prevent further neurological consequences and quickly reestablish normal quality of life. Even though LETM is a rare neurological complication of epidural anaesthesia in childbirth, it should be taken into account and diagnosed promptly so that the patient can recover as soon as possible and dedicate all of her strength to her child.

REFERENCES

1. *Loo CC, Dahlgren G, Irestedt L.* Neurological complications in obstetric regional anaesthesia. Int J Obstet Anesth 2000; 9(2): 99124.
2. *Duncan A, Patel S.* Neurological complications in obstetric regional anesthetic practice. J Obstet Anaesth Crit Care 2016; 6(1): 3–10.
3. *Nightingale H, Witherick J, Wilkins A.* Diagnosis of longitudinally extensive transverse myelitis. BMJ Case Rep 2011; 2011: bcr1020103444.
4. *Pandit L.* Transverse myelitis spectrum disorders. Neurol India 2009; 57(2): 126–33.
5. *Chen HC, Lai JH, Juan CJ, Kuo SY, Chen CH, Chang DM.* Longitudinal myelitis as an initial manifestation of systemic lupus erythematosus. Am J Med Sci 2004; 327(2): 105–8.
6. *Kitazaki Y, Ueno A, Maeda K, Asano R, Satomi H, Nishio T,* et al. A case of longitudinally extensive transverse myelitis with an isolated pontine lesion following epidural and spinal anesthesia for cesarean section. eNeurologicalSci 2020; 21: 100264.

Received on September 1, 2022
Revised on October 27, 2022
Accepted on October 28, 2022
Online First November 2022

CASE REPORT

UDC: 616.5-006-031.6::616.714.1]:: 616-006-07/-08
DOI: https://doi.org/10.2298/VSP210226100S

Squamous cell carcinoma of the scalp with intracranial extension – the importance of various imaging modalities

Planocelularni karcinom poglavine sa intrakranijalnim širenjem – značaj različitih modaliteta snimanja

Srdjan Stošić*†, Mirela Juković*†, Jagoš Golubović†‡, Milana Panjković†§, Sanja Stojanović*†

University Clinical Center of Vojvodina, *Center for Radiology, ‡Clinic for Neurosurgery, §Center for Pathology and Histology, Novi Sad, Serbia; †University of Novi Sad, Faculty of Medicine, Novi Sad, Serbia

Abstract

Introduction. Around 2% of all cutaneous neoplasms arise in the scalp and can be classified as either primary or metastatic. The intracranial extension is rare in cutaneous malignancies but can generally occur if left untreated. Squamous cell carcinoma (SCC) is the second most common type of nonmelanoma skin cancer after basal cell carcinoma. About 3–8% of SCCs are located on the scalp and can cause skull and dural invasion in rare cases. **Case report.** A 49-year-old male patient presented with a large and painful lesion in the parietooccipital region of the head. Magnetic resonance imaging (MRI) revealed a large inhomogeneous, necrotic lesion with infiltration of the underlying skull and dura. The patient underwent surgical removal of the tumor with excision of invaded skin, bone, and dura with a safety margin of 1 cm, followed by custom prefabricated 3D-printed cranioplasty with polymethylmetacrilate. Pathohistological analysis revealed invasive SCC with immunohistochemistry staining revealing CK5/6 and CK7 positivity. **Conclusion.** Some cases of scalp SCCs can cause invasion of the underlying skull and dura if left untreated. Imaging modalities like computed tomography (CT) and MRI play a crucial role in evaluating the degree of neoplastic extension and potential calvarial and dural invasion, thus being of significant importance in preoperative planning and management.

Key words:
diagnosis; histological techniques; immunohistochemistry; magnetic resonance imaging; neoplasm invasiveness; neoplasms, squamous cell; neurosurgical procedures; scalp.

Apstrakt

Uvod. Oko 2% svih neoplazmi kože javlja se na poglavini, i mogu biti klasifikovane kao primarne i metastatske. Intrakranijalno širenje je retko kod maligniteta kože, ali se generalno može javiti kada se lečenje odlaže. Planocelularni karcinom (PCK) je drugi najčešći tip nemelanomskog karcinoma kože posle bazocelularnog karcinoma. Oko 3–8% PCK lokalizovano je na poglavini, i u retkim slučajevima mogu se širiti intrakranijalno i infiltrisati tvrdu moždanu opnu (duru). **Prikaz bolesnika.** Bolesnik star 49 godina javio se na pregled sa velikom, bolnom tumefakcijom na levoj parijetookcipitalnoj regiji glave. Na snimku dobijenom magnetnom rezonancom (MR) uočene su velike, nehomogene, nekrotične lezije, sa infiltracijom podležuće lobanje i dure. Bolesniku je tumor hirurški odstranjen ekscizijom infiltrisane kože, lobanje i dure sa bezbednosnom marginom od 1 cm, posle čega je urađena kranioplastika korišćenjem prethodno specifično konstruisanog 3D grafta od polimetilmetakrilata. Patohistološkom analizom utvrđen je invazivni PCK, a imunohistohemijskom analizom je nađena CK5/6 i CK7 pozitivnost. **Zaključak.** U nekim slučajevima, kada se lečenje odlaže, PCK poglavine može izazvati invaziju podležuće lobanje i dure. Modaliteti snimanja kao što su kompjuterizovana tomografija i MR igraju važnu ulogu u proceni širenja tumora i potencijalne invazije svoda lobanje (kalvarje) i dure, zauzimajući važno mesto u preoperativnom planiranju i zbrinjavanju.

Ključne reči:
dijagnoza; histološke tehnike; imunohistohemija; magnetska rezonanca, snimanje; neoplazme, invazivnost; karcinom, planocelularni; neurohirurške procedure; skalp.

Correspondence to: Srđan Stošić, University Clinical Center of Vojvodina, Center for Radiology, Hajduk Veljkova 1–3, 21 000 Novi Sad, Serbia. E-mail: srdjan.stosic@mf.uns.ac.rs

Introduction

Around 2% of all cutaneous neoplasms arise in the scalp and can be classified as either primary scalp tumors (epithelial, melanocytic, adnexal) or metastatic [1, 2]. In adult populations, 93–98% of scalp lesions are benign, with the most common lesion being trichilemmal cysts, followed by epidermal cysts, lipoma, nevi, and sebaceous cysts, while primary malignant tumors of the scalp are rare [3–6]. Skull and dural infiltration is rare in cutaneous malignancies but can generally occur if left untreated [6, 7]. Squamous cell carcinoma (SCC) is the second most common subtype of nonmelanoma skin cancer after basal cell carcinoma (BCC), representing about 20% of these tumors. Like BCCs, the incidence of SCCs is increasing throughout the world, with risk factors including ultraviolet radiation exposure, age, fair skin, history of skin cancer, actinic damage, and immunosuppression [8]. About 3–8% of SCCs are located on the scalp and, if left untreated, can cause skull and dural invasion [4].

We present a case of a large, initially untreated scalp lesion, proven to be SCC with invasion of the underlying calvaria and dura.

Case report

A 49-year-old male patient presented with a large and painful cutaneous lesion in the left parietooccipital region of the head. Physical examination revealed a large cauliflower-like, partially necrotic, painful lesion with peripheral subcutaneous induration and erythema. The lesion had previously been neglected for some time, and the patient finally got consulted because of rapid growth in the few months leading up to the examination. There were no signs of neurological impairment, and no other symptoms were present. Magnetic resonance imaging (MRI) revealed a large inhomogeneous lesion in the left parietooccipital region with intracranial extension and dural infiltration. The tumor was predominantly T2 weighted (T2W)/T1 weighted (T1W) isointense with prominent zones of T2W hyperintensity, suggesting cystic degeneration or necrosis (Figure 1). There were no signs of diffusion restriction. No foci of succeptibility weighted imaging (SWI) hypointense signal were detected. The lesion showed significant inhomogeneous contrast enhancement with extensive zones of hypovascularity, suggesting necrosis. The lesion was localized near the displaced superior sagittal sinus (SSS) without an evident defect after administration of paramagnetic contrast (Figure 2). The specificity of this lesion is in its size, location, and invasivity, as similar lesions have been rarely encountered, let alone treated and pathohistologically verified, due to the often poor condition of the patient. Owing to his good clinical condition, the patient underwent surgical removal of the tumor with excision of invaded skin, bone, and dura with a safety margin of 1 cm; as the invasion of SSS was not observed intraoperatively, gross total removal was confirmed by the neurosurgeon. The excised dural portion was reconstructed with an autograft that was taken from the fascia lata. Craniotomy planning was performed preoperatively virtually, followed by three-dimensional (3D) printing of craniotomy bone cutting guide and, subsequently, after 3D-guided preplanned craniotomy, the cranial implant was custom prefabricated *via* 3D-printed molds used to shape the polymethylmetacrilate implant under sterile conditions, which had a perfect fit intraoperatively. That was an important treatment step needed to achieve better functional and aesthetic outcomes as well as speed up the surgery time and reduce complications rate such as bleeding, primarily, and the need for excessive drilling that could potentially lead

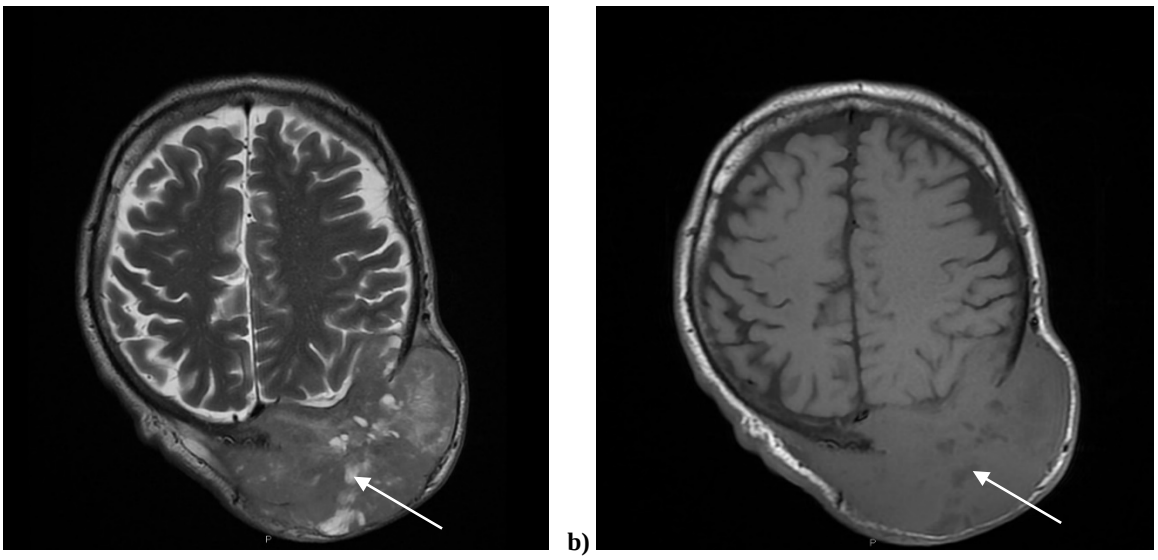

Fig. 1 – Magnetic resonance imaging of the brain. a) Transversal T2W image; b) Transversal T1W image. Large inhomogeneous tumor in the left parietooccipital region with intracranial extension. The lesion is predominantly T2W/T1W isointense with zones of T2W hyper/T1W hypointensity (indicated by arrow). T2W – T2 weighted; T1W – T1 weighted.

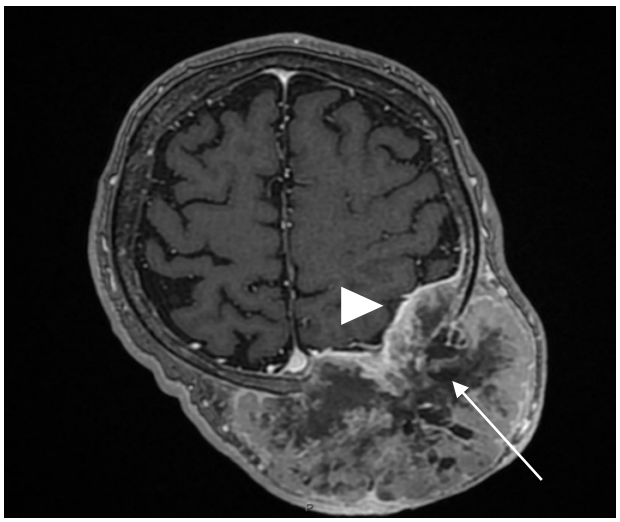

Fig. 2 – Magnetic resonance imaging of the brain. Transversal 3DT1W images after paramagnetic contrast administration. Prominent inhomogeneous signal alteration of the lesion with extensive zones of hypovascularity suggesting necrosis (indicated by →). Signs of dural infiltration (indicated by ►). The lesion is localized near the displaced superior sagittal sinus with no evident contrast defect. 3DT1W – 3D T1 weighted image.

to dural and/or thermic injury. Pathohistological (PH) analysis revealed invasive SCC (Figure 3) with immunohistochemistry staining, which revealed CK5/6 and CK7 positivity (Figure 4). A postoperative computed tomography (CT) scan was performed, which showed no signs of surgical complications (Figure 5).

Discussion

SCCs of the scalp are usually diagnosed before the invasion of the skull due to their progressive and slow extension. However, the possibility of skull and dural infiltration exists in the late stages of development, with very

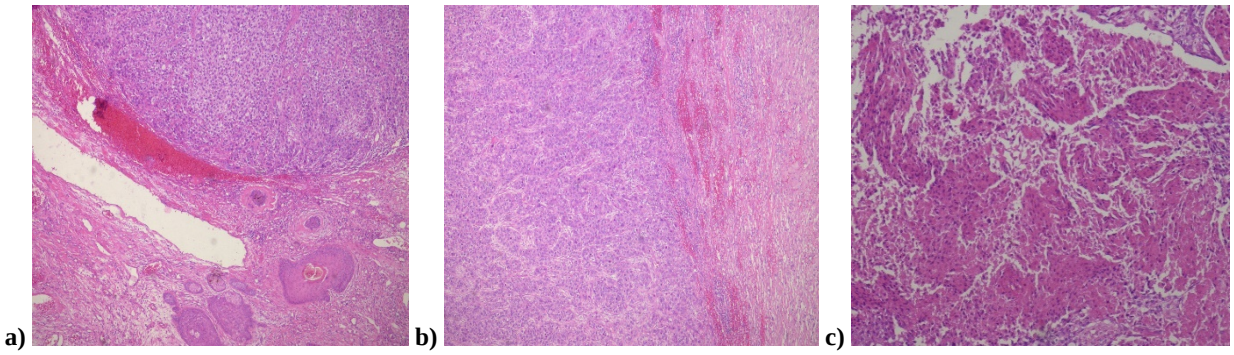

Fig. 3 – Pathohistology, hematoxylin and eosin staining; a) Squamous cell carcinoma (SCC) in the dermis; b) Dural invasion; c) Dyskeratosis in SCC. Magnifications ×50 (a,b), ×100 (c).

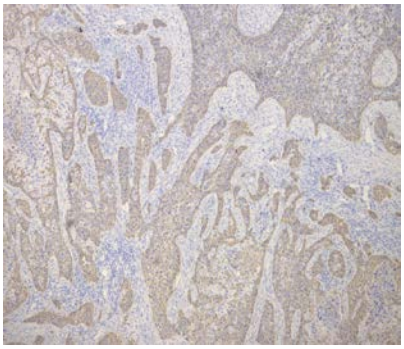

Fig. 4 – Immunohistochemistry finding shows CK5/6 positive reaction verifying squamous differentiation of tumor (magnification ×50).

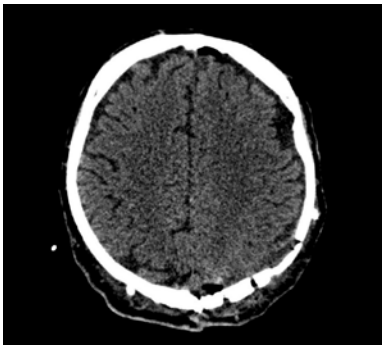

Fig. 5 – Postoperative computed tomography, axial non-contrast slices. No signs of surgical complications.

few cases involving the adjacent brain [9]. As some SCCs of the scalp are diagnosed at this advanced stage, this location may be considered an independent risk factor for poor prognosis [4, 10].

BCC and SCC are the two most common types of malignant cutaneous tumors of the scalp accounting for 41% and 17% of cases, respectively, with 12–18% of BCCs and 3–8% of SCCs being located on the scalp [4, 10, 11]. Other, albeit less common, malignant lesions of the scalp include malignant melanoma, angiosarcoma, Merkel cell carcinoma, and metastasis. BCCs and SCCs are indistinguishable on MRI, with both tumors showing nonspecific T1W hypointensity and iso-hyperintensity on T2W images, and both lesions often having central recesses [12]. A scalp-localized dermatofibrosarcoma protuberans (DFSP), which is a rare locally aggressive sarcoma of the dermis, can have a similar imaging presentation, although the lesion is much slower growing and painless. On T1W images, DFSP is isointense, with a variable T2W signal, mostly hyperintense, sometimes iso- or hypointense. Contrast enhancement pattern in DFSP ranges from mild to markedly heterogeneous or homogeneous [13].

While the vast majority of skin cancers can be treated based on clinical features alone, large and aggressive tumors that may compromise vital structures demand radiologic imaging for a detailed assessment and further optimal management. Skin cancers that most frequently require imaging are SCC, BCC, DFSP, and Merkel cell carcinoma [14]. Both locally aggressive BCCs and SCCs of the forehead and scalp have been shown to potentially infiltrate the underlying bone, with dural and brain parenchyma invasion in very rare cases, more common in BCCs [15, 16]. The presence of a large, firm, tender mass of the scalp, with focal tenderness over a bony margin, should raise suspicion of bony invasion and warrant imaging [14].

Imaging modalities (CT and MRI) are of great value in evaluating potential skull and dural involvement and thus play an important role in planning a preoperative strategy. CT is more accurate for identifying bony invasion, while MRI is superior in detecting dural and brain involvement [7]. Depth of invasion of SCC is a significant factor for the prognosis and outcome of patients, and these radiology modalities play a significant role in detecting any changes in the brain structure [17].

The rate of a correct preoperative diagnosis for scalp lesions is usually lower among general surgery, neurosurgery, and plastic surgery departments, which may be caused by a lack of diagnostic expertise in scalp lesions [3, 10]. Therefore, careful assessment and understanding of imaging characteristics are important in forming a more accurate preoperative diagnosis while the definitive diagnosis is established with PH verification. Additionally, the importance of this specific lesion lies in the specific clinical steps administered preoperatively and intraoperatively concerning the rarity, location, invasiveness, and aesthetical appearance of the lesion.

The surgical approach and management strategy are dependent on the degree of infiltration, with cooperation among different specialists required in the most complex of cases. In tumors with calvarial and dural involvement, generous excision of all small tissues with parts of the invaded skull and dura offers the best chance for preventing tumor recurrence with adequate dural reconstruction, preferably with autograft, followed by bone reconstruction with novel reconstruction techniques and materials, if available [6, 18, 19].

Furthermore, CT and MRI modalities are of great importance for bone reconstruction because 3D printing is performed on their basis using images, which indicates the even greater importance of radiological tools in many clinical areas. That serves to emphasize the current need to embrace the technology so the best treatment of surgical outcomes can be achieved [20, 21].

Conclusion

If left untreated, some cases of scalp SCCs can cause invasion of the underlying skull and dura. Imaging modalities like CT and MRI play a crucial role in evaluating the degree of neoplastic extension and potential calvarial and dural invasion, thus being of significant importance in preoperative planning, management, and clinical outcome of the patient.

REFERENCES

1. *Dika E, Patrizi A, Veronesi G, Manuelpillai N, Lambertini M.* Malignant cutaneous tumours of the scalp: always remember the head. J Eur Acad Dermatol Venereol 2020; 34(10): 2208–15.
2. *Katz TM, Silapunt S, Goldberg LH, Jih MH, Kimyai-Asadi A.* Analysis of 197 female scalp tumors treated with Mohs micrographic surgery. J Am Acad Dermatol 2005; 52(2): 291–4.
3. *Türk CÇ, Bacanli A, Kara NN.* Incidence and clinical significance of lesions presenting as a scalp mass in adult patients. Acta Neurochir 2015; 157(2): 217–23.
4. *Prodinger CM, Koller J, Laimer M.* Scalp tumors. J Dtsch Dermatol Ges 2018; 16(6): 730–53.
5. *García-Rojo B, García-Solano J, Sánchez-Sánchez C, Montalbán-Romero S, Martínez-Parra D, Pérez-Guillermo M.* On the utility of fine needle aspiration in the diagnosis of primary scalp lesions. Diagn Cytopathol 2001; 24(2): 104–11.
6. *Soma PF, Chibbaro S, Makiese O, Marsella M, Diemidio P, Fricia M,* et al. Aggressive scalp carcinoma with intracranial extension: A multidisciplinary experience of 25 patients with long-term follow-up. J Clin Neurosci 2008; 15(9): 988–92.
7. *Wollina U, Kittner T, Nowak A.* Nonmelanoma skin cancer with skull infiltration and cranial involvement. Open Access Maced J Med Sci 2019; 7(18): 3030–3.
8. *Alam M, Armstrong A, Baum C, Bordeaux JS, Brown M, Busam KJ,* et al. Guidelines of care for the management of cutaneous squamous cell carcinoma. J Am Acad Dermatol 2018; 78(3): 560–78.
9. *Chabaane M, Ayadi K, Rkhami M, Drissi C, Houimli S, Bahri K,* et al. Management of a recurrence of a squamous cell carcinoma of the scalp with extension to the brain: A case report and literature review. Surg Neurol Int 2020; 11: 347.

10. *Kawaguchi M, Kato H, Matsuo M.* CT and MRI features of scalp lesions. Radiol Med 2019; 124(10): 1049–61.
11. *Chiu CS, Lin CY, Kuo TT, Kuan YZ, Chen MJ, Ho HC,* et al. Malignant cutaneous tumors of the scalp: a study of demographic characteristics and histologic distributions of 398 Taiwanese patients. J Am Acad Deramtol 2007; 56(3): 448–52.
12. *Kim JH, Kim JY, Chun KA, Jee WH, Sung MS.* MR imaging manifestation of skin tumors. Eur Radiol 2008; 18(11): 2652–61.
13. *Millare GG, Guha-Thakurta N, Sturgis EM, El-Naggar AK, Debnam JM.* Imaging findings of head and neck dermatofibrosarcoma protuberans. Am J Neuroradiol 2014; 35(2): 373–8.
14. *Humphreys TR, Shah K, Wysong A, Lexa F, MacFarlane D.* The role of imaging in the management of patients with nonmelanoma skin cancer. When is imaging necessary? J Am Acad Dermatol 2017; 76(4): 591–607.
15. *Hay A, Strahan JE, Torres A, Kim JY.* Basal cell carcinoma with calvarium invasion. Dermatol Surg 2011; 37(3): 399–401.
16. *Kleydman Y, Manolidis S, Ratner D.* Basal cell carcinoma with intracranial invasion. J Am Acad Dermatol 2009; 60(6): 1045–9.
17. *Suk S, Shin HW, Yoon KC, Kim J.* Aggressive cutaneous squamous cell carcinoma of the scalp. Arch Craniofac Surg 2020; 21(6): 363–7.
18. *Bolly HM, Faried A, Jembise TL, Wirakusumah FF, Arifin MZ.* The ideal selection criteria for duraplasty material in brain surgery: a review. Interdiscip Neurosurg 2020; 22: 100800.
19. *Zanotti B, Zingaretti N, Verlicchi A, Robiony M, Alfieri A, Parodi PC.* Cranioplasty: Review of materials. J Craniofac Surg 2016; 27(8): 2061–72.
20. *da Silva Júnior EB, de Aragão AH, de Paula Loureiro M, Lobo CS, Oliveti AF, de Oliveira RM,* et al. Cranioplasty with three-dimensional customised mould for polymethylmethacrylate implant: a series of 16 consecutive patients with cost-effectiveness consideration. 3D Print Med 2021; 7(1): 4.
21. *Juković M, Stojić I, Till V.* Potentials of three dimensional printing in radiology: a case of a knee injury. Med Pregl 2019; 72(9–10): 307–11.

Received on February 26, 2021
Revised on November 14, 2022
Accepted on November 16, 2022
Online First November 2022

CASE REPORT

UDC: 616.834-002.152-06-07
DOI: https://doi.org/10.2298/VSP200511001M

Neurophysiological confirmation of phrenic nerve affection in a patient with dyspnea and herpes zoster

Neurofiziološka potvrda zahvaćenosti freničnog nerva kod bolesnika sa dispnejom i herpesom zosterom

Vesna Martić*†, Aleksandar Stojanov‡

***Military Medical Academy, Clinic for Neurology, Belgrade, Serbia; †University of Defence, Faculty of Medicine of the Military Medical Academy, Belgrade, Serbia; ‡University Clinical Center Niš, Clinic for Neurology, Niš, Serbia**

Abstract

Introduction. Herpetic lesion of the phrenic nerve is quite uncommon. These lesions are usually unilateral, and for most clinicians, the clinical manifestation of herpes zoster in the cervical or thoracic region and diaphragmatic paralysis on the same side is sufficient for making a diagnosis of segmental herpes zoster phrenic nerve palsy. We report a patient with a classic clinical picture, in which we confirmed phrenic nerve affection on nerve conduction study. **Case report.** A 58-year-old female patient came for an examination due to shortness of breath. The patient had a herpetic rash on her right shoulder two and a half months earlier. The elevation of the right hemidiaphragm was seen on chest X-ray imaging. Asymmetry was evident in the nerve conduction study of the phrenic nerve: prolonged latency and reduced amplitude of her right phrenic nerve. The patient was treated with acyclovir, pregabalin, and B complex vitamins. After six months, the motor deficit was reduced completely. **Conclusion.** A nerve conduction study of the phrenic nerve is useful in making the definitive diagnosis. Good outcome, as in this patient, is rare in patients with this diagnosis and may be linked to timely treatment with acyclovir.

Key words:
diagnosis; electrodiagnosis; herpes zoster; nerve conduction studies; phrenic nerve.

Apstrakt

Uvod. Herpetična lezija freničnog nerva je veoma retka. Te lezije su obično jednostrane i za većinu kliničara je klinička manifestacija herpes zostera u cervikalnom ili torakalnom regionu, uz paralizu dijafragme na istoj strani, dovoljna za postavljanje dijagnoze segmentne paralize freničnog nerva. Prikazujemo bolesnicu sa tipičnom kliničkom slikom kod koje je zahvaćenost freničnog nerva potvrđena ispitivanjem provodljivosti nerva. **Prikaz bolesnika.** Bolesnica stara 58 godina javila se na pregled zbog tegoba sa disanjem u vidu „kratkog" daha. Bolesnica je dva i po meseca ranije imala herpetični osip na koži desnog ramena. Rendgenskim snimkom grudnog koša utvrđena je podignuta desna hemidijafragma. Ispitivanjem provodljivosti freničnog nerva utvrđena je jasna asimetrija: produžena latencija i redukovana amplituda desnog freničnog nerva. Bolesnica je lečena aciklovirom, pregabalinom i vitaminima B kompleksa. Šest meseci kasnije, motorički deficit se potpuno povukao. **Zaključak.** Ispitivanje provodljivosti freničnog nerva je korisno za postavljanje definitivne dijagnoze. Povoljan ishod, kao kod prikazane bolesnice, redak je kod bolesnika sa tom dijagnozom i može biti povezan sa blagovremenim lečenjem aciklovirom.

Ključne reči:
dijagnoza; elektrodijagnostika; herpes zoster; živci, provodljivost, ispitivanje; frenični nerv.

Introduction

The diaphragm is innervated by the phrenic nerve, which originates from the anterior horn of the spinal cord (mainly C4 and partially C3 and C5 roots). Therefore, the phrenic nerve plays a crucial role in breathing. It is believed that reactivated varicella-zoster virus (VZV), from initial infection during chickenpox in childhood, can lead to the development of diaphragmatic paralysis and shortness of breath. Herpetic lesions of the phrenic nerve and consecutive diaphragmatic paralysis are extremely uncommon, and there are no accurate data about their frequency [1]. Cervical herpes zoster (HZ) and diaphragmatic paralysis were first described in 1949 [2]. Herpetic lesions of the phrenic nerve are usually

Correspondence to: Vesna Martić, Military Medical Academy, Clinic for Neurology, Crnotravska 17, 11 000 Belgrade, Serbia.
E-mail: vesnamartic.bgd@gmail.com

unilateral, and for most clinicians, the clinical manifestation of HZ in the cervical or thoracic region and diaphragmatic paralysis on the same side is sufficient for making a diagnosis of segmental HZ phrenic nerve palsy [3]. There are only a few publications on the neurophysiological confirmation of phrenic nerve damage in segmental HZ paresis [1].

Case report

We present a 58-year-old female patient with paresis of the right hemidiaphragm and neurophysiologically demonstrated affection of the phrenic nerve as the reason for this weakness. She consulted her doctor because of shortness of breath. The patient had no previous history of smoking, malignancy, trauma, or chest surgery. Two and a half months earlier, she had a herpetic rash on her right shoulder, accompanied by intense pain. She noted weakness in her right shoulder and arm after that, along with the withdrawal of herpetic rash. During the inspection of the patient, dyspnea reduced respiratory excursions; the use of intercostal and accessory inspiratory muscles during inspiration in the region of the right hemithorax was noted. There was a pale herpetic rash in the area of her right shoulder (Figure 1). Moderate weakness during abduction of her upper right arm [Muscle Power Assessment (MRC) 4/5] was present; the right triceps reflex was abolished, and dysesthesia in the right shoulder region was evidenced. On the chest X-ray imaging, the elevation of the right hemidiaphragm was seen (Figure 2). Furthermore, no other pathological findings and possible causes of the phrenic nerve compression were noted on this scan. To prove diaphragmatic paralysis originating from phrenic nerve involvement, we performed a nerve conduction study (NCS) of this nerve and needle electromyography (EMG) of the diaphragm. We noted prolonged latency (11 ms) and reduced amplitude (0.1 mV) of the right phrenic nerve. The left phrenic nerve latency was 6.63 ms, and the amplitude was 0.45 mV (Figure 3). EMG of the diaphragm on the left side recorded a rhythmic electrical activity of inspiration as bursts of an interference pattern, separated by regular intervals of electrical silence during passive expiration. No such activity was noticed on the affected right side. EMG of her right arm revealed the existence of a neurogenic pattern and fibrillation in the right deltoid muscle. On the left side, the results of electrodiagnostic tests were normal. We performed a magnetic resonance imaging of the cervical spine, which showed only mild degenerative lesions, with no compressive radicu-

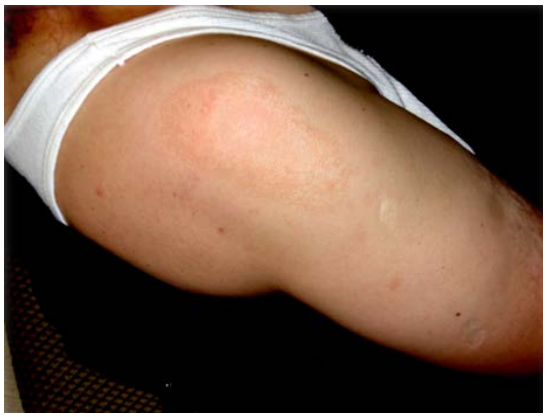

Fig. 1 – Herpetic rash on the patient's shoulder.

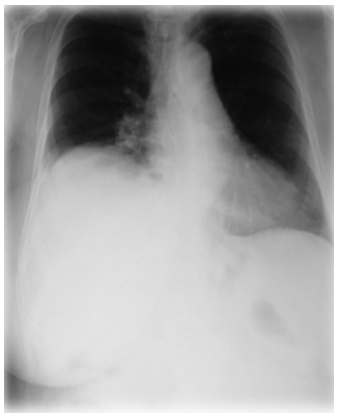

Fig. 2 – Chest X-ray imaging shows the elevation of the right hemidiaphragm.

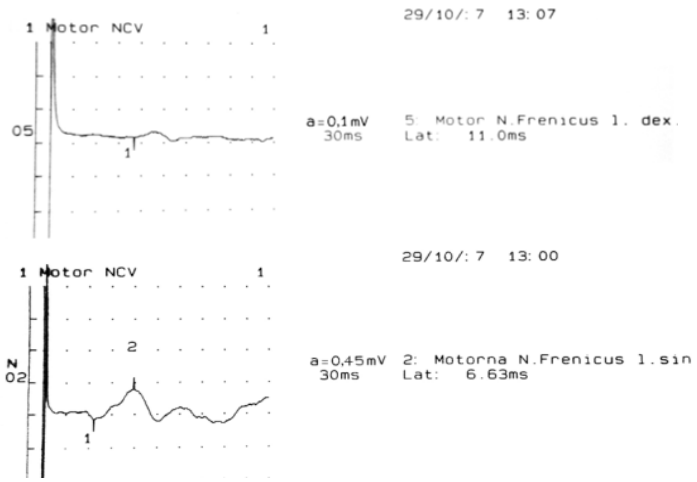

Fig. 3 – Phrenic nerve conduction studies. Note the right phrenic nerve M-response with reduced amplitude and prolonged latency. M – motor response, NCV– nerve conduction velocity.

lopathy or myelopathy. It was concluded that the patient has C5 radiculopathy due to the HZ infection (post-infectious radiculitis). The patient was treated with acyclovir (1,500 mg for 14 days), pregabalin (450 mg a day), and B complex vitamins. After six months, the motor deficit was completely reduced.

Discussion

The experience of an increase in the rate of HZ infection in patients older than 50 due to a decline in cell-mediated immunity with age is confirmed by the case of the presented patient (58 years old) [4]. Except for hypertension, the patient did not have any other diseases commonly seen in a population of patients with HZ, such as malignancy, diabetes mellitus, etc. According to the literature data, the maximal rash-to-weakness interval in patients with segmental limb paresis was 19 days [5]. A delay of 4–5 months is documented in patients with diaphragmatic paralysis [6]. That could be explained by the fact that the phrenic nerve is the longest motor nerve in the body, and, therefore, the time required for retrograde migration of VZV is longer. In the case of this specific patient, diaphragmatic weakness took two and a half months to appear after the HZ infection – much longer compared to the time of development of limb paresis. For most clinicians, the clinical manifestation of HZ in the cervical or thoracic region and ipsilateral diaphragmatic paralysis, when other known causes of phrenic nerve paralysis are excluded, is sufficient for making the diagnosis of segmental HZ paresis of the phrenic nerve [6]. Hemidiaphragm elevation was seen on chest radiography or computed tomography (CT) scans that had been used in the majority of previous papers for the confirmation of the diagnosis. The presence of hemidiaphragmatic paralysis may be suspected in patients who complain of dyspnea. It should be noted that half of the cases with diaphragmatic paralysis due to HZ had no symptoms referable to the respiratory system [7]. Furthermore, there are cases with normal chest CT which indicates insufficiency of this diagnostic measure [8]. Raised and immobile diaphragm is not by itself evidence of paralysis. It is necessary to demonstrate the paradoxical movement of the diaphragm after sudden inspiration on fluoroscopy or to prove phrenic nerve palsy (confirmed by the affection of the diaphragm motor action potential after phrenic nerve stimulation) [7, 9]. Only a few authors used neurophysiology to confirm the phrenic nerve paralysis [1, 7]. Electrodiagnostic confirmation of the phrenic nerve affection was used in the case of the presented patient. Because of prolonged reinnervation of the diaphragm due to the relatively long course of the phrenic nerve, the prognosis in patients with diaphragmatic paralysis is not good as it is segmental zoster paresis of limbs. In the case of phrenic nerve palsy, a lack of spontaneous recovery is not surprising. It is common for zoster-associated diaphragmatic paralysis to be permanent; still, recovery has occasionally been reported after seven and twelve months. That being said, in this case, the patient recovered completely within six months. Treatment of these patients with acyclovir has been reported only in a few patients [7, 8]. Only in one previous case report did the patient receive acyclovir intravenously [9]. Famciclovir was the therapy in one patient [10]. The presented patient was treated with acyclovir for two weeks with the complete withdrawal of the symptoms over the next six months. As postherpetic neuralgia is not rare in the cases of segmental zoster paresis, medicaments for neuropathic pain are recommended. In the presented patient, pregabalin was used for pain treatment.

Conclusion

We present a rare form of diaphragmatic HZ paralysis with electrophysiological confirmation of phrenic nerve involvement. Phrenic nerve conduction study is useful in making the definitive diagnosis. A favorable outcome, as in this case, is rare in patients with this diagnosis and may be linked to timely treatment with acyclovir.

Conflict of interest

The authors report no conflict of interest.

REFERENCES

1. *Bahadir C, Kalpakcioglu AB, Kurtulus D.* Unilateral diaphragmatic paralysis and segmental motor paresis following herpes zoster. Muscle Nerve 2009; 38(2): 1070–3.
2. *Halpern LS, Covner AH.* Motor manifestations of herpes zoster, report of a case of associated permanent paralysis of phrenic nerve. Arch Intern Med (Chic) 1949; 84(6): 907–16.
3. *Melcher WL, Dietrich RA, Whitlock WL.* Herpes zoster phrenic neuritis with respiratory failure. West J Med 1990; 152(2): 192–4.
4. *Yawn B, Gilden D.* The global epidemiology of herpes zoster. Neurology 2013; 81(10): 928–30.
5. *Reda H, Watson J, Jones L.* Zoster associated mononeuropathies: a retrospective series. Muscle Nerve 2012; 45: 734–9.
6. *Stowasser M, Cameron J, Oliver WA.* Diaphragmatic paralysis following cervical herpes zoster. Med J Aust 1990; 153(9): 555–6.
7. *Soler JJ, Perpiña M, Alfaro A.* Hemidiaphragmatic paralysis caused by cervical herpes zoster. Respiration 1996; 63(6): 403–6.
8. *Liu Y, Wu BY, Ma ZS, Xu JJ, Yang B, Li H,* et al. A retrospective case series of segmental zoster paresis of limbs: clinical, electrophysiological and imaging characteristics. BMC Neurol 2018; 18(1): 121.
9. *Berger R.* Case of Hiccups. J Emerg Med 2013; 44 (1): 107–8.
10. *Oike M, Naito T, Tsukada M, Kikuchi Y, Sakamoto N, Otsuki Y,* et al. A case of diaphragmatic paralysis complicated by herpes-zoster virus infection. Intern Med 2012; 51(10): 1259–63.

Received on May 11, 2020
Revised on December 25, 2022
Accepted on December 27, 2022
Online First January 2023

INSTRUCTIONS TO THE AUTHORS

The VSP publishes only papers not published before, nor submitted to any other journals, in the order determined by the Editorial Board. Any attempted plagiarism or self-plagiarism will be punished. When submitting a paper to the VSP electronic editing system **(http://aseestant.ceon.rs/index.php)**, the following should be enclosed: a statement on meeting any technical requirements, a statement signed by all the authors that the paper on the whole and/or partly has not been submitted nor accepted for publication elsewhere, a statement specifying the actual contribution of each author, no conflict of interest statement that make them responsible for meeting any requirements set. What follows subsequently is the acceptance of a paper for further editing procedure. The manuscripts submitted to the VSP pass in-house and external peer review. All authors pay "Article Processing Charge" for coverage all editing and publishing expenses. Domestic authors pay 5,000 RSD, and those from aboard 150 euros. The editing and publishing fee is required for substantive editing, facts and references validations, copy editing, and publishing online and in print by editorial staff of the Journal. No additional fees, other than stated above, are required even if an author who already paid the fee would have more articles accepted for publishing in the year when fee was paid. All authors who pay this fee may, if want, receive printed version of the Journal in year when fee is payed. Please note that the payment of this charge does not guarantee acceptance of the manuscript for publication and does not influence the outcome of the review procedure. The requirement about paying "Article Processing Charge" does not apply to reviewers, members of the Editorial Board and the Publisher's Council of the Journal, young researchers and students, as well as any of the subscribers of the Journal.

The VSP publishes: **editorials, original articles**, **short communications**, **reviews**/**meta-analyses, case reports**, **medical history** (general or military), personal views, invited comments, letters to the editor, reports from scientific meetings, book reviews, and other. Original articles, short communications, meta-analyses and case reports are published with abstracts in both English and Serbian.

General review papers will be accepted by the Editorial Board only if the authors prove themselves as the experts in the fields they write on by citing not less than 5 self-citations.

Papers should be written on IBM-compatible PC, using 12 pt font, and double spacing, with at least 4 cm left margin. **Bold** and *italic* letters should be avoided as reserved for subtitles. Original articles, reviews, meta-analyses and articles from medical history should not exceed 16 pages; current topics 10; case reports 6; short communications 5; letters to the editor and comments 3, and reports on scientific meetings and book reviews 2.

All measurements should be reported in the metric system of the International System of Units (SI), and the standard internationally accepted terms (except for mmHg and °C).

MS Word for Windows (97, 2000, XP, 2003) is recommended for word processing; other programs are to be used only exceptionally. Illustrations should be made using standard **Windows** programs, **Microsoft Office** (**Excel**, **Word Graph**)**.** The use of colors and shading in graphs should be avoided.

Papers should be prepared in accordance with the **Vancouver Convention**.

Papers are reviewed anonymously by at least two editors and/or invited reviewers. Remarks and suggestions are sent to the author for final composition. Galley proofs are sent to the corresponding author for final agreement.

Preparation of manuscript

Parts of the manuscript are: **Title page; Abstract with Key words; Text; Acknowledgements** (to the authors' desire), **References**, **Enclosures**.

1. ***Title page***

a) The title should be concise but informative, while subheadings should be avoided;

b) Full names of the authors signed as follows: ***, †, ‡, §, ‖, ¶, **, ††, ...** .

c) Exact names and places of department(s) and institution(s) of affiliation where the studies were performed, city and the state for any authors, clearly marked by standard footnote signs;

d) Conclusion could be a separate chapter or the last paragraph of the discussion;

e) Data on the corresponding author.

2. ***Abstract and key words***

The second page should carry a structured abstract (250-300 words for original articles and meta-analyses) with the title of the article. In short, clear sentences the authors should write the **Background**/**Aim**, major procedures – **Methods** (choice of subjects or laboratory animals; methods for observation and analysis), the obtained findings – **Results** (concrete data and their statistical significance), and the **Conclusion**. It should emphasize new and important aspects of the study or observations. A structured abstract for case reports (up to 250 words) should contain subtitles **Introduction, Case report, Conclusion**). Below the abstract **Key words** should provide 3–10 key words or short phrases that indicate the topic of the article.

3. ***Text***

The text of the articles includes: **Introduction**, **Methods**, **Results**, and **Discussion**. Long articles may need subheadings within some sections to clarify their content.

Introduction. After the introductory notes, the aim of the article should be stated in brief (the reasons for the study or observation), only significant data from the literature, but not extensive, detailed consideratuion of the subject, nor data or conclusions from the work being reported.

Methods. The selection of study or experimental subjects (patients or experimental animals, including controls) should be clearly described. The methods, apparatus (manufacturer's name and address in parentheses), and procedures should be identified in sufficient detail to allow other workers to reproduce the results. Also, give references to established methods, including statistical methods. Identify precisely all drugs and chemicals used, with generic name(s), dose(s), and route(s) of administration. State the approval of the Ethnics Committee for the tests in humans and animals.

Results should be presented in logical sequence in the text, tables and illustrations. Emphasize or summarize only important observations.

Discussion is to emphasize the new and significant aspects of the study and the conclusions that result from them. Relate the observations to other relevant studies. Link the conclusions with the goals of the study, but avoid unqualified statements and conclusions not completely supported by your data.

References

References should be superscripted and numerated consecutively in the order of their first mentioning within the text. All the authors should be listed, but if there are more than 6 authors, give the first 6 followed by *et al*. Do not use abstracts, secondary publications, oral communications, unpublished papers, official and classified documents. References to papers accepted but not yet published should be cited as "in press". Information from manuscripts not yet accepted should be cited as "unpublished data". Data from the Internet are cited with the date of citation.

Examples of references:

Jurhar-Pavlova M, Petlichkovski A, TrajkovD, Efinska-Mladenovska O, Arsov T, Strezova A, et al. Influence of the elevated ambient temperature on immunoglobulin G and immunoglobulin G subclasses in sera of Wistar rats. Vojnosanit Pregl 2003; 60(6): 657–612.

DiMaio VJ. Forensic Pathology. 2nd ed. Boca Raton: CRC Press; 2001.

Blinder MA. Anemia and Transfusion Therapy. In: Ahya NS, Flood K, Paranjothi S, editors. The Washington Manual of Medical Therapeutics, 30th edition. Boston: Lippincot, Williams and Wilkins; 2001. p. 413-28.

Christensen S, Oppacher F. An analysis of Koza's computational effort statistic for genetic programming. In: *Foster JA, Lutton E, Miller J, Ryan C, Tettamanzi AG*, editors. Genetic programming. EuroGP 2002: Proceedings of the 5th European Conference on Genetic Programming; 2002 Apr 3-5; Kinsdale, Ireland. Berlin: Springer; 2002. p. 182-91.

Abood S. Quality improvement initiative in nursing homes: the ANA acts in an advisory role. Am J Nurs [serial on the Internet]. 2002 Jun [cited 2002 Aug 12]; 102(6): [about 3 p.]. Available from: http://www.nursingworld.org/AJN/2002/june/Wawatch.htm

Tables

Each table should be typed double-spaced 1,5 on a separate sheet, numbered in the order of their first citation in the text in the upper left corner and supplied with a brief title each. Explanatory notes are printed under a table. Each table should be mentioned in the text. If data from another source are used, acknowledge fully.

Illustrations

Any forms of graphic enclosures are considered to bi figures and should be submitted as additional databases in the System of Assistent. Letters, numbers, and symbols should be clear and uniform, of sufficient size that when reduced for publication, each item will still be legible. Each figure should have a label on its back indicating the number of the figure, author's name, and top of the figure (**Figure 1**, **Figure 2** and so on). If a figure has been published, state the original source.

Legends for illustrations are typed on a separate page, with Arabic numbers corresponding to the illustrations. If used to identify parts of the illustrations, the symbols, arrows, numbers, or letters should be identified and explained clearly in the legend. Explain the method of staining in photomicrographs.

Abbreviations and acronyms

Authors are encouraged to use abbreviations and acronyms in the manuscript in the following manner: abbreviations and acronyms must be defined the first time they are used in the text consistently throughout the whole manuscript, tables, and graphics; abbreviations should be used only for terms that appear more than three times in text; abbreviations should be sparingly used.

An alphabetical list of all abbreviations used in the paper, followed by their full definitions, should be provided on submission.

Detailed Instructions are available at the web site:

www.vma.mod.gov.rs/vsp

UPUTSTVO AUTORIMA

VSP objavljuje radove koji nisu ranije nigde objavljivani, niti predati za objavljivanje redosledom koji određuje uređivački odbor. Svaki pokušaj plagijarizma ili autoplagijarizma kažnjava se. Prilikom prijave rada u sistem elektronskog uređivanja „Vojnosanitetskog pregleda“**(http://aseestant.ceon.rs/index.php)** neophodno je priložiti izjavu da su ispunjeni svi postavljeni tehnički zahtevi uključujući i izjavu koju potpisuju svi autori da rad nije ranije ni u celini, niti delimično objavljen niti prihvaćen za štampanje u drugom časopisu. Izjavu o pojedinačnom doprinosu svakog od autora rada potpisanu od svih autora, treba skenirati i poslati uz rad kao dopunsku datoteku. Takođe, autori su obavezni da dostave i potpisanu izjavu o nepostojanju sukoba interesa čime postaju odgovorni za ispunjavanje svih postavljenih uslova. Ovome sledi odluka o prihvatanju za dalji uređivački postupak. Rukopisi pristigli u Redakciju časopisa podležu internoj i eksternoj recenziji. Svi autori dužni su da plate “Article Processing Charge” za pokriće troškova jezičke, stručne i tehničke obrade rukopisa, kao i njegovog objavljivanja. Domaći autori plaćaju iznos od 5 000 dinara, a inostrani 150 eura. Dodatna plaćanja nisu predviđena čak i u slučaju da autor koji je već prethodno platio traženi iznos, ima više prihvaćenih radova za objavljivanje u godini u kojoj je izvršio uplatu. Svi autori koji su platili “Article Processing Charge” mogu, ukoliko žele, dobijati štampanu verziju časopisa tokom godine u kojoj je izvršena uplata. Plaćanje ovog iznosa ne garantuje prihvatanje rukopisa za objavljivanje i ne utiče na ishod recenzije. Od obaveze plaćanja pokrića navedenih troškova oslobođeni su recenzenti, članovi Uređivačkog odbora i Izdavačkog saveta VSP, studenti i mladi istraživači, kao i pretplatnici časopisa.

U VSP-u se objavljuju **uvodnici**, **originalni članci, prethodna** ili **kratka saopštenja**, revijski radovi tipa **opšteg pregleda** (uz uslov da autori navođenjem najmanje 5 autocitata potvrde da su eksperti u oblasti o kojoj pišu), **aktuelne teme, metaanalize**, **kazuistika, seminar praktičnog lekara,** članci iz **istorije medicine**, lični stavovi, naručeni komentari, pisma uredništvu, izveštaji sa naučnih i stručnih skupova, prikazi knjiga i drugi prilozi. Radovi tipa originalnih članaka, prethodnih ili kratkih saopštenja, metaanalize i kazuistike **objavljuju se uz apstrakte na srpskom i engleskom jeziku**.

Rukopis se piše sa proredom 1,5 sa levom marginom od **4 cm**. Koristiti font veličine 12, a načelno izbegavati upotrebu **bold** i *italic* slova, koja su rezervisana za podnaslove. Originalni članci, opšti pregledi i metaanalize i članci iz istorije medicine ne smeju prelaziti 16 stranica (bez priloga); aktuelne teme – deset, seminar praktičnog lekara – osam, kazuistika – šest, prethodna saopštenja – pet, a komentari i pisma uredniku – tri, izveštaji sa skupova i prikazi knjiga – dve stranice.

U celom radu obavezno je korišćenje međunarodnog sistema mera (SI) i standardnih međunarodno prihvaćenih termina (sem mm Hg i °C).

Za obradu teksta koristiti program **Word for Windows** verzije 97, 2000, XP ili 2003. Za izradu grafičkih priloga koristiti standardne grafičke programe za **Windows**, poželjno iz programskog paketa **Microsoft Office** (**Excel, Word Graph**). Kod kompjuterske izrade grafika izbegavati upotrebu boja i senčenja pozadine.

Radovi se pripremaju u skladu sa **Vankuverskim dogovorom**.

Prispeli radovi kao anonimni podležu uređivačkoj obradi i recenziji najmanje dva urednika/recenzenta. Primedbe i sugestije urednika/recenzenata dostavljaju se autoru radi konačnog oblikovanja. Pre objave, rad se upućuje autoru određenom za korespodenciju na konačnu saglasnost.

Priprema rada

Delovi rada su: **naslovna strana, apstrakt sa ključnim rečima, tekst** rada, zahvalnost (po želji), literatura, prilozi.

1. ***Naslovna strana***

a) Poželjno je da naslov bude kratak, jasan i informativan i da odgovara sadržaju, podnaslove izbegavati.

b) Ispisuju se puna imena i prezimena autora sa oznakama redom: *, †, ‡, §, ‖, ¶, **, ††, ...

c) Navode se puni nazivi ustanove i organizacijske jedinice u kojima je rad obavljen mesta i države za svakog autora, koristeći standardne znake za fusnote.

d) Zaključak može da bude posebno poglavlje ili se iznosi u poslednjem pasusu diskusije.

e) Podaci o autoru za korespodenciju.

2. ***Apstrakt i ključne reči***

Na drugoj stranici nalazi se strukturisani apstrakt (250-300 reči za originalne članke i meta-analize) sa naslovom rada. Kratkim rečenicama na srpskom i engleskom jeziku iznosi se **Uvod/Cilj** rada, osnovne procedure **– Metode** (izbor ispitanika ili laboratorijskih životinja; metode posmatranja i analize), glavni nalazi **– Rezultati** (konkretni podaci i njihova statistička značajnost) i glavni **Zaključak**. Naglasiti nove i značajne aspekte studije ili zapažanja. Strukturisani apstrakt za kazuistiku (do 250 reči), sadrži podnaslove **Uvod, Prikaz bolesnika** i **Zaključak**). Ispod apstrakta, „Ključne reči“ sadrže 3–10 ključnih reči ili kratkih izraza koje ukazuju na sadržinu članka.

3. ***Tekst članka***

Tekst sadrži sledeća poglavlja: **uvod**, **metode**, **rezultate** i **diskusiju**. **Uvod.** Posle uvodnih napomena, navesti cilj rada. Ukratko izneti razloge za studiju ili posmatranje. Navesti samo važne podatke iz literature a ne opširna razmatranja o predmetu rada, kao ni podatke ili zaključke iz rada o kome se izveštava.

Metode. Jasno opisati izbor metoda posmatranja ili eksperimentnih metoda (ispitanici ili eksperimentne životinje, uključujući kontrolne). Identifikovati metode, aparaturu (ime i adresa proizvođača u zagradi) i proceduru, dovoljno detaljno da se drugim autorima omogući reprodukcija rezultata. Navesti podatke iz literature za uhodane metode, uključujući i statističke. Tačno identifikovati sve primenjene lekove i hemikalije, uključujući generičko ime, doze i načine davanja. Za ispitivanja na ljudima i životinjama navesti saglasnost nadležnog etičkog komiteta.

Rezultate prikazati logičkim redosledom u tekstu, tabelama i ilustracijama. U tekstu naglasiti ili sumirati samo značajna zapažanja.

U **diskusiji** naglasiti nove i značajne aspekte studije i izvedene zaključke. Posmatranja dovesti u vezu sa drugim relevantnim studijama, u načelu iz poslednje tri godine, a samo izuzetno i starijim. Povezati zaključke sa ciljevima rada, ali izbegavati nesumnjive tvrdnje i one zaključke koje podaci iz rada ne podržavaju u potpunosti.

Literatura

U radu literatura se citira kao superskript, a popisuje rednim brojevima pod kojima se citat pojavljuje u tekstu. Navode se svi autori, ali ako broj prelazi šest, navodi se prvih šest i *et al*. Svi podaci o citiranoj literaturi moraju biti tačni. Literatura se u celini citira na engleskom jeziku, a iza naslova se navodi jezik članka u zagradi. Ne prihvata se citiranje apstrakata, sekundarnih publikacija, usmenih saopštenja, neobjavljenih radova, službenih i poverljivih dokumenata. Radovi koji su prihvaćeni za štampu, ali još nisu objavljeni, navode se uz dodatak „u štampi“. Rukopisi koji su predati, ali još nisu prihvaćeni za štampu, u tekstu se citiraju kao „neobjavljeni podaci“ (u zagradi). Podaci sa interneta citiraju se uz navođenje datuma pristupa tim podacima.

Primeri referenci:

Đurović BM. Endothelial trauma in the surgery of cataract. Vojnosanit Pregl 2004; 61(5): 491–7. (Serbian)

Balint B. From the haemotherapy to the haemomodulation. Beograd: Zavod za udžbenike i nastavna sredstva; 2001. (Serbian)

Mladenović T, Kandolf L, Mijušković ŽP. Lasers in dermatology. In: *Karadaglić Đ*, editor. Dermatology. Beograd: Vojnoizdavački zavod & Verzal Press; 2000. p. 1437–49. (Serbian)

Christensen S, Oppacher F. An analysis of Koza's computational effort statistic for genetic programming. In: *Foster JA, Lutton E, Miller J, Ryan C, Tettamanzi AG*, editors. Genetic programming. EuroGP 2002: Proceedings of the 5th European Conference on Genetic Programming; 2002 Apr 3-5; Kinsdale, Ireland. Berlin: Springer; 2002. p. 182-91.

Abood S. Quality improvement initiative in nursing homes: the ANA acts in an advisory role. Am J Nurs [serial on the Internet]. 2002 Jun [cited 2002 Aug 12]; 102(6): [about 3 p.]. Available from: http://www.nursingworld.org/AJN/2002/june/Wawatch.htm

Tabele

Sve tabele pripremaju se sa proredom 1,5 na posebnom listu. Obeležavaju se arapskim brojevima, redosledom pojavljivanja, u levom uglu (**Tabela 1**), a svakoj se daje kratak naslov. Objašnjenja se daju u fus-noti, ne u zaglavlju. Svaka tabela mora da se pomene u tekstu. Ako se koriste tuđi podaci, obavezno ih navesti kao i svaki drugi podatak iz literature.

Ilustracije

Slikama se zovu svi oblici grafičkih priloga i predaju se kao dopunske datoteke u sistemu **aseestant**. Slova, brojevi i simboli treba da su jasni i ujednačeni, a dovoljne veličine da prilikom umanjivanja budu čitljivi. Slike treba da budu jasne i obeležene brojevima, onim redom kojim se navode u tekstu (**Sl. 1; Sl. 2** itd.). Ukoliko je slika već negde objavljena, obavezno citirati izvor.

Legende za ilustracije pisati na posebnom listu, koristeći arapske brojeve. Ukoliko se koriste simboli, strelice, brojevi ili slova za objašnjavanje pojedinog dela ilustracije, svaki pojedinačno treba objasniti u legendi. Za fotomikrografije navesti metod bojenja i podatak o uvećanju.

Skraćenice i akronimi

Skraćenice i akronimi u rukopisu treba da budu korišćeni na sledeći način: definisati skraćenice i akronime pri njihovom prvom pojavljivanju u tekstu i koristiti ih konzistentno kroz čitav tekst, tabele i slike; koristiti ih samo za termine koji se pominju više od tri puta u tekstu; da bi se olakšalo čitaocu, skraćenice i aktinome treba štedljivo koristiti.

Abecedni popis svih skraćenica i akronima sa objašnjenjima treba dostaviti pri predaji rukopisa.

Detaljno uputstvo može se dobiti u redakciji ili na sajtu: www.vma.mod.gov.rs/vsp